NOAA Technical Memorandum NOS 25

TECHNICAL PAPERS ON AIRBORNE LASER HYDROGRAPHY (MARCH - DECEMBER 1978)

Rockville, Md.
February 1979

noaa NATIONAL OCEANIC AND ATMOSPHERIC ADMINISTRATION / National Ocean Survey

NOAA TECHNICAL MEMORANDUMS

National Ocean Survey Series

Survey (NOS) provides charts and related information for the safe navigation of merce. The survey also furnishes other Earth science data--from geodetic, hydro- ic, geomagnetic, seismologic, gravimetric, and astronomic surveys or observations, measurements--to protect life and property and to meet the needs of engineering, al, industrial, and defense interests.

NOAA Technical Memorandums NOS series facilitate rapid distribution of material that may be preliminary in nature and which may be published formally elsewhere at a later date. Publications 1 through 8 are in the former series, ESSA Technical Memoranda, Coast and Geodetic Survey Technical Memoranda (C&GSTM). Beginning with 9, publications are now part of the series, NOAA Technical Memorandums NOS.

Publications listed below are available from the National Technical Information Service (NTIS), U.S. Department of Commerce, Sills Bldg., 5285 Port Royal Road, Springfield, VA 22161. Price varies for paper copy; $3.00 microfiche. Order by accession number (in parentheses) when given.

ESSA Technical Memoranda

C&GSTM 1 Preliminary Measurements With a Laser Geodimeter. S. E. Smathers, G. B. Lesley, R. Tomlinson, and H. W. Boyne, November 1966. (PB-174-649)

C&GSTM 2 Table of Meters to Fathoms for Selected Intervals. D. E. Westbrook, November 1966. (PB-174-655)

C&GSTM 3 Electronic Positioning Systems for Surveyors. Angelo A. Ferrara, May 1967. (PB-175-604)

C&GSTM 4 Specifications for Horizontal Control Marks. L. S. Baker, April 1968. (PB-179-343)

C&GSTM 5 Measurement of Ocean Currents by Photogrammetric Methods. Everett H. Ramey, May 1968. (PB-179-083)

C&GSTM 6 Preliminary Results of a Geophysical Study of Portions of the Juan de Fuca Ridge and Blanco Fracture Zone. William G. Melson, December 1969. (PB-189-226)

C&GSTM 7 Error Study for Determination of Center of Mass of the Earth From Pageos Observations. K. R. Koch and H. H. Schmid, January 1970. (PB-190-982)

C&GSTM 8 Performance Tests of Richardson-Type Current Meters: I. Tests 1 Through 7. R. L. Swanson and R. H. Kerley, January 1970. (PB-190-983)

NOAA Technical Memorandums

NOS 9 The Earth's Gravity Field Represented by a Simple Layer Potential From Doppler Tracking of Satellites. Karl-Rudolf Koch and Bertold U. Witte, April 1971. (COM-71-00668)

NOS 10 Evaluation of the Space Optic Monocomparator. Lawrence W. Fritz, June 1971. (COM-71-00768)

NOS 11 Errors of Quadrature Connected With the Simple Layer Model of the Geopotential. Karl-Rudolf Koch, December 1971. (COM-72-10135)

NOS 12 Trends and Variability of Yearly Mean Sea Level 1893-1971. Steacy D. Hicks, March 1973. (COM-73-10670)

NOS 13 Trends and Variability of Yearly Mean Sea Level 1893-1972. Steacy D. Hicks and James E. Crosby, March 1974. (COM-74-11012)

NOS 14 Some Features of the Dynamic Structure of a Deep Estuary. Michael Devine, April 1974. (COM-74-10885)

NOS 15 An Average, Long-Period, Sea-Level Series for the United States. Steacy D. Hicks and James E. Crosby, September 1975. (COM-75-11463)

(Continued on inside back cover)

NOAA Technical Memorandum NOS 25

TECHNICAL PAPERS ON AIRBORNE LASER HYDROGRAPHY (MARCH - DECEMBER 1978)

Gary C. Guenther, Lowell R. Goodman,
and David B. Enabnit
Engineering Development Laboratory
Office of Marine Technology

Robert W.L. Thomas and Robert N. Swift
Wolf Research
Washington Analytical Sciences Center
EG&G

Rockville, Md.
February 1979

UNITED STATES
DEPARTMENT OF COMMERCE
Juanita M. Kreps, Secretary

NATIONAL OCEANIC AND
ATMOSPHERIC ADMINISTRATION
Richard A. Frank, Administrator

National Ocean
Survey
Allen L. Powell, Director

CONTENTS

TECHNICAL PAPERS ON AIRBORNE LASER HYDROGRAPHY (March - December 1978)

Gary C. Guenther, Lowell R. Goodman, and David B. Enabnit
Engineering Development Laboratory, Office of
Marine Technology, NOS, Rockville, MD

Robert W.L. Thomas and Robert N. Swift
Wolf Research, EG&G, Riverdale, MD 20840

ABSTRACT. Six papers are presented on the early results of an experimental and theoretical investigation into the technical aspects of airborne laser bathymetry. These papers were presented at technical meetings between March and December 1978.

1. INTRODUCTION

The National Ocean Survey (NOS) has been evaluating airborne laser bathymetry for several years. This work is aimed at determining the capabilities of the technique, as well as its cost effectiveness and the impacts of using it. The results of this evaluation will be used to determine if the potential benefits sufficiently outweigh the cost and risks for NOS to procure and implement such a system.

A major factor in the evaluation of this high technology system is performance. How accurate is laser bathymetry? How deep will it penetrate? What is the effect of turbidity? To study performance, the Engineering Development Laboratory of NOS is carrying out a theoretical and experimental program to quantify system behavior. The experimental program uses a prototype laser system belonging to NASA, the Airborne Oceanographic Lidar, to measure performance in a series of field tests. The continuing theoretical effort is being used to explain the experimental results and to extrapolate those results to an optimum laser bathymetric system.

A series of papers have been given at technical meetings as the work has progressed. Those papers document intermediate results, procedures, supporting analyses, and status. Since it is unlikely that these intermediate results, procedures, and analyses will be documented elsewhere, the papers have been collected and printed here as a single report. A certain amount of redundancy was unavoidable by printing the papers, but each has some unique information in it.

LASER BATHYMETRY FOR NEAR-SHORE CHARTING APPLICATION

(A STATUS REPORT)

Gary C. Guenther
David B. Enabnit
NOAA/National Ocean Survey
EDL, C61
Rockville, Maryland 20852

Abstract

Near-shore bathymetric measurements by NOAA/National Ocean Survey (NOS) are presently accomplished primarily with down-looking acoustic (sonar) equipment mounted in small boats which work along linear track lines at relatively low speeds. A scanning airborne laser bathymetric system has the potential to provide a higher quality product with more timely and less costly results in critical coastal and inland waters, and, as a member of the hydrographic team, also promises new or improved services.

1. Introduction

The objectives of the Laser Hydrography Development Project within NOS are: to determine, through field tests of an existing bathymetric laser system, the capability of an optimized airborne laser system to meet or exceed NOS near-shore vertical accuracy requirements within a bounding set of system variables and environmental parameters; to assess its cost effectiveness under "typical" operational conditions; to perform preliminary design work on a realizable, NOS operations oriented system; and to investigate the impact of such a system on NOS operations such as fleet utilization, chart production, and survey requirements.

2. AOL Field Tests

Background:

During the past ten years, a number of increasingly sophisticated airborne laser ranging (lidar) devices have been tested to determine technical feasibility for hydrographic and other oceanographic applications. (Ref. 1) In 1974, a development program for a versatile airborne laser and data acquisition system, to be sponsored by the NASA Advanced Applications Flight Experiment (AAFE) program, was proposed jointly by NASA/Wallops Flight Center and AVCO Everett Research Laboratory, Inc. Requirements, specifications, evaluation procedures, and applications for this "Airborne Oceanographic Lidar" (AOL) system were solicited and established through a series of meetings with interested parties. (Refs. 2-5) The system evolved with two major and separate

modes of operation: bathymetric lidar, and fluorosensing. Preliminary shakedown and experimentation with the AOL instrument in the bathymetric mode, installed in a NASA/Wallops Flight Center C-54 aircraft, has been sponsored by NOAA/National Ocean Survey (NOS) and the Defense Mapping Agency (DMA), and conducted jointly by NASA and NOS. In this section we shall discuss the results of the NOS test program. (Ref. 6)

Goals:

The goals of the NOS flight test program with the AOL system are to: validate the overall feasibility of a bathymetric lidar system to provide high quality data under typical operations-oriented circumstances; determine vertical error under a bounding range of system variables and environmental parameters and correlate error contributions with sources; quantify system and environmental usage constraints to establish the operational "window"; and model major contributions in a return signal strength equation to provide a sound basis for extrapolation of these results to the design specifications of an NOS prototype bathymetric lidar system.

Two test sites were selected (Ref. 7): one in the Atlantic Ocean over Winter Quarter Shoal (several miles offshore from Assateague Island), and one in Chesapeake Bay -- Tangier Sound between Janes Island and Smith Island. These dissimilar sites provided the opportunity to investigate the effects of diversity in water clarity, depth, wind, and surface wave structure.

Hardware:

The AOL bathymetric configuration (Ref. 8) includes the following: neon/nitrogen laser with appropriate optics; a 56 cm scanner mirror with drive motor and 14-bit angle encoder; a 30.5 cm diameter Cassegranian f/4 receiver telescope with adjustable field stop and baffles (0–20 milliradian field of view); a narrow band (4Å) interference filter to suppress ambient background; a photomultiplier tube (PMT) detector with appropriate electronics; 40 charge digitizers (A/D converters); and a computer controlled data acquisition, processing, display, and recording subsystem. The laser wavelength of 5401Å (green) is near the minimum of the Jerlov (Ref. 9) curves of diffuse attenuation coefficient for coastal water types. The laser output power is typically 2 kilowatts (peak), while approximately 500 watts (peak) exits the aircraft in the primary beam. Divergence is variable from 0-20 milliradians, and maximum pulse repetition rate is 400 Hz. Water depths are determined for each laser pulse by measuring the time of flight difference between that portion of the pulse reflected back to the receiver from the water's surface and that reflected by the underwater "bottom" topography.

Test Program:

The performance of the AOL is limited primarily by the product of water depth and optical attenuation coefficient. The latter is, for a given location and season, modulated temporally by wind, waveheight, precipitation, and

currents; also affecting performance are such things as bottom reflectivity and solar illumination. These parameters interact with system variables such as receiver field-of-view, altitude, scanner angle, and beam divergence to yield a highly complex set of interactions which must be unraveled to permit the quantization of specific effects. Adequate testing of the AOL thus depended on the quality and quantity of ground data specifically tailored to meet needs. Primary support data acquired in conjunction with the flight tests include vertical control, horizontal control, water clarity, sea surface conditions, meteorology, and bottom reflectivity. The data was obtained as near to the time of overflights as possible. A total of over one hundred vessel "sorties" or "cruises" were mounted in support of the program.

In 1977, 18 missions were flown with a total of 161 separate passes for an estimated total distance of 1000 linear nautical miles and 400 minutes of recorded data comprised of five million soundings. Aircraft speed was maintained at approximately 150 knots with altitudes ranging from 150 to 600 meters. Missions were flown in river, bay, and ocean waters, in hot and cold weather, clear and cloudy, night and day, for winds from 0 to 15 knots, with and without capillary waves, in water clarities with narrow beam attenuation coefficients varying from less than $1m^{-1}$ to greater than $4m^{-1}$, and with water depths from 0 to over 10 m.

Engineering:

Penetration capability is probably the most important performance parameter for a laser bathymetric system next to accuracy. The maximum penetration depth, in general, is dependent on a large number of variables and parameters including laser power, altitude, water clarity, bottom reflectivity, off-nadir angle, receiver aperture, receiver field of view, receiver sensitivity, noise sources, and many more (Ref. 6); but for a given (appropriately designed and operated) system, the ultimate concern is water clarity. The reduction in bottom return signal strength with increasing depth can be described by the expression:

$$SSB \sim e^{-2kD}$$

where

SSB = bottom signal strength,

D = depth, and

k $\equiv$ "system" attenuation coefficient as defined by this expression.

The coefficient, k, has no particular theoretical basis, but simply provides a straightforward empirical parameter for describing system performance.

It has been established (Ref. 10) that for a sufficiently large receiver field of view, the value of "k" somewhat coincidentally approaches very close to the value of depth averaged diffuse attenuation coefficient ($\bar{K}$) for the water in question. Calculation of "k" for the AOL (from the slope of ℓn SSB vs. D curves)

resulted in values generally consistent with $\bar{K}$. Because of this fact, the product of $\bar{K}$ and the depth beyond which successful returns cannot be detected (D_{max}) is commonly referred to as the "extinction coefficient" ($\bar{K} D_{max}$); and penetration capability is frequently reported in terms of this unitless parameter. In addition, because an apparently linear relationship ($\alpha \cong 5K$) (Ref. 11) exists between diffuse attenuation coefficient (K) and beam attenuation coefficient (α) for water clarities of interest in coastal waters, extinction coefficients may also be reported in terms of $\bar{\alpha} D_{max}$. (AOL results will take this form because most cruise data is for α rather than K).

Maximum extinction coefficients observed in processed AOL data are $\bar{\alpha} D_{max} = 12$ during the day and $\bar{\alpha} D_{max} = 15$ at night! The latter was accomplished in December off Janes Island with $\bar{\alpha} = 2.75 m^{-1}$ and $D_{max} = 5.5m$. These results, considered to be excitingly high for such a low power laser, were defined at the maximum extent of high quality data, where hit probabilities remain in excess of 90% and precision (pulse to pulse agreement) remains no worse than 15-20 cm. Because of the sophisticated processing techniques applied to the raw signals (Ref. 12), the loss of soundings at extinction tends to occur quite abruptly at bottom return signal strengths not greatly in excess of the minimum hardware digitization level. Projecting these results to a higher laser power system (100-200 kW peak) leads to expectations of $\bar{\alpha} D_{max}$ in the 18-20 range. Such estimates are consistent with independent high power results (K. Petri, Naval Air Development Center, personal communication, 1978).

Wind and wind generated waves (throughout the entire wavelength spectrum from capillaries to off-shore swell) unquestionably influence system performance through a number of interactions, but few are overly significant except at the extremes -- considered for our purposes to be 2-20 knots wind speed. Surface return energy from non-nadir scanner angles reaches the receiver only if capillary waves are excited sufficiently to present a large number of tiny facets perpendicular to the beam. These capillaries tend to die out below about 2 knots, and, as noted above, this leads to a reduced hit probability. On the other end of the spectrum, high winds generate waves with sufficient energy and depth to resuspend bottom sediments and decrease water clarity to unacceptable levels. From 2-20 knots, beam spreading through the air/sea interface due to wave slope augmented refraction is not large compared to beam spreading in the water column due to scattering. Surface return amplitudes at higher off-nadir scanner angles actually benefit slightly from higher winds where less variation of amplitude with angle is also noted.

Dark, muddy bottoms, typical in Chesapeake Bay, caused no bottom detection difficulties. Reflectivities for sediments consisting of various grades of mud, sand, and shell fragments ranged between 4% and 12% with a median of approximately 9%. Significant bottom vegetation was present in neither test site. Future testing of the system will be planned for bottoms populated by various forms of broad and narrow leaf plants. It is expected that various types of vegetation will attenuate the bottom signal or cause a shallow bias in soundings.

Sunglint proved to be no problem in AOL testing, because scanner off-nadir angles were not large enough to permit viewing of the glint pattern at the 38° latitude of the test sites. For low latitudes, noon-time summer operations might be difficult, and a system with larger scan angle could experience a glint problem.

Results:

Accuracy is divided into two basic measures: precison and bias. Precision is a measure of self-consistency and is related to random noise, while bias errors are determined by comparison with an external "standard" and are fixed offset or "systematic" errors.

A mean precision of 4-5 cm for data with reasonable signal strengths was observed during a low wind/wave test (without wave correction) with a 15° offnadir scan angle. This value compares favorably with simulation results (Ref. 13) undertaken to derive a model of expected system performance based on laser pulse width and shape, charge digitizer gate width, photon arrival rates, pulse detection algorithms, and similar matters. At low bottom return signal strengths (several times the minimum detectable limit) the precision may typically increase into the 10-20 cm range (trending as predicted by the simulation). Because of limitations in the AOL altitude intervalometer (minimum discrete jumps of 15 cm, as operated), the mean precision for wave corrected data generally has a minimum of about 10 cm. Wave correction thus adds about 5 cm error to the optimum performance level, but on the other hand performs admirably for the more usual case where wave heights above 10 cm predominate.

A bathymetric survey of the Tangier Sound flightline was conducted by an NOS vessel from the Atlantic Marine Center utilizing standard, automated, acoustic techniques. Horizontal control for this survey was a line-of-sight, high frequency electronic positioning system with ground stations. Tide control was furnished by three continuously recording NOS tide gages at appropriate locations. Navigation and positioning of the aircraft were accomplished with the tracking radar and plot-board capabilities available at NASA/Wallops Flight Center. Radar data, smoothed with a Kalman filter program to provide the highest possible accuracy, are merged with AOL data offline during processing.

Fully automated comparisons of AOL soundings with NOS acoustic soundings are not yet available (though pending), and the comparison has consequently involved comparisons of several data sets by hand--a tedious task. Results in general are encouraging. Datum free comparisons of laser and acoustic bottom profiles yield mean RMS deviations in the range of 5-15 cm. With appropriate datums applied, however, distinct biases of about 30 cm have been observed in several cases. Careful analysis of the data indicates no apparent fault with the basic techniques, and hardware anomalies are suspected. Ground test data (from simulated bottom and surface targets), presently being analyzed to test this hypothesis, appear to contain somewhat similar inconsistencies. Biases as a class are generally causal and hence correctable; the high "precision" noted in the data is considered to be a better measure of system performance at this point in time. Ultimately, biases of less than

approximately ± 15 cm are desired. Detailed error budgets, calculated for the AOL and for an optimized design (Ref. 14), indicate that this is a quite reasonable goal in the reasonably shallow coastal waters of interest.

Conclusions:

1) The feasibility of obtaining high precison (5-20 cm) bathymetric soundings in a typical operational environment with a scanning airborne lidar system has been confirmed.

2) Excellent penetration ($\bar{\alpha}$ D≅12-15) of typical coastal waters has been achieved with a relatively low power laser.

3) Performance in the scanning mode at off-nadir angles up to 15^{o} is satisfactory for performing bathymetry.

4) The operational window for various sytem variables and environmental parameters is not unduly restrictive and should not lead to unreasonable misson constraints.

5) The mean precision of AOL soundings is excellent (typically less than 20 cm) and predictable with an existing model.

6) Biases of up to 30 cm presently noted in a limited number of soundings are slightly greater than NOS accuracy standards but are expected to be explainable (in terms of hardware instabilities) if not correctable. Such biases are not expected to appear in a well designed system.

7) Wave correction using altitude intervalometer data has been successfully demonstrated for non-scanning data. Further work is required to extend this result to scanning data.

8) Sophisticated peak detection and location software has been developed and is performing well in low signal-to-noise ratio conditions.

3. Cost Benefit Analysis

Technological advances, of themselves, do not provide a rationale for replacement of existing techniques. Significant benefits must be demonstrated before a major realignment may be seriously entertained. Before embarking on the AOL field test program, NOS sponsored a preliminary investigation (Ref. 15) of the predicted survey costs involved with scanning airborne laser hydrography compared to estimates of present expenditures. The conclusions reached in this study indicated that an airborne laser system appears to offer significant cost reduction potential.

With the growing success of AOL test activities, significant refinements of the airborne laser hydrography costs were dictated. As a result, a computerized cost model was developed by GKY & Associates (Ref. 16) to permit rapid iteration with varying inputs, and sensitivity analysis for identification of the most significant of the cost contributors. The beauty of this approach is that controversies over appropriate inputs can easily be evaluated for their meaningfulness, and impact on the final costs is clearly resolved. At the same time, the benefits accrued from such a system must be identified; for, ultimately, the cost benefit ratio for the system within its expected operational and physical environments will dictate managerial actions.

The study was aimed at defining capital, operational, and total survey costs estimated on a cost per square nautical mile basis. Capital costs include purchasing of aircraft, laser systems, horizontal control equipment, and the like. Operational costs include salaries, maintenance, and expendables. Survey costs are expressed as functions of annual costs, survey coverage rate, and total yearly flight hours over the target. Outputs are "first" (capital) costs, amortized first costs, operational maintenance, total annual costs, unit operaging costs, and unit total cost. The cost model is made most useful for decisions by additionally presenting unit costs as a function of chart production rate.

The sensitivity analysis, including 19 parameters, is based on a $\pm$ 10% change in individual inputs. A 95% confidence range for unit costs is also estimated. The input parameters having the greatest impact on unit costs (ranked in descending order) are coverage rate, flight time over target (tie), overtime/difficulty factor, aircraft dedication factor, and crew dedication factor.

Because the survey coverage rate strongly impacts the overall analysis, an in-depth study of its physical attributes was conducted. Survey rate relates to operational flight techniques as dictated by physical characteristics of the survey area. The key parameter in coverage rate determinations was defined as the ratio of water surface area to total miles of shoreline (A/S) for a given study area; twenty case study areas were selected covering the entire East Coast and Gulf Coast (from Maine to Texas) and the five Great Lakes. A "typical" and a "difficult" area were then selected for specific analysis (Oregon Inlet, North Carolina and Tangier Sound of Chesapeake Bay, respectively).

Flight geometry was then determined (for the assumption of 20% overlap of swath width) by identifying typical values for altitude, speed, distance between tracks, laser pulse rate, scan angle, aircraft turning radius, etc. The areal coverage rate was then derived by dividing the water surface area to be surveyed for the selected regions by the sum of the times required to make all the turns and fly the total number of flight tracks plus 15% extra for overhead. The results of the study indicate coverage rates (square nautical miles per hour) as follows: "typical" coastline, 7.4; "smooth" coastline, 8.3; "irregular" coastline, 4.5. The mean value between smooth and irregular coastlines, 6.4 nmi^2/hr, is close to the typical value (on the conservative side) and was utilized for the subsequent modelling with a $\pm$ 30% range based on the twenty case studies.

Annual chart production (the product of coverage rate and time over target) potential for this system was estimated (based on the 6.4 nmi^2/hr) at 1920 square nautical miles per year. The resultant data could easily overwhelm the verification process (which today typically handles the equivalent of about 400 square nautical miles per year) if appropriate upgrading is not accomplished. This possibility led to the inclusion of chart production rate as a functional in the analysis which is based on two situations providing upper and lower bounds on "realistic" operations. These two cases are: 1) the assumption that the laser/aircraft system is completely dedicated, and that as chart production is reduced, men and equipment will be idle (a completely dedicated system); and 2) the assumption that the aircraft and its crew and the laser system crew can use all the free time on other projects (a completely shared system). Figure 1 presents model results as total unit cost (dollars per square nautical mile) as a function of chart production (square nautical miles per year) for these two extremes along with 95% confidence bounds.

As previously noted, lack of water clarity in the coastal waters has great potential for hindering short-term laser bathymetric survey operations. Consequently, the study addresses operational success probabilities on a regional basis for the specified study areas as well as a detailed look at the "typical" Oregon Inlet (North Carolina) site. Probability of successful bottom returns was calculated as the product of the probabilities that the wind was between 5 and 20 knots, that there was no precipitation, that there was no ice cover, and (based on data from the EPA STORET files) that water clarity was sufficient for operation at a 5.5 meter depth. Results for the various areas ranged between 14% and 65% with a 35% mean. Because the planned aircraft utilization factor is only 3.4%, this would seem to be more than adequate for operational purposes. The result is that while water clarity may permanently preclude operations in certain limited areas, the problem is basically one of scheduling flights at appropriate times.

Results of the cost model indicate that baseline utilization of the system (1920 nmi^2/year) should result in a mean estimated cost of $422 per square nautical mile ($\pm$ 33%). As seen in Figure 1, unit survey costs based on lower production volumes can be significantly reduced by sharing the aircraft and crew with other programs. Cost estimates for present near-shore acoustic hydrography range from $1000 to $10,000 per square nautical mile; the authors' estimate is $5000/$nmi^2$. It is evident that, from this standpoint, the development and use of an airborne laser system is a substantially more cost effective technique for acquiring bathymetric information for chart production purposes than the launch-borne sonar system presently in use.

The cost model will be refined as better estimates are developed for the various parameters. Many of the inputs are certainly open to question, and other values may easily be substituted to investigate their overall impact on this result. The magnitude of the difference between the two systems is so great, however, that it is considered unlikely that the conclusion will change.

4. Limited System Design

The AOL system was designed, built, and tested as an unrefined, multi-role scientific tool, not as a bathymetric prototype. The characteristics of such a prototype are vital to the cost benefit study, to aircraft requirements, and to risk assessment as part of the technical extrapolation phase of the NOS Laser Hydrography Development Project. A "Limited System Design" (Ref. 14) was conducted by AVCO Everett Research Laboratory to provide a basic functional design, sizing, cost, and risk assessment for a typical bathymetric prototype, but not a detailed design for fabrication. The design included as many AOL results as were available at the time as well as performance simulation predictions.

Major areas of emphasis in the design were the sizing of the system to fit a small aircraft -- the system design was configured for the cabin of a Beechcraft "King Air" 200T -- and the selection of a prime laser candidate. The choice of a laser was based on expected availability in a 3-5 year time frame. Three lasers (neon, copper vapor, and frequency doubled Nd:YAG) were rated within 13 categories such as peak power, pulse repetition rate, pulse duration, wavelength, efficiency, volume, weight, power requirements, scalability, projected reliability, and development risk. Although copper vapor offers promise farther in the future, the frequency doubled Nd:YAG laser was clearly the preferred instrument for this application.

Other items covered at length were optical system design; scanner configurations; electronics system design; data acquisition, processing, display, and storage; navigation and positioning requirements, including attitude monitoring unit and an error budget model; signal to noise ratio required for chosen detection and false alarm probabilities; and eye safety.

5. Present Program

The original questions asked in the laser hydrography evaluation were: can an airborne laser hydrographic system collect bathymetric soundings meeting NOS vertical accuracy standards in a routine, operational manner, and is it cost effective? The AOL flight tests, Cost Benefit Analysis, and Limited System Design were directed at those questions. Because the preliminary results are favorable, the NOS Laser Hydrography Development Project has broadened its scope to address other questions needed for a complete evaluation of the technique. These remaining areas of study can be categorized as technical, economic, operational, and impact.

The technical evaluation tasks address vertical accuracy, horizontal accuracy, and environmental constraints. The vertical accuracy work is a continuation of the investigations, described earlier in this paper, of the accuracy of AOL bathymetric soundings. In the horizontal accuracy tasks, the ability to assign geographic coordinates to each sounding within NOS horizontal accuracy standards will be determined. The ability to navigate an aircraft along preselected flight lines with sufficient accuracy for optimal coverage will

also be tested. The environmental constraints task will yield an estimate of the total area surveyable by laser under the constraints of depth, water clarity, bottom composition, vegetation, and weather. A model for predicting when local environmental conditions are satisfactory for surveying will also be developed. Such a model is considered necessary for laser bathymetry to be worthwhile.

The economic evaluation tasks continue the investigation of cost benefits arising from the use of an airborne laser hydrographic system. To better determine those benefits, refined operating cost estimates for both the existing acoustic systems and for the laser system are being developed. The refined estimates will be used in a model of operating costs which describes the total cost to survey an area using any combination of systems. With this model, costs and cost savings should be predicted realistically. Such a model also permits determiantion of the optimum mix of systems, based on economic grounds, for inclusion in the NOS inventory.

The operational tasks address utilization problems expected with an airborne laser hydrographic system. Through an operational scenario, such problems will be anticipated to insure that the systems benefits are not degraded through operational constraints. Also to be considered are operational tools, such as real time data quality indicators, which should be demonstrated before a system is acquired.

Finally, the project will consider the impact of an airborne laser hydrographic system on other activities in NOS. The major such impact anticipated will be in the data processing and chart production system. At nearly one billion soundings per year, the laser system will surpass NOS' ability to verify, process, store, and convert the data into charts with present techniques. Determining how this mass of soundings can be appropriately handled without choking the data processing and chart production system will be a major factor in the desirability of a laser hydrographic system for NOS. Other impacts to be considered are: impact on the existing hydrographic fleet; impact of new capabilities and applications made possible by a laser system; impact of sharing an aircraft with another activity; and determination of survey requirements in areas chartable by laser.

Once the technical, economic, operational, and impact analyses are completed, NOS will have a complete evaluation of the capabilities, benefits, and impacts of an airborne laser hydrographic system. On the basis of this evaluation, NOS will decide whether or not to commit resources to establishing a major new technology.

References

1. Kim, H., P. Cervenka, and C. Lankford, "Development of an Airborne Laser Bathymeter," NASA Technical Note TND-8079, October 1975.

2. "Laser Hydrography User Requirements Workshop Minutes," edited by L.R. Goodman, NOAA; January 1975.

3. "Minutes of the Laser Fluorosensor Workshop," NERC/Las Vegas, S.R. Melfi, Chairman, February 1975.

4. "Laser Hydrography Technical Review Workshop Minutes," edited by L.R. Goodman, NOAA; August 1976.

5. "Presentation for Airborne Oceanographic Lidar System Applications Workshop Seminar," AVCO-Everett Research Laboratories, Inc., December 1976.

6. "Laser Hydrography Development Project Plan, A Working Document," L.R. Goodman, February 1977.

7. Swift, R.N., "Preliminary Report on Pre-Flight Seatruthing for the Airborne Oceanographic Lidar Project," prepared for NASA/Wallops Flight Center, February 1977.

8. "Airborne Oceanographic Lidar System," NASA Contractor Report CR-141407, prepared under contract # NAS6-2653 by AVCO-Everett Research Laboratory, Inc., October 1975.

9. Jerlov, N.G., Optical Oceanography, (Elsevier, Amsterdam), 1968.

10. Witt, A.K., et. al., "Air/Underwater Laser Radar Test Results, Analysis, and Performance Predictions," Naval Air Development Center Report #NADC-76005-20, January 1976, (Report is classified "CONFIDENTIAL").

11. Shannon, J.G., "Correlation of Beam and Diffuse Attenuation Coefficients Measured in Selected Ocean Waters," SPIE Ocean Optics, Vol. 64, p. 3, 1975.

12. "Airborne Oceanographic Lidar Post-flight Bathymetry Processor Program Documentation, Version 4.0," K. Borman, EG&G/WASC Planetary Sciences Department Report #004-78, March 1978.

13. "A Quantitative Analysis of Errors in the Interpretation of AOL Charge Digitizer Output," R.W.L. Thomas, EG&G/WASC Report #4820-10, January 1977.

14. "Airborne Hydrography System Limited Design Report," prepared under contract #7-35373 for NOAA/NOS by AVCO-Everett Research Laboratory, Inc., January 1978.

15. "Laser Hydrography Analysis (A Cost Comparison Study)," prepared under contract for NOAA/NOS by GKY & Associates, Inc., January 1977.

16. "Cost Benefit Analysis Study of Airborne Laser Hydrography," prepared under contract #7-35364 for NOAA/NOS by GKY & Associates, Inc., February 1978.

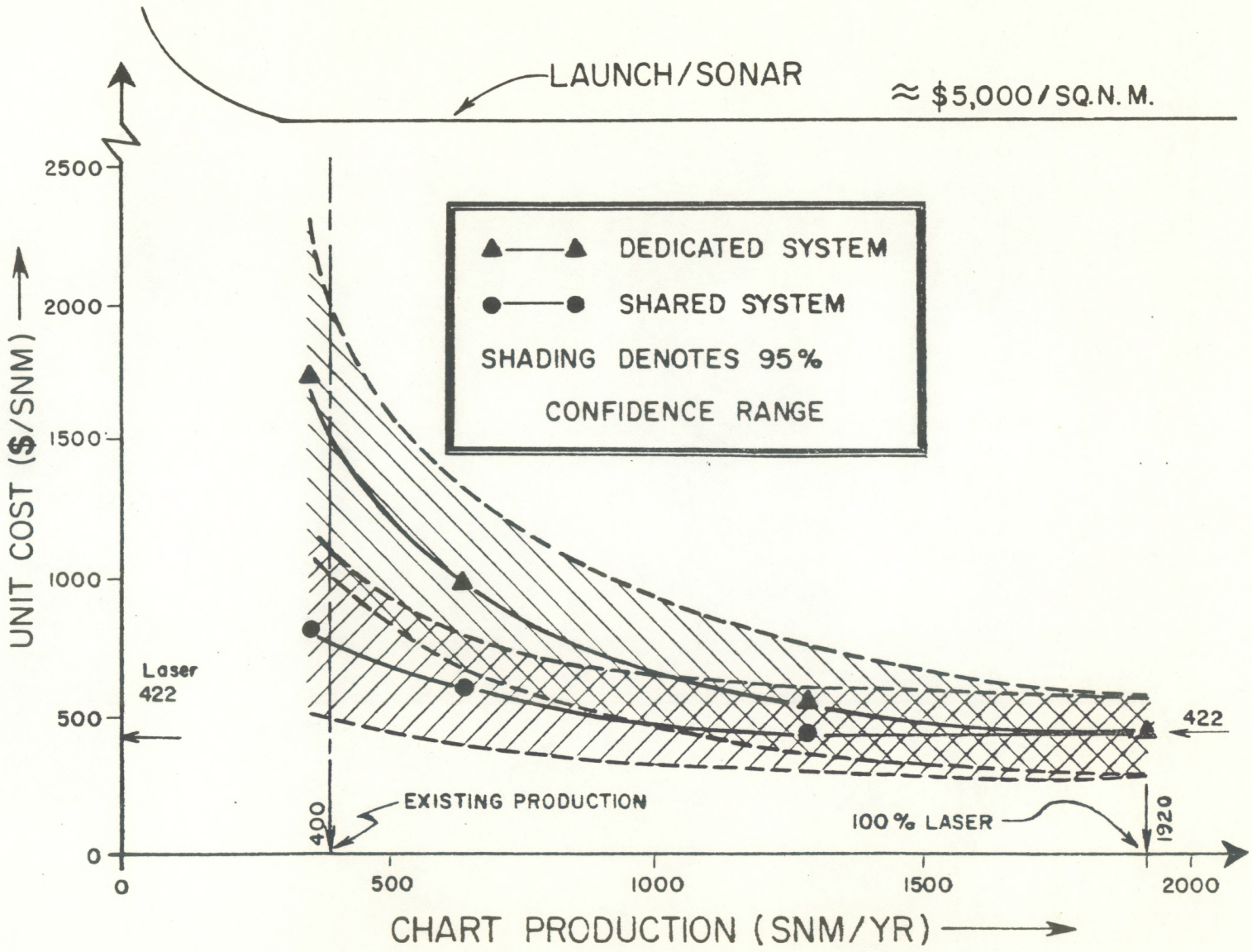

LASER UNIT COST vs. PRODUCTION

FIGURE 1

LASER HYDGROGRAPHY

Lowell R. Goodman, LCDR, NOAA
National Ocean Survey
Engineering Development Laboratory
6001 Executive Blvd.
Rockville, Maryland 20852

Lt. Cdr. Goodman, an officer in the National Oceanic and Atmospheric Administration Commissioned Corps, has a B.S. in Electrical Engineering from the University of Arkansas. For the past nine years he has been active in the area of remote sensing, ranging from tidal currents development work to a laison assignment with the National Aeronautics & Space Administration on a geodetic/oceanographic satellite (GEOS-C) to project manager of the Laser Hydrography Development Project.

ABSTRACT

The Engineering Development Laboratory of the National Ocean Survey has, for the past two years, been actively engaged in the evaluation of the "technique" of airborne laser hydrography. Through the rigorous adherence to an overall project plan and associated follow-up flight test plan, the project team has completed a series of paper studies, modeling efforts, software development, data acquisition flights, and data analyses focused as a total systems approach to the complex problems posed by the technique of potential airborne laser hydrography. This paper summarizes the NOS Laser Hydrography Project and highlights the flight test results as well as operational bounds of the laser hydrography "technique".

1.0 INTRODUCTION

The evaluation of airborne hydrography by the National Ocean Survey over the past couple of years has been directed toward the following two project objectives:

- Determination of the capability of an airborne laser system to meet the NOS vertical accuracy requirements, and
- Assessment of the cost/effectiveness of a realizeable NOS operations oriented system.

In order to address the first objective NOS was fortunate to have been able to use the NASA funded Airborne Oceanographic Lidar (AOL)* developed under their Advanced Applications Flight Experiments (AAFE) program as an "engineering model" for field testing and evaluation. These field tests were a cooperative effort involving the National Ocean Survey, the Naval Oceanographic Research and Development Activity, and the National Aeronautics and Space Administration.

---

* Refer to the previous paper, Airborne Oceanographic Lidar System Description, Joe Nunes, AVCO Everett Research Laboratories, Inc. for AOL system details.

2.0 PROJECT STRUCTURE AND DOCUMENTATION

The NOS Project was structured around the flight testing of the AOL mounted in the NASA C-54 aircraft. Both the overall aspects of the NOS project and the detailed technical approach for each of eight specific tasks are documented in the Laser Hydrography Development Project Plan, Lowell R. Goodman, February 1977. The eight tasks within the project are:

1. Cost Comparison Study
2. Flight Test and Data Analysis Planning
3. Experimentation Software
4. Flight Tests
5. Experimental Data Analysis
6. Performance Characterization
7. Technical Extrapolation
8. Cost Benefit Analysis

The major findings and conclusions of these eight tasks are given in three separate reports. These are:

- Laser Hydrography Project Summary (report in progress)
- Airborne Hydrography Limited Design Report
- Cost Benefit Analysis Study of Airborne Laser Hydrography

The Laser Hydrography Project summary, as the name implies, covers key aspects of the entire project with emphasis on preliminary results and conclusions from the flight experiments (tasks 4, 5, and 6 above).

The Airborne Hydrography System Limited Design Report addressed the technical extrapolation task (task 7) of the project and was based on a performance assessment of the AOL system. The primary objective of the design study was to optimize the projected performance of an NOS operations oriented system, while, at the same time minimize development risks.

The Cost Benefit Analysis Study of Airborne Laser Hydrography fulfilled the requirements for a final cost benefit study (task 8). This study followed an earlier preliminary cost comparison study (task 1) and tackled the difficult task of quantifying the various cost factors to arrive at dollars per square nautical mile of hydrography.

3.0 FLIGHT TEST REQUIREMENTS

The actual flight tests and associated "sea truth" efforts were driven by a detailed flight test plan (task 2) and centered around the following set of scientific objectives:

- Validate feasibility of the "technique" of laser hydrography.
- Determine the overall vertical system error under a bounding range of system variables and parameters; correlate error contributions to variables and parameters.
- Quantify system and environmental usage constraints.
- Model all major contributions to the signal equation to provide a sound basis for extrapolation of these results to the design specifications of an NOS operations oriented system.

In order to thoroughly address the science objectives, a complete set of "independent" and "dependent" variables and parameters were defined. The "independent" variables chosen for investigation are: water depth, water clarity, wind speed, wave height, solar illumination, bottom character, aircraft altitude, receiver polarization, receiver field of view, transmitter beam divergence, and scanner off nadir angle. The "dependent" variables studied for effects of the above are: hit probabilities, accuracy (precision and bias), repeatability, extinction coefficients, minimum resolveable depth, surface and bottom return signal strengths, noise levels, and pulse detection algorithms.

A wide variety of ancillary supporting data was required for each mission in order to permit quantitative description of system performance and environmental bounds. Vertical control consists of standard NOS hydrography and tide control. A hydrographic survey of the Tangier Sound flightlines was conducted in December, 1977 by NOS personnel using standard automated acoustic techniques and the normal microwave, line of sight electronic positioning system for horizontal control. Navigation and positioning of the aircraft were accomplished with NASA C-band radar and their associated real-time plot boards. Water clarity measurements were made with a narrow beam transmissometer as well as a secchi disc. The wind field structure at various levels was recorded at Wallops Island and visual estimates of wind and sea conditions were taken on the flightline along with the water clarity data. A total of over one hundred sea truth "cruises" were made in support of the project with all data from each cruise cataloged in computer card image format.

The scientific data requirements dictated the development of two separate test sites. The primary site was at Winter Quarter Shoal, located approximately 8 nautical miles east of the island of Chincoteague, Virginia. The secondary site consisted of several flightline configurations in the Tangier Sound area of Chesapeake Bay just west of Crisfield, Maryland. These dissimilar sites provided the opportunity to investigate the effects of diversity in water clarity, depth, wind, and surface wave structure. Both sites were within a 25 nautical mile radius of the NASA Wallops Island radar tracking facility.

4.0 FLIGHT TESTS

A typical mission (flight) lasted one to two hours and consisted of 10 to 15 passes over a pre-determined flightline. A detailed plan was written for each mission which attempted to optimize the combinations of variables and parameters for which data was to be taken. The data base for each mission includes a mission plan, the AOL system output tape, a digitized flight log of equipment settings, a digitized sea truth data log, filtered radar tracking tapes, pre and post flight ground calibration data, measured tide correctors and voice annotated video tape from a down looking video camera.

Throughout the user flight test phase which ran from September 1 through December 16, 1977, a total of 12 missions were flown. These missions accumulated 400 minutes of laser data in 161 passes over preselected flightlines. This translates to 5,000,000 soundings (or 1000 linear nautical miles).

5.0 DEEP WATER CALIBRATION

One of the problems encountered in the project was that of excessive systematic noise which masked the bottom return signal. A major noise source was the bank of charge digitizers which were used to slice each laser return into 40 time bins of 2.5 nanoseconds each. This was not totally unexpected, since this area of high pulse repetition rate (PRR) and narrow time bin digitizing was one in which the state of the art in hardware at the time of the AOL design was pushed to the limit.

The solution to the noise problem evolved into what is now referred to within the project as the deep water calibration. In simplistic terms, this process consists of building a calibration matrix from data taken over water too deep to "sound" the bottom and then applying the appropriate calibration vector from this matrix to each laser return. In this process the choice of the vector to be used is based on the amplitude of the surface return. The various bottom detection algorithms are then applied to the residual between the calibration vector and the raw signal return.

As a result of the deep water calibration procedure, both system and environmental systematic noise were significantly reduced. Excellent resolution of bottom returns were thus achieved even for very weak signals approaching the digitization limit of the system. With these calibration procedures applied, typical bottom profile precision is 20 cm or better, and approaches 6 cm with stronger signals. In addition this technique provides an effective means of "pulling" the bottom out of the trailing edge of the surface return for the very shallow water cases. Results to date show the capability of consistently recording depths as shallow as 30 cm.

6.0 DATA PROCESSING

The application of the above mentioned calibration procedures and the correlation of the laser and supportive data requires a variety of complex computer software packages.

The primary analysis program, the "processor", unpacks the AOL data tape, identifies the surface and bottom return, and quantifies their location and amplitude under control of a highly parameterized, selectable tracking algorithm, performs wave height corrections, prints and plots altitudes, depths, waveforms, and statistics, and supplies regressions and correlation values for all combinations of eleven chosen parameters.

7.0 BOUNDS

In order to determine the operational feasibility of an airborne laser, the environmental and system bounds must be determined. Two of the eight project tasks which addressed these bounds were the performance characterization (characterization of the AOL) and the technical extrapolation (estimated bounds of the "technique") tasks. Tables 1 and 2 summarize these bounds.

Table 1
AOL SYSTEM ENVIRONMENTAL BOUNDS
(PERFORMANCE CHARACTERIZATION)

Wind	-	2 kts to 10 kts. tested
Sun Angle	-	sun glint not a constraint
Cloud Cover	-	supresses background noise (aids technique)
Altitude	-	500 - 2000 ft.
Incidence Angle	-	15° half angle
Precipitation	-	will likely prohibit operations (untested however)
Night Operations	-	provides optimal conditions; maximum available power; and best signal to noise ratio conditions (narrow band filter not required)
Penetration	-	$\alpha D \approx 6$ to 12 (1.5 to 2.0 times secchi depth)

Table 2
EXTRAPOLATED TECHNIQUE OPERATIONAL BOUNDS

Wind	-	0 to (10 - 20 kts.); depends on fetch
Sun Angle	-	sun glint not a constraint
Altitude	-	500 - 3000 ft. (driver by power; inversely proportional to the square of the altitude)
Incidence Angle	-	25° half angle
Precipitation	-	will likely prohibit operations
Cloud Cover	-	suppresses background noise (aids technique)
Night Operations	-	provides optimal conditions; maximum available power; and best signal to noise ratio conditions (narrow band filter not required)
Penetration	-	$\alpha D \approx 15$ to 18 (3 to 4 times secchi depth)

From a technical standpoint, and outside the scope of this paper, there are a multitude of factors which affect (qualify and further quantify) each of the numbers in both tables. However, in the generation of these numbers, the project attempted to be conservative in that the numbers quoted could be deemed operational bounds, i.e., conditions under which at least 90% probability of acceptable bottom returns could be expected.

8.0 CONCLUSIONS

The feasibility of obtaining high precision swath type bathymetric soundings with an airborne scanning laser system in typical NOS charting environments has been confirmed. This conclusion is particularly strengthened by the excellent penetration ($\alpha D \approx 15$) of coastal waters achieved with relatively low laser output power. Additionally the low signal to noise ratio conditions precipitated the development of a variety of bottom detection and location algorithms which will be advantageous to future designs.

In summary, the project's total systems approach to the laser hydrography problem has moved the technique from the technically feasible state to the operationally feasible state, thus putting within reach, a step function in hydrography at least equal to the transition from "lead line" to acoustic fathometer.

REFERENCES

1. "Laser Hydrography Development Project Plan," a working Document," L. R. Goodman, February, 1977.

2. "Laser Hydrography Analysis (a cost comparison study)," prepared under contract for NOAA/NOS by GKY Associates,Inc. January, 1977.

3. "Laser Hydrography User Requirements Workshop Minutes," edited by L.R. Goodman, NOAA; January 1975.

4. "Airborne Oceanographic Lidar System," NASA Contractor Report CR - 141407, prepared under contract #NASA-2693 by AVCO - Everett Research Laboratory, Inc. October, 1975.

5. "Airborne Hydrography System Limited Design Report," prepared under contract #7-35378 for NOAA/NOS by AVCO - Everett Research Laboratory, Inc. January 1978.

6. "Airborne Oceanographic Lidar Post-flight Bathymetry Processor Program Documentation, version 4.0," K. Borman, EG&G/WASC Planetary Sciences Department Report #004-78, March 1978.

7. "Laser Hydrography Technical Review Workshop Minutes," edited by L.R. Goodman, NOAA, August 1976.

8. "Cost Benefit Analysis Study of Airborne Laser Hydrography," prepared under contract #7-35364 for NOAA/NOS by GKY & Associates, Inc., February 1978.

9. "Preliminary Report on Preflight Seatruthing for the Airborne Oceanographic Lidar Project," prepared for NASA/Wallops Flight Center, February 1977.

10. "A Quantitative Analysis of Errors in the Interpretation of AOL Charge Digitizer Output," R.W.L. Thomas, EG&G/WASC Report #4820-10, January 1978.

BATHYMETRY INTERCOMPARISON: LASER VS. ACOUSTIC

Gary Guenther
NOAA/National Ocean Survey
EDL, C61
Rockville, Maryland 20852

BIOGRAPHICAL SKETCH

Mr. Guenther is Chief Scientist for the National Ocean Survey's Laser Hydrography Development Project. In his four years with NOS he has also headed projects dealing with underway water sampling and remote buoy tracking. After obtaining B.S. and M.S. degrees in engineering and physics respectively from Northwestern University, he joined the National Security Agency with which he had already gained several years experience as a co-op student. There he engaged in research and development on mass memory computer architecture, holographic optical correlator, and electron beam interactions with materials before joining NOS.

ABSTRACT

Airborne Oceanographic Lidar (AOL) bathymetric results are examined and compared to a standard National Ocean Survey (NOS) automated acoustic hydrographic survey. Spatial data densities, horizontal control, pulse detection and tracking, beam spreading, extinction depths, and wave correction techniques are discussed. Precision, profile correlation, and bias are presented along with precision predictions from a Poisson simulation of the hardware configuration.

INTRODUCTION

The Airborne Oceanographic Lidar (AOL) scanning, pulsed laser system, built by AVCO Everett Research Laboratory Inc. (Ref. 1) for the NASA Advanced Applications Flight Experiment (AAFE) program, and the National Ocean Survey (NOS) Laser Hydrography Development Project (Ref. 2), dedicated, in part, to field testing this instrument, have been discussed in detail in the two preceeding papers. The AOL was designed in a compromise configuration which permits either lidar bathymetry or active fluorosensing to be conducted at the advanced research or preliminary development level. Because of its unique dual nature, it was not possible to optimize performance in either mode separately. Because of the recognized inherent limitations of the AOL, the technical evaluation of the general "technique" of laser bathymetry for application to NOS requirements was broken into two parts: evaluation of results from AOL field test data and extrapolation of these results, via analytic models and computer simulations, to the ultimate expected performance of the "technique".

The primary goals of AOL flight testing were the determination of vertical accuracy and operational usage constraints over a wide range of systems variables and environmental parameters. In this paper the extremely promising preliminary results of the AOL bathymetric field test are presented and concluded with brief comments on technical extrapolation.

AOL BATHYMETRY TESTS

Preliminary:

Site selection for the AOL field tests (Ref. 3) was based on the following criteria: depths must range between one and ten meters; a combination of both flat and relatively high relief topography is preferred; radar tracking of the aircraft is imperative due to poor performance of the LTN-51 Inertial Navigation System; the sites must be logistically easy to reach by both aircraft and ground support vessels; the area must have suitable tide "control"; typical water clarities must be appropriate to permit penetration to the bottom over sufficiently long portions of a flightline; and adequate meteorological support should be available 24 hours in advance for daily mission go/no-go decisions.

Two test sites meeting these requirements were selected: one in the Atlantic Ocean over Winter Quarter Shoal (several miles offshore from Assateaque Island), and one in Chesapeake Bay -- Tangier Sound between Jane's Island and Smith Island. These dissimilar sites provided the opportunity to investigate the effects of diversity in water clarity, depth, wind, and surface wave structure. The probability of successful missions in the Wallops Island vicinity based on precipitation, fog, and wind speed data from histrocial records was calculated and found to be acceptable (Refs. 3 and 4).

A wide variety of ancillary supporting data was required for the flight tests in order to permit quantitative description of the system performance and the environmental restrictions on the operational window. The performance of the AOL is limited primarily by the product of water depth and optical attenuation coefficient. The latter is, for a given location and season, modulated temporally by wind, waveheight, precipitation, and currents; also affecting performance are such things as bottom reflectivity and solar illumination. These parameters interact with system variables such as receiver field-of-view, altitude,

scanner angle, and beam divergence to yield a complex set of interactions which must be unraveled to permit the quantization of specific effects. Primary support data acquired in conjunction with the flight tests include vertical control, horizontal control, water clarity, sea surface conditions, meteorology, and bottom reflectivity.

In 1977, 18 missions were flown with a total of 161 separate passes for an estimated total distance of 1000 linear nautical miles and 400 minutes of recorded data comprised of five million soundings. Aircraft speed was maintained at approximately 150 knots with altitudes ranging from 150 to 600 meters. Missions were flown in river, bay, and ocean waters, in summer and winter, clear and cloudy, night and day, for winds from 0 to 15 knots, with and without capillary waves, in water clarities with narrow beam attenuation coefficients varying from less than $1m^{-1}$ to greater than $4m^{-1}$, and with water depths from 0 to over 10 m. At this point only a fraction of the data has been analyzed in depth.

Performance Constraints:

"Independent" variables and parameters chosen for investigation during the test phase are: water depth, water clarity, wind speed/wave height, solar illumination, bottom character, aircraft altitude, scanner off-nadir angle, receiver field of view, and transmitter beam divergence. "Dependent" variables studied for effects of the above are accuracy (precision, profile correlation, and bias), repeatability, hit probabilities, extinction coefficients, system attenuation coefficients, minimum resolvable depth, surface return signal strengths, bottom return signal strengths, noise levels, and detection algorithms.

Bottom returns as low as 100 nanowatts can be tracked successfully. Surface returns range from ten to several hundred times larger. Probability of a successful surface return under most circumstances approaches 100% rapidly as the mean surface return signal strength reaches several times the trigger threshold. Typically for the AOL this occurs at about 2.5 microwatts optical power into the scanner. A glassy or mirror-like water surface during totally calm wind conditions causes the surface return probability to decrease while the dynamic range of amplitudes and overall mean amplitude increase. Operation under these conditions would not be recommended.

Next to accuracy, penetration capability is probably the most important performance parameter for a laser bathymetric system. The maximum penetration depth, in general, is dependent on a large number of variables and parameters including laser wavelength and power, altitude, water clarity, bottom reflectivity, off-nadir angle, receiver aperture, receiver field of view, receiver sensitivity, noise sources, and many more (Ref. 1); but for a given (appropriately designed and operated) system, the ultimate concern is water clarity. The AOL bathymetric laser configuration uses neon gas to produce a green (5401 Å) pulse which falls very near the minimum diffuse attenuation coefficient for coastal waters (Ref. 5).

The reduction in bottom return signal strength with increasing depth can be described by the expression:

$$SSB \sim e^{-2kD}$$

where

SSB = bottom signal strength,

D = depth, and

k ≡ "system" attenuation coefficient as defined by this expression.

The coefficient, k, has no particular theoretical basis, but simply provides a straightforward empirical parameter for describing system performance.

It has been established (Ref. 6) that for a sufficiently large receiver field of view, the value of "k" somewhat coincidentally approaches very close to the value of depth averaged diffuse attenuation coefficient ($\overline{K}$) for the water in question. Because of this fact, the product of $\overline{K}$ and the depth beyond beyond which successful returns cannot be detected (D_{max}) is commonly referred to as the "extinction coefficient" ($\overline{K}D_{max}$); and penetration capability is frequently reported in terms of this unitless parameter. In addition, because an apparently linear relationship ($\alpha \cong 5K$) (Ref. 7) exists between diffuse attenuation coefficient (K) and beam attenuation coefficient (α) for water clarities of interest in coastal waters, extinction coefficients may also be reported in terms of $\overline{\alpha}D_{max}$. (AOL results will take this form because most cruise data is for α rather than K).

Calculation of "k" for the AOL (from the slope of ln SSB vs. D curves) resulted in values generally consistent with K. Maximum extinction coefficients observed in processed AOL data are $\overline{\alpha}D_{max} = 12$ during the day and $\overline{\alpha}D_{max} = 15$ at night. The latter was accomplished in December off Janes' Island with $\overline{\alpha} = 2.75m^{-1}$ and $D_{max} = 5.5m$. These results, considered to be excitingly high for such a low power laser, were defined at the maximum extent of high quality data, where hit probabilities remain in excess of 90% and precision (pulse to pulse agreement) remains no worse than 15-20 cm. Because of the sophisticated processing techniques applied to the raw signals, the loss of soundings at extinction tends to occur quite abruptly at bottom return signal strengths not greatly in excess of the minimum hardware digitization level. Projecting these results to a higher laser power system (100-200 kW peak) leads to expectations of $\overline{\alpha}D_{max}$ in the 18-20 range. Such estimates are consistent with independent high power results (K. Petri, Naval Air Development Center, personal communication, 1978).

Wind and wind generated waves (throughout the entire wavelength spectrum from capillaries to off-shore swell) unquestionably influence system performance through a number of interactions, but few are overly significant except at the extremes--considered for our purposes to be 2-20 knots wind speed. Surface return energy from non-nadir scanner angles reaches the receiver only if capillary waves are excited sufficiently to present a large number of tiny facets perpendicular to the beam. These capillaries tend to die out below about 2 knots, and, as noted above, this leads to a reduced hit probability. On the other end of the spectrum, high winds generate waves with sufficient energy and depth to resuspend bottom sediments and decrease water clarity to unacceptable levels. From 2-20 knots, beam spreading through the air/sea interface due to wave slope augmented refraction is not large compared to beam spreading in the water column due to scattering. Surface return amplitudes at higher off-nadir scanner angles actually benefit slightly from higher winds where less variation of amplitude with angle is also noted.

If mean surface return signal strength versus altitude data are

estimated with power law curves, the exponents thus obtained range between 1.0 and 2.0 for altitudes from 150-600m. No correlation between the value of the exponent and any variable or parameter (such as off-nadir angle or wind speed) could be established; rather, the value seems to be a complex function of these plus the direction of the beam relative to the wind direction. The median exponent value observed is approximately 1.3, which indicates that the surface returns generally contain a high specular component, rather than being diffuse in nature (for typical illuminated areas from 0.5-6m in diameter at the water's surface).

The effect of altitude on bottom return signal strength is indirect. The amount of bottom return energy reaching the receiver depends on the fraction of the bottom return energy refracted through the air/sea interface (in the direction of the receiver) within the field of view of the receiver. The factors determining that fraction are water clarity, depth, altitude, wind speed, and receiver field of view. An analytic model has been developed which calculates the field of view necessary to intercept 90% of the potential bottom return energy for specific values of the other parameters. This model is in good agreement with experimental data and can be used for future system design applications.

The off-nadir "scanner" angle affects both surface and bottom return signal strengths. Surface returns at nadir are quite strong and can easily exceed the input capabilities of the system. With increasing off-nadir angle, the returns decrease rapidly in the first five degrees and then much more slowly thereafter. Bottom return signal strength is also highest at nadir but falls off more gradually with increasing angles. A scanner pattern which does not intersect the nadir is highly desirable because it avoids the dynamic range problem caused by the strong nadir surface returns. Although the AOL was configured for a maximum off-nadir angle of 15^{o}, extrapolations of test data indicate that angles of up to 30^{o} or more may not be unreasonable. At such large angles, calculations of a depth bias due to pulse stretching from long slant ranges would become increasingly more important.

The transmitter beam divergence, varied from 2 to 10 milliradians, had virtually no effect on results. The only potential restriction is that the beam must be large enough to provide high surface return probability; resolution is not degraded with a larger divergence because the beam spreading in the water is several orders of magnitude greater.

Dark, muddy bottoms, typical in Chesapeake Bay, caused no bottom detection difficulties. Reflectivities for sediments consisting of various grades of mud, sand, and shell fragments ranged between 4% and 12% with a median of approximately 9%. Significant bottom vegetation was present in neither test site. Future testing of the system will be planned for bottoms populated by various forms of broad and narrow leaf plants. It is expected that various types of vegetation will attenuate the bottom signal or cause a shallow bias in soundings.

Sunglint proved to be no problem in AOL testing, because scanner off-nadir angles were not large enough to permit viewing of the glint pattern at the 38^{o} latitude of the test sites. For low latitudes, noon-time summer operations might be difficult, and a system with larger scan angle could experience a glint problem.

Software:

The tremendous volume of data acquired on even a single pass causes computer analysis to be mandatory. A wide variety of programs on a number of computers have been developed for data verification, reduction display, analysis, and troubleshooting. The primary analytic tool for AOL data analysis is a sophisticated multi-function program called the "Processor" (Ref. 8). Briefly, the Processor unpacks and interpolates the asynchronous system data tape, identifies surface and bottom returns and quantifies their location and amplitude under control of a highly parameterized tracking algorithm, performs wave height correction, prints and plots altitudes, depths, waveforms, statistics, and other requested information, and supplies regressions and correlation values for all combinations of eleven specially selected parameters. An additional program is being developed to automatically compare airborne lidar soundings with corresponding launch acoustic soundings and regress differences against a given parameter set.

Return waveforms from the initial flight tests were badly contaminated with electronic ringing and other spurious but repeatable noise sources whose amplitudes were greater than those of the desired bottom returns. To suppress this noise, a processing technique was developed which subtracts the system response to a surface return in deep water (with no possible bottom return) from the waveforms with bottom returns to yield a "residual" waveform in which only the bottom return pulse (and any uncorrected noise) appears. This subtraction is parameterized on surface return amplitude which drives the system response. Excellent resolution of bottom returns was achieved for even very weak returns approaching the digitization limit of the system (approximately 50 nanowatts at the scanner). An added benefit of this technique is the resultant subtraction of the surface return (and average solar noise and volume backscatter signal as well) which permits resolution of bottom returns at very shallow depths where they might otherwise be masked. Results indicate bottom resolution as shallow as approximately 30 cm.

An altitude intervalometer, operating in conjunction with a surface return detector, triggers the electronics upon detection of the surface return and permits digitization of just the event data--automatically, independent of aircraft altitude. Delay lines are used to permit digitization of the surface return, as well as the bottom return, in the same output vector. (This feature is extremely important, as it allows use of the surface return shape and location for subsequent analysis.) The altitude data is also utilized to facilitate the removal of wave height variations and boat wakes from the depth calculations; this permits correction of the depths to mean sea level.

Precision:

Investigation of the basic sounding accuracy of the system to date has been based on data acquired in the "fixed" or non-scanning mode at various off-nadir angles. This technique permits simple comparisons with acoustic data and precludes additional errors due to possible uncertainties in wave correction procedures. (Scanning data contains large variations in air to sea slant range caused by scanner eccentricity and aircraft roll and pitch.) Wave correction procedures for scanning data, based on careful modeling of the aircraft and scanner parameters, are presently being investigated. Wave correction for non-scanning data is accomplished with a simple averaging technique based on altitude

intervalometer data.

Precision is a measure of self-consistency and is related to random noise. Dominant environmental noise sources for a lidar bathymetric system are solar background reflection in daylight and volume backscattering of the laser pulse in the water column at night. A narrowband interference filter centered on the laser wavelength reduces solar background level by a large factor. AC-coupling in the electronics further reduces this noise source. Volume backscatter has not been particularly evident in the relatively murky waters used for AOL testing because it occurs very close to the surface return, and because the deep water subtraction technique effectively removes it.

An upper bound on the actual system precision under given conditions can be estimated as the lower bound of the RMS deviation of given data about a linear fit to the data over a representative interval (40 points, or about 15 meters of track length). This is true, because this measure also unavoidably includes actual small bottom variations and residual uncorrected wave noise in addition to actual system random noise components. This worst case measure will henceforth be called "precision" for purposes of discussion.

A mean "precision" of 4-5 cm for data with reasonable signal strengths was observed during a low wind/wave test (without wave correction) with a 15^{o} off-nadir scan angle. This value compares favorably with simulation results (Ref. 9) undertaken to derive a model of expected system performance based on laser pulse width and shape, charge digitizer gate width, photon arrival rates, pulse detection algorithms, and similar matters. At low bottom return signal strengths (several times the minimum detectable limit) the "precision" may typically increase into the 10-20 cm range (trending as predicted by the simulation). Because of limitations in the AOL altitude intervalometer (minimum discrete jumps of 15 cm, as operated), the mean precision for wave corrected data generally has a minimum of about 10 cm. Wave correction thus adds about 5 cm error to the optimum performance level, but on the other hand performs admirably for the more usual case where wave heights above 10 cm predominate.

When speaking of AOL depth precision, it must be recalled that the AOL was not conceived with high precision bathymetry in mind. This is evidenced by the following equivalencies of distance (depth) measures related to AOL timing parameters: physical pulse length (7.5 ns) = 84 cm; gate length (4 ns) = 45 cm; gate separation (2.5 ns) = 28 cm. The 10 cm mean precisions quoted are the result of intensive and complex processing software necessitated by the crudeness of the AOL design. This software, however, has performed so successfully that similar techniques are also expected to be applied to the superior hardware of an NOS prototype system.

Bias:

The primary potential causes of bias, or depth offset, in AOL results are pulse stretching and off-nadir angles of incidence and refraction. Pulse stretching results from beam spreading in the water column due to scattering. The effective "cone" half-angle enclosing a fraction (say 90%) of the light incident on the bottom can easily be as much as 45^{o} for $\overline{KD}$'s near extinction. The late arrival at the receiver of light traveling longer paths from the outside fringes of the "cone" results in an increased duration or "stretching" of the bottom return

pulse at the receiver. This in turn can cause a slightly deeper depth indication (dependent on $\overline{KD}$) if it is not understood and compensated. In the second case, off-nadir passage of the pulse through the water column results in a "slant range" slightly greater than the "true" depth. It is ironic that this bias is effectively removed by the aforementioned beam spreading--because off-nadir angles are generally less than 15^{o}, and beam spreading casues some of the off-axis energy to travel down the nadir.

The primary theoretical cause of bias is thus pulse stretching as it distorts (by lengthening) the bottom return pulse. The effect will be at its worst for the case of deep clear water (due to the long "throw" distance). It is expected that this can be successfully predicted, modelled, and removed in the course of data processing.

COMPARISON

Controls:

Vertical control consists of bathymetry and tide control. A high density bathymetric survey of the Tangier Sound flightline was conducted by an NOS vessel from the Atlantic Marine Center utilizing standard, automated, acoustic techniques. Tide control for both acoustic and laser missions was furnished by three continuously recording NOS tide gages at appropriate locations. Horizontal control for this survey was a line-of-sight, high frequency electronic positioning system with ground stations. Positions have an expected uncertainty of 5m.

Two flightlines in the Chesapeake Bay were surveyed. The first extends completely across Tangier Sound between Janes' Island and Smith Island (a distance of approximately 12 kilometers), and the second is centered on a line of buoys (off Janes' Island) approximately 3 kilometers long. The former was accomplished with 25 meter line spacings, while a more concentrated effort on the latter led to roughly 10 meter line spacings on the average. Depths were digitized every six seconds or approximately 25 meters along the tracks, and a continuous low depth resolution analog record was also maintained to investigate major peaks or valleys between digitizations.

Even with such close spacing of "truth" measurements, it is interesting to note that a small (and typical for the area) linear slope of 2^{o} produces a vertical deflection of 0.35 meter (more than one foot) in 10 meters. Practically, this means that a one foot high feature can reside between lines spaced 25 m apart, given only a scant 2^{o} slope. Because of this, the acoustic data, while vital, is not the ultimate in "truth"; and differences between the two systems are classed as "residuals", not errors .

Navigation and positioning of the aircraft were accomplished primarily with the tracking radar and plot-board capabilities available at NASA/ Wallops Flight Center. The on-board LTN-51 Inertial Navigation System was prone to drift and used only for a rough indication of general location (as well as roll and pitch data). The accuracy of real time radar vectoring at the low elevation angles required for the test site location was limited to about $\pm$100m. Visual aids for the pilots, such as buoys, lights, flags, etc., were only marginally successful. Consequently, attempts to fly particular, precisely located flight paths were not generally successful; each pass typically had an individual character and location within the stated bounds. After the missions, radar data

are smoothed with a Kalman filter program to provide the highest possible accuracy. The post flight aircraft position data have an expected uncertainty of at least 10 m. Combining this in quadrature with the 5 m uncertainty from the acoustic bathymetry leads to a combined uncertainty of about 11 m. Because a vertical error of 35 cm can accrue in this distance for only a typical 2^{o} slope, agreement between laser and acoustic data sets to better than 30 cm must be considered a success. Unfortunately, it was hoped to assess the accuracy of the laser system to perhaps the 5-10 cm level. This is still possible, but it could not be expected even if the AOL were a "perfect" system.

Results:

Fully automated comparisons of AOL soundings with NOS acoustic soundings are not yet available (though pending), and the comparison has consequently involved comparisons of several data sets by hand. Results in general are quite encouraging. Datum free comparisons of laser and acoustic bottom profiles yield mean RMS deviations in the range of 5-15 cm (Fig. 1). With appropriate datums applied, however, distinct biases of about 30 cm have been observed in several cases (Fig. 2); while in others (Fig. 3), agreement remains in the 5-15 cm range.

Careful analysis of the data indicates no apparent fault with the basic techniques, and hardware anomalies are suspected rather than, or in addition to, potentially disparate "truth" measurements as previously mentioned. Ground test data (from simulated bottom and surface targets), presently being analyzed to test this hypothesis, appear to contain somewhat similar inconsistencies. Biases as a class are generally causal and hence correctable; the high "precision" noted in the data is considered to be a better measure of system performance at this point in time.

Ultimately, biases of less than approximately $\pm$15 cm are desired. Detailed error budgets, calculated for the AOL and for an optimized design, indicate that this is a quite reasonable goal in the reasonably shallow coastal waters of interest.

CONCLUSIONS

1) The feasibility of obtaining high precision bathymetric soundings in a typical operational environment with a scanning airborne lidar system has been confirmed.

2) Excellent penetration ($\overline{\alpha} D_{max} \cong 15$) of typical coastal waters has been achieved with a relatively low power laser.

3) Performance in the scanning mode at off-nadir angles up to 15^{o} is satisfactory for performing bathymetry.

4) The operational window for various system variables and environmental parameters is not unduly restrictive and should not lead to unreasonable mission constraints.

5) The mean precision of AOL soundings is excellent (typically less than 20 cm) and predictable with an existing model.

6) Biases of up to 30 cm presently noted in a limited number of soundings are slightly greater than NOS accuracy standards but are expected to be explainable (in terms of hardware instabilities) if not correctable. Such biases are not expected to appear in a well designed system.

7) Wave correction using altitude intervalometer data has been successfully demonstrated for non-scanning data. Further work is required to extend this result to scanning data.

8) Sophisticated peak detection and location software has been developed and is performing well in low signal-to-noise ratio conditions.

9) Separate studies indicate that a relatively high powered (200 kW peak), eye safe, lidar bathymetry system can be configured to operate from a small (Beech "King Air") aircraft (Ref. 10) and should provide a significant gain in cost-effectiveness over present acoustic techniques (Refs. 11 and 12).

ACKNOWLEDGEMENTS

AOL bathymetry mode testing could not have been accomplished without the dedication of over forty individuals. We wish to specifically thank Frank Arbusto, Wayne Barbley, Chris Blue, Kurt Borman, Marion Butler, Bob Chase, Earl Frederick, Tom Harmon, Frank Hoge, Doug Mason, Roger Navarro, and Bill Townsend for their assistance, and the aircrew who flew long, tedious missions at low altitude. Finally, we owe a special debt of gratitude to Bill Krabill whose faith, support, and ideas made it all possible.

REFERENCES

1. "Airborne Oceanographic Lidar System," NASA Contractor Report CR-141407, prepared under contract # NAS6-2653 by AVCO-Everett Research Laboratory, Inc., October 1975.

2. "Laser Hydrography Development Project Plan, A Working Document," L. R. Goodman, February 1977.

3. Swift, R. N., "Preliminary Report on Pre-Flight Seatruthing for the Airborne Oceanographic Lidar Project," prepared for NASA/ Wallops Flight Center, February 1977.

4. Scott, R., "Probability of Success of AOL Bathymetry," NOS Internal Report, December 1976.

5. Jerlov, N. G., Optical Oceanography, (Elsevier, Amsterdam), 1968.

6. Witt, A. K., et. al., "Air/Underwater Laser Radar Test Results, Analysis, and Performance Predictions," Naval Air Development Center Report # NADC-76005-20, January 1976, (Report is classified "CONFIDENTIAL").

7. Shannon, J. G., "Correlation of Beam and Diffuse Attenuation Coefficients Measured in Selected Ocean Waters," SPIE Ocean Optics, Vol. 64, p. 3, 1975.

8. "Airborne Oceanographic Lidar Post-flight Bathymetry Processor Program Documentation, Version 4.0," K. Borman, EG&G/WASC Planetary Sciences Department Report # 004-78, March 1978.

9. "A Quantitative Analysis of Errors in the Interpretation of AOL Charge Digitizer Output," R. W. L. Thomas, EG&G/WASC Report # 4820-10, January 1977.

10. "Airborne Hydrography System Limited Design Report," prepared under contract # 7-35373 for NOAA/NOS by AVCO-Everett Research Laboratory, Inc., January 1978.

11. "Laser Hydrography Analysis (A Cost Comparison Study)," prepared under contract for NOAA/NOS by GKY & Associates, Inc., January 1977.

12. "Cost Benefit Analysis Study of Airborne Laser Hydrography," prepared under contract # 7-35364 for NOAA/NOS by GKY & Associates, Inc., February 1978.

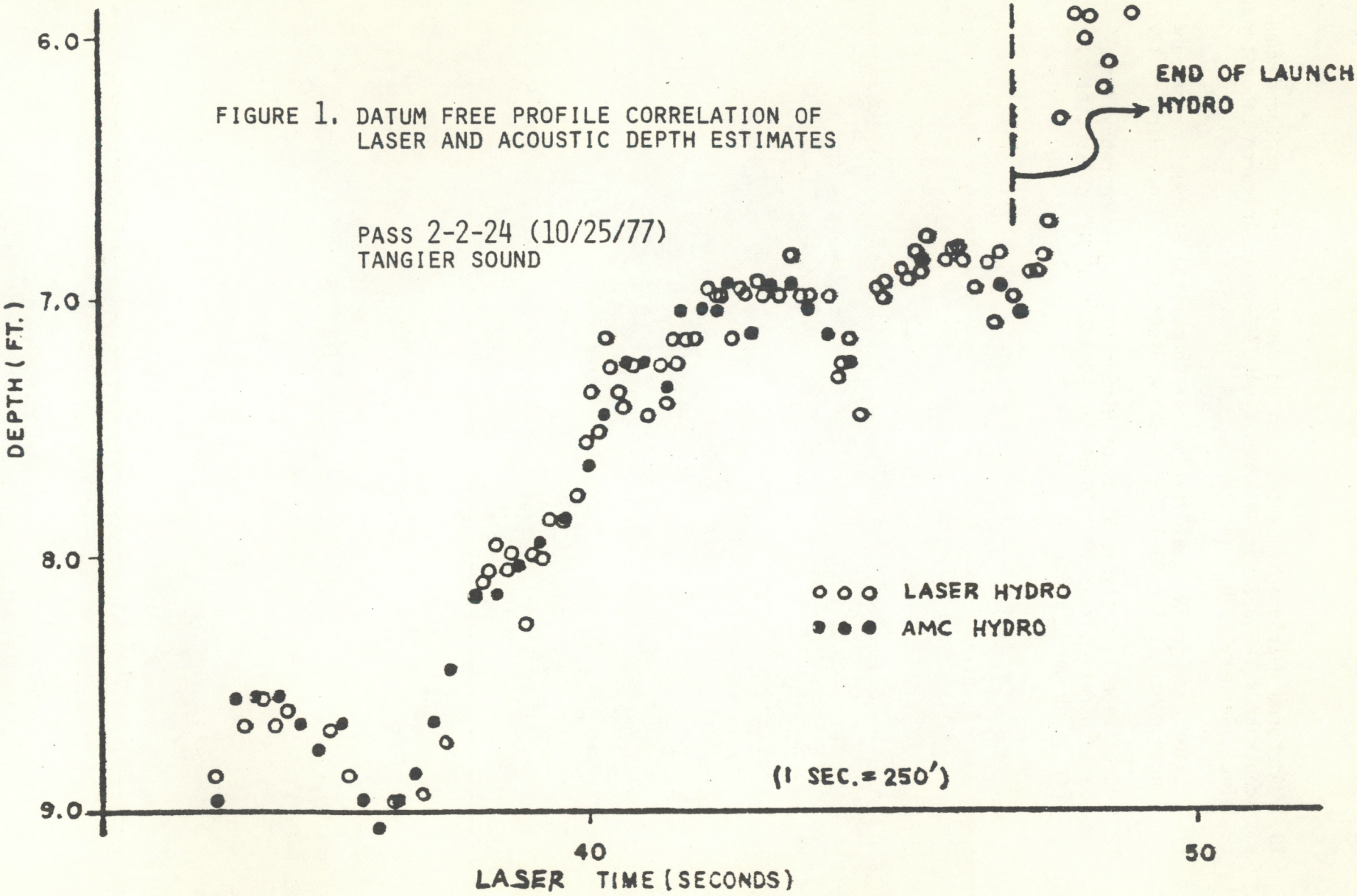

FIGURE 1. DATUM FREE PROFILE CORRELATION OF LASER AND ACOUSTIC DEPTH ESTIMATES

FIGURE 2. COMPARISON OF LASER AND ACOUSTIC DEPTH ESTIMATES INDICATING 1 FOOT BIAS

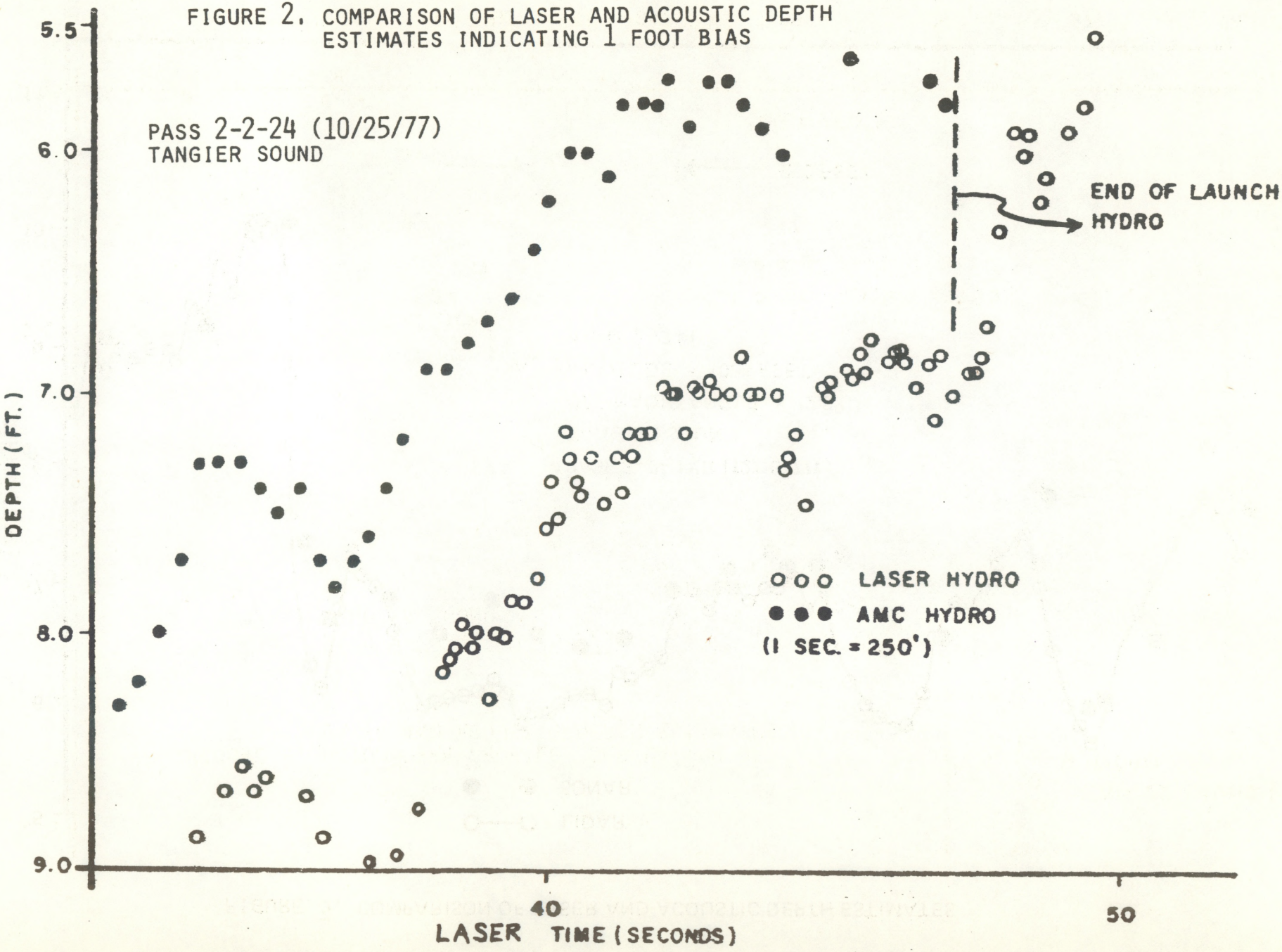

FIGURE 3. COMPARISON OF LASER AND ACOUSTIC DEPTH ESTIMATES

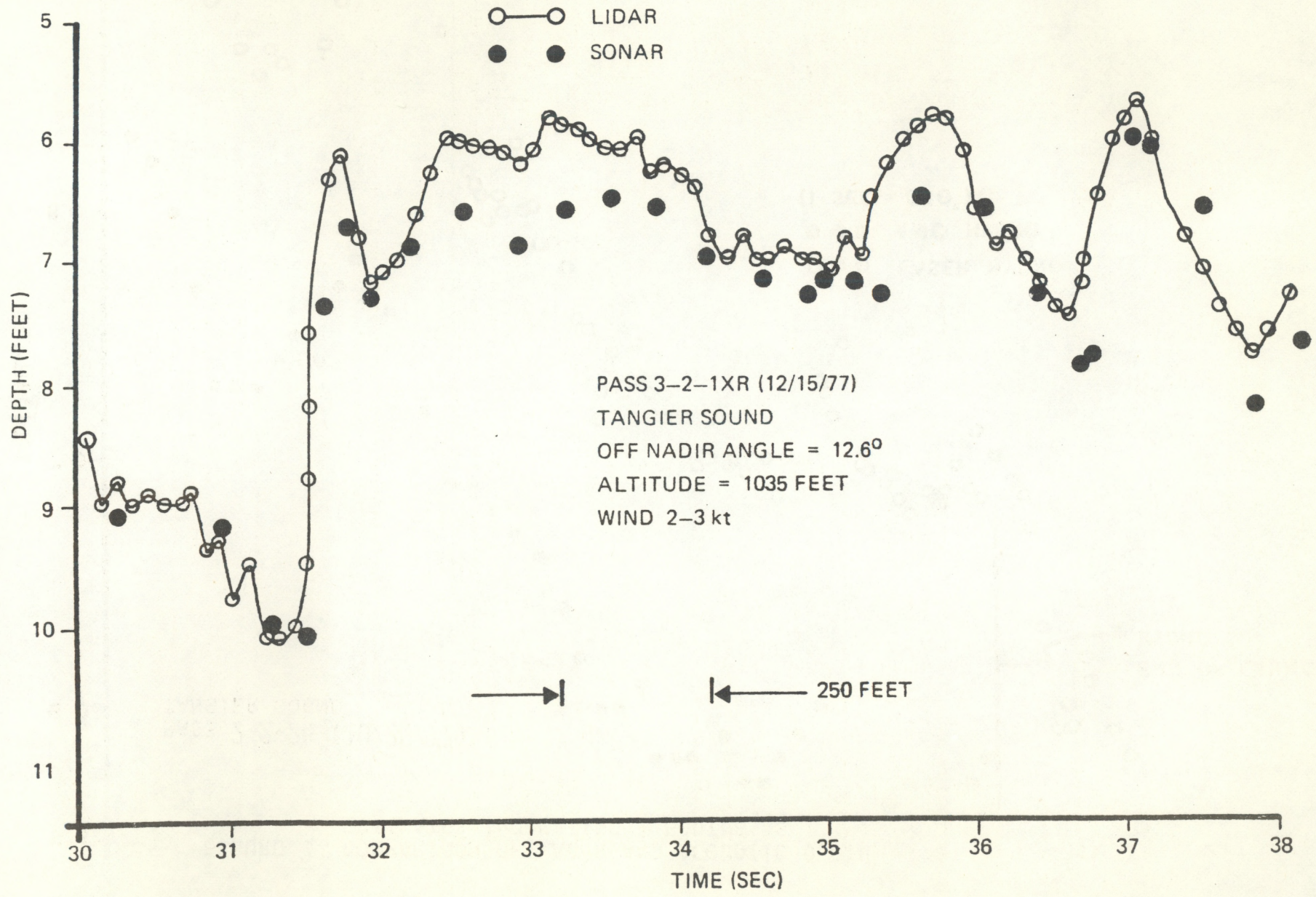

LASER APPLICATIONS FOR NEAR-SHORE NAUTICAL CHARTING

Gary C. Guenther
Lowell R. Goodman
NOAA/National Ocean Survey
EDL, C61
Rockville, Maryland 20852

Abstract

Flight testing of an airborne, scanning lidar bathymetric system has been conducted to determine vertical accuracy, operational constraints, and the effects of system variables. Test results are described, and an analytic performance model based on optical interactions is presented.

Introduction

Background

During the past ten years, a number of increasingly sophisticated airborne laser ranging (lidar) devices have been tested to determine technical feasibility for hydrographic and other oceanographic applications.(1) In 1974, a development program for a versatile airborne laser and data acquisition system, to be sponsored by the NASA Advanced Applications Flight Experiment (AAFE) program, was proposed jointly by NASA/Wallops Flight Center and AVCO Everett Research Laboratory, Inc. Requirements, specifications, evaluation procedures, and applications for this "Airborne Oceanographic Lidar" (AOL) system were solicited and established through a series of meetings with interested parties.(2-5) The concept evolved with two major and separate modes of operation: bathymetric lidar, and fluorosensing. The system was designed and built by the AVCO Everett Research Laboratory. Preliminary shakedown and experimentation with the AOL instrument in the bathymetric mode, installed in a NASA/Wallops Flight Center C-54 aircraft, has been sponsored by NOAA/National Ocean Survey (NOS) and the Defense Mapping Agency (DMA) through the Naval Oceanographic Research and Development Activity (NORDA), and conducted jointly by NASA and NOS.

The objectives of the Laser Hydrography Development Project within NOS are: to determine, through field tests of the AOL bathymetric laser system, the capability of an optimized airborne laser system to meet or exceed NOS near-shore vertical accuracy requirements within a bounding set of system variables and environmental parameters; to assess its cost effectiveness under "typical" operational conditions; to perform preliminary design work on a realizable, NOS operations oriented system; and to investigate the impact of such a system on NOS operations such as fleet utilization, chart production, and survey requirements.

The goals of the NOS flight test program with the AOL system are to: validate the overall feasibility of a bathymetric lidar system to provide high quality data under typical operations-oriented circumstances; determine vertical error under a bounding range of system variables and environmental parameters and correlate error contributions with sources; quantify system and environmental usage constraints to establish the operational "window"; and model major contributions in a return signal strength equation to provide a sound basis for extrapolation of these results to the design specifications of an NOS bathymetric lidar system.

The AOL was designed in a compromise configuration which permits either lidar bathymetry or active fluorosensing to be conducted at the advanced research or preliminary development level. Because of its unique dual nature, it was not possible to optimize performance in either mode separately. In view of the recognized inherent limitations of the AOL, the technical evaluation of the general "technique" of laser bathymetry for application to NOS requirements was broken into two parts: evaluation of results from AOL field test data and extrapolation of these results, via analytic models and computer simulations, to the ultimate expected performance of the "technique".

AOL System Description

The AOL system(6) is installed in the NASA/Wallops Flight Center C-54 aircraft. Water depths are determined for each laser pulse by measuring the time of flight difference between that portion of the pulse reflected back to the receiver from the water's surface and that reflected by the underwater "bottom" topography. An open hatch is used to pass transmitted and received energy to and from a large scanning mirror which is mounted between the floor and exterior skin of the aircraft.

The AOL bathymetric configuration consists of three major subsystems: optics, electronics, and computer. The optical subsystem includes: an AVCO C-5000 gas (neon/nitrogen) laser with an unstable resonator (to improve beam divergence), an adjustable beam expander (for divergence control), and an optional polarizer; a 56 cm scanner mirror with drive motor and 14-bit angle encoder; a 30.5 cm diameter Cassegranian f/4 receiver telescope with adjustable field stop and baffles (0-20 milliradian field of view) and an optional polarizer; a narrow band (4A) interference filter to suppress ambient background; and a photomultiplier tube (PMT) detector. The laser wavelength of 5401A (green) is near the minimum of the Jerlov(7) curves of diffuse attenuation coefficient for coastal water types. The laser output power is typically 2 kilowatts (peak), while approximately 500 watts (peak) exits the aircraft in the primary beam. Divergence is variable from 0-20 milliradians, and pulse repetition rate is variable up to a maximum of 400 Hz.

The scanner is a nutating design whose mirror axis is offset slightly from the axis of rotation. The resulting pattern on the earth's surface is a tightly interlocked series of pseudo-ellipses (actually slightly "egg"-shaped) which provides relatively uniform areal coverage. The scanner can be operated either at a 5 Hz rotation rate or locked in a fixed position for non-scanning (fixed off-nadir angle) data acquisition. The nominal angle of the output beam with respect to the nadir is adjustable in 5^{o} increments between 0^{o} and 15^{o} maximum deflection (this angle varies slightly during scanner rotation).

The electronics subsystem includes: amplification, discrimination, fanout, timing and gating functions; 40 charge digitizers (A/D converters); CAMAC interface; and appropriate power and control provisions. The 40 charge digitizers are gated sequentially at 2.5 ns intervals to provide 100 ns (or approximately 10 meters) of usable depth range. The digitized signals are transmitted through the CAMAC interface to a Hewlett-Packard 21 MX minicomputer with disk and tape storage and CRT display capability. The computer controls data acquisition, elementary processing, display, and recording functions. An altitude intervalometer, operating in conjunction with a surface return detector, triggers the digitization process slightly prior to detection of the expected surface return. This permits digitization of the surface return and bottom return in the same data vector; this is very important, as it provides the surface return shape and location for subsequent offline analysis. The altitude data can also be utilized to facilitate the removal of wave height variations and boat wakes from the depth calculations; this permits correction of the depths to the desired mean sea level.

Aircraft attitude and rough positional data are supplied to the computer from a Litton LTN-51 Inertial Navigation System (INS). A Universal Time Code Translator interfaced with the system provides precise "real time of day" for each laser pulse. The entire system (electronics, laser, optics, and computer for both bathymetry and fluorosensing modes) weighs 2100 pounds and fits comfortably in a small section of the C-54 cabin.

Test Program

The performance of the AOL is limited primarily by the product of water depth and optical attenuation coefficient. The latter is, for a given location and season, modulated temporally by wind, waveheight, precipitation, microorganisms, and currents; also affecting performance are such things as bottom relectivity and solar illumination. These parameters interact with system variables such as receiver field-of-view, altitude, scanner angle, and beam divergence to yield a highly complex set of relationships which must be unraveled to permit the quantization of specific effects. Adequate testing of the AOL thus depended on the quality and quantity of ground data specifically tailored to meet needs.

Two test sites were selected[8]: one in the Atlantic Ocean over Winter Quarter Shoal (several miles offshore from Assateague Island), and one in Chesapeake Bay -- Tangier Sound between Janes Island and Smith Island. These dissimilar sites provided the opportunity to investigate the effects of diversity in water clarity, depth, wind, and surface wave structure. Primary support data acquired in conjunction with the flight tests include vertical control, horizontal control, water clarity, sea surface conditions, meteorology, and bottom reflectivity. The data were obtained as near to the time of overflights as possible. A total of over one hundred vessel sorties or "cruises" were mounted in support of the program.

Water clarity measurements were made throughout the water column with a narrow beam transmissometer and were backed up with Secchi disk readings. (A well correlated linear regression of beam attenuation coefficient (α) against inverse Secchi depth was noted. This lends credence to both sets of readings.) Measurements were made in the vicinity of the flightline before, during, and after overflights. Attempts to measure diffuse attenuation coefficients (K) were foiled, with few exceptions, by baulky equipment. The observed relationship between α and K, based on a very small data set, is not inconsistent with the Shannon[9] equation ($K \cong \alpha/5 + 0.04$).

Navigation and positioning of the aircraft were accomplished with the tracking radar and plot-board capabilities available at NASA/Wallops Flight Center. Radar data are smoothed with a Kalman filter program to provide the highest possible accuracy. Radar data are merged with AOL data offline during processing to assign geographic coordinates to each laser sounding.

"Independent" variables and parameters chosen for investigation during the test phase are: water depth, water clarity, wind speed/wave height, solar illumination, bottom character, aircraft altitude, scanner off-nadir angle, receiver field of view, transmitter beam divergence, and detection algorithms. "Dependent" variables studied for effects of the above are accuracy (precision, profile correlation, bias, and repeatability), hit probabilities, extinction coefficients, system attenuation coefficients, minimum resolvable depths, surface return signal strengths, bottom return signal strengths, and noise levels.

In 1977, 18 missions were flown with a total of 161 separate passes for an estimated total distance of 1000 linear nautical miles and 400 minutes of recorded data comprised of five million soundings. Aircraft speed was maintained at approximately 150 knots with altitudes ranging from 150 to 600 meters. Missions were flown in river, bay, and ocean waters; in summer and winter; clear and cloudy; night and day; for winds from 0 to 15 knots; with and without capillary waves; in water clarities with narrow beam attenuation coefficients varying from less than $1m^{-1}$ to greater than $4m^{-1}$; and with water depths from 0 to over 10 m. This data base has been carefully archived and serves as the basis for an ongoing analysis program.

The primary analytic tool for AOL data analysis is a multifunction program called the "Processor"[10]. This program is extremely versatile because it is based on a freeform "keyword" input procedure with liberal defaults. The Processor unpacks and interpolates the asynchronous system data tape, identifies surface and bottom returns and quantifies their location and amplitude under control of a highly parameterized tracking algorithm, performs wave height correction, prints and plots altitudes, depths, waveforms, statistics, and other requested information, and supplies regressions and correlation values for all combinations of eleven specially selected parameters. An additional program is being developed to compare airborne lidar soundings with launch acoustic soundings and regress differences against a given parameter set.

Performance

Typical surface return signal strengths range from 1.0 to 25 microwatts optical power into the scanner; this is ten to several hundred times larger than typical bottom return signal strengths. The probability of a successful surface return, under most circumstances, approaches 100% rapidly as the mean surface return signal strength reaches several times the surface return detector trigger threshold. Typically for the AOL this occurs at about 2.5 microwatts.

Wind and wind generated waves (throughout the entire wavelength spectrum from capillaries to off-shore swell) influence system performance through a number of interactions, but few are overly significant except at the extremes--considered for our purposes to be 2 and 20 knots wind speed. Surface return energy from off-nadir scanner angles reaches the receiver only if capillary waves are excited sufficiently to present a large number of tiny facets perpendicular to the beam. These capillaries tend to die out below about 2 knots. A glassy or mirror-like water surface during calm wind conditions causes the surface return probability to decrease while the dynamic range of amplitudes and overall mean amplitude increase. Operation under these conditions is not effective. On the other end of the spectrum, high winds generate waves with sufficient energy and depth to resuspend bottom sediments and decrease water clarity to unacceptable levels. Such winds also make flying at low altitudes uncomfortable and unduly dangerous.

The off-nadir "scanner" angle affects both surface and bottom return signal strengths. Surface returns at nadir are quite strong and can easily exceed the input capabilities of the system. Results of an investigation of lidar returns from water (11)indicate that for low winds (under approximately 3 knots) the surface return is very strong at nadir and drops off very rapidly with increasing off-nadir angle. For higher winds the return is increasingly lower at nadir, but falls off more slowly with off-nadir angle. Surface return strengths at off-nadir angles benefit under some circumstances from higher winds. An additional benefit of higher winds is a reduction in the dynamic range of surface return amplitudes compared to nadir. A scanner pattern which does not intersect the nadir is highly desirable because it avoids the dynamic range problem altogether. Bottom return signal strength is also highest at nadir but, compared to surface return strength, falls off more gradually with increasing angles. (12) The major contributions to this drop are the decrease in the bottom energy distribution with increasing angle, the longer average path length through the water, and the significant asymmetric elongation of the return and subsequent loss of return energy from the down-beam direction. Sun glint proved to be no problem in AOL testing, because scanner off-nadir angles were not large enough to permit viewing of the glint pattern at the 38^{o} latitude of the test sites. For low latitudes, noon-time summer operations might be difficult, and a system with larger scan angle could experience a glint problem. Although the AOL was configured for a maximum off-nadir angle of 15^{o}, extrapolations of test data indicate that considerably larger angles may not be unreasonable for a higher powered system. The Navy system described by Witt, et al.,(12) has been successfully tested for off-nadir angles as large as 45^{o}.

Two dissimilar techniques for correcting individual, wave contaminated soundings to mean water level can be postulated. In the first, a very narrow transmitter divergence is required so that, from the flight altitude, the transmitter surface spot size is smaller than the size of the waves requiring removal. In the non-scanning test case, the profile of these waves then appears in the lidar determined altitude data; aircraft motion frequencies are much lower and do not interfere. Wave heights for individual pulses are calculated from variations about a mean altitude, or a linear fit to the altitude, over an appropriate time span (typically 20 to 40 pulses) and added to or subtracted from the depth measurement to correct it to mean water level. The technique has been used very successfully in certain AOL data sets, but, in at least one case, it failed; this is presently under investigation. The scanning case is further complicated by variations in slant range to the water which depend on the scan pattern and the roll and pitch of the aircraft. These variations must be predictable from the scan parameters and measured attitude data to an accuracy reasonably smaller than the wave heights requiring correction. This capability has not been demonstrated but is under study. The very small surface spot size required for this technique potentially conflicts with several other requirements. The surface return probability must be maintained at nearly 100%, and a high powered operational system must remain eye-safe. The transmitter beam divergence, varied between 2 and 10 milliradians, had very little effect on surface return peak powers or probabilities. This is an important result because it means that capillary waves provide sufficient return power even from the sloped faces of single waves. Eye safety could be a much more significant problem. It has been estimated that a 200 kW peak power system will be eye-safe from an altitude of 300 m if the transmitter beam divergence is at least 5 milliradians. This configuration produces a minimum surface spot diameter of 1.5 m which is most likely large enough to hinder or confuse direct wave removal. This leads to the second major technique which involves direct determination of the mean water level by using a surface spot size large enough to integrate over several typical wavelengths. In this situation, laser pulse duration becomes important, because it must be short enough that the temporal spreading of the surface return due to typical waveheights is separable from the transmitted pulse. For a 15 cm peak to trough wave, the spreading is only 1 ns; resolution of this amount would dictate a laser pulse of certainly less than the 5 ns duration which is presently considered to be a design goal. More analysis is needed in the area of wave height removal before a firm design judgement can be reached.

If mean surface return peak power versus altitude data are estimated with power law curves, the exponents thus obtained for altitudes from 150-600 m range between 1.0 and 2.0. The median exponent value observed is approximately 1.3, which indicates that the surface returns generally contain a high specular component, rather than being diffuse in nature (for typical illuminated areas from 0.5 to 6 m in diameter and with winds from 2 to 15 knots). This result is expected (11) for low wind speed with many nearly specular returns, but not for high winds with well developed wave structure and larger wave slopes. The expected correlation between exponent and wind speed could not be extracted, indicating that the surface return peak power data may be contaminated due to a recognized temperature dependent response instability of the system.

Next to accuracy, which will be discussed in a later section, penetration capability is the most important performance parameter for a laser bathymetric system. The maximum penetration depth, in general, is dependent on a large number of variables and parameters including laser wavelength and power, altitude, water clarity, bottom reflectivity, off-nadir angle, receiver aperture, receiver field of view, receiver sensitivity, noise sources, and many more[6,12] ; but for a given (appropriately designed and operated) system, the ultimate concern is water clarity. The reduction in bottom return peak power with increasing depth is typically described by the empirical expression:

$$P_B \propto e^{-2kD} \qquad (1)$$

where P_B = bottom return peak power

D = depth, and

$k \equiv$ "system" attenuation coefficient as defined by this expression.

The coefficient, k, has no theoretical basis and simply provides a straightforward parameter for describing system performance. This relationship has not been tested over a wide range of water clarities and requires further confirmation, particularly near extinction.

It has been established[12] that, for a sufficiently large receiver field of view, the value of "k" somewhat coincidentally approaches very close to the value of diffuse attenuation coefficient (K) for the water in question. Calculation of "k" for the AOL (from the slope of ℓn SSB vs. D curves) resulted in values usually consistent with K. Because of this fact, the product of K and the depth beyond which successful returns cannot be detected (D_{max}) is commonly referred to as the "extinction coefficient" (KD_{max}); and penetration capability is frequently reported in terms of this unitless parameter. In addition, because an apparently linear relationship ($\bar{\alpha} \cong 5K-0.2$) exists between diffuse attenuation coefficient (K) and depth averaged beam attenuation coefficient ($\bar{\alpha}$) for water clarities of interest in coastal waters,[9] extinction coefficients may also be reported in terms of $\bar{\alpha}D_{max}$. Although KD_{max} is the preferred form, AOL results will take the latter form because most recorded cruise data is for α rather than K. As a reference point, the Secchi depth is approximately equivalent to an $\bar{\alpha}D$ of 5.5 or a KD of about 1.2.

A healthy controversy exists regarding the advantages of using either K or $\bar{\alpha}$ as a measure of water clarity for underwater lidar applications. The two parameters are completely dissimilar in nature: α is a well defined, reproducible point measure of scattering and absorption properties independent of illumination and depth; K is an inherently integrated quantity (for the water column between the surface and the sensor) whose value, for homogeneous water, varies with depth and depends on the diffusivity of solar illumination at the time of the measurement. Both have certain advantages: K automatically integrates the water column in one measurement, while a series of measurements at various depths are needed to obtain $\bar{\alpha}$; α, however, can be obtained equally well night or day, while K is more difficult to measure at night. Conceptually, α regards all scattered light to be "gone", while K retains a useful fraction which has been scattered only over small collective angles. This is the chief reason for the applicability of K to the lidar scenario. Considering all these factors, it seems most logical to measure both parameters as simultaneously as possible. By making comparisons of α versus K and both against lidar results, one can retain the general utility of K and the rigor and night capability of α until either one measure becomes unnecessary or the pair become an inseparable team.

Dark, muddy bottoms, typical in Chesapeake Bay, caused no bottom detection difficulties. Reflectivities for sediments consisting of various grades of mud, sand, and shell fragments ranged between 4% and 12% with a median of approximately 9%. Significant bottom vegetation was present in neither test site. Maximum $\bar{\alpha}D_{max}$ extinction coefficients observed in processed AOL data are 12 during the day (over twice the Secchi depth) and 15 at night (nearly three times the Secchi depth). The latter was accomplished in December off Janes Island with $\bar{\alpha} = 2.7m^{-1}$ and $D_{max} = 5.5m$. These results, considered to be excitingly high for such a low power laser, were defined at the maximum extent of high quality data, where successful sounding probabilities remain in excess of 90% and precision (pulse to pulse agreement) remains no worse than 15-20 cm. Because of the sophisticated processing techniques applied to the raw signals, the loss of soundings at extinction tends to occur quite abruptly at bottom return signal strengths not greatly in excess of the minimum hardware digitization level. Bottom returns as low as 100 nanowatts can be tracked successfully with the AOL. Projecting these results to a higher power laser system (100-200 kW peak) leads to expectations of $\bar{\alpha}D_{max}$ in the 18-20 range (3.5 times Secchi). Such estimates are consistent with independent high power results (K. Petri, Naval Air Development Center, personal communication, 1978).

The effect of altitude on bottom return signal strength is indirect. One key parameter is the dimension of the region at the surface which falls within the receiver field of view--this depends on the field of view and the altitude. The dimension of the effective bottom return energy passing through the water/air interface depends on water clarity, depth, and, to a lesser extent, wind speed and transmitter beam divergence. The percentage of the available energy reaching the receiver depends on the ratio of these two dimensions. A model derived to quantify these relationships is presented in the next section.

Fundamentals

Physical Interactions

Several expressions previously derived[6,12] for the bottom return peak power of air to underwater lidar systems did not formally include the effect of receiver spot size at the water's surface relative to the extent there of bottom return energy. This relationship is important from an engineering point of view because it affects aircraft altitude and receiver

field of view requirements which, in turn, affect size, weight, scanning parameters, laser divergence and pulse repetition rate, and other important variables. Measurements and predictions of the bottom return peak power distribution versus receiver field of view, over a range of αD, are also important, because they provide insight into the bottom resolution capabilities of the system.

In order to model this relationship, one must first perceive the optical geometry. The three major contributions to the angular extent of the energy incident on the bottom are the original transmitter beam divergence, geometric refraction from waves at the surface, and, generally by far the dominant component, scattering in the water column. The angular energy density distribution on a spherical cap for a laser source in water, over a broad range of αD and α/a (the ratio of the attenuation coefficient to the absorption coefficient), has been measured and empirically described by Duntley.(13) These results permit the definition of effective cone angles within which a fixed percentile of the total energy is contained. The solution can be extended to the flat plate case to describe the incident energy distribution at the bottom. (The resulting energy percentile cone angles are somewhat smaller for the flat plate due to increased attenuation at the cone extremities with path lengths increased by the secant of the angle. The fractional reduction in effective percentile cone angles is greatest for large αD products because of the shape of the secant function.) The reflection from the bottom is assumed to be diffuse; this leads to a broad, virtually flat energy density distribution returning to the underside of the water/air interface.

The critical aspect of the model is the identification of the boundary and radial distribution of that portion of the bottom return energy which has passed through the interface in the direction of the receiver. The optical receiver will "see" the energy returning from the bottom reflection through the water/air interface as an apparent energy source at the water's surface which has a certain effective diameter. From geometric optics one can see that bottom reflected energy reaching the surface at a given angle cannot be refracted to the vertical (the effective direction of the receiver to within half the field of view) if that angle is greater than approximately one quarter of the effective wave slopes. The mean squared wave slope as a function of wind speed has been estimated (14) to be $\langle S^2 \rangle = 0.00267 \times W(\text{knots}) + 0.003$, with S in radians. For a 10 knot wind this yields approximately 10^o slopes; thus the maximum off-nadir angle in the water for energy reaching the receiver is about 2.5^o (or 3.4^o for a 20 knot wind). The fractional error incurred in neglecting this small angle and approximating the effective surface source diameter with the effective bottom source diameter is $\tan(S_{RMS}/4)$, or 4% for a ten knot wind. The Duntley irradiance expression is unbounded for very small scattering angles; this causes normalization problems for qualitative shape comparisons. Normalizing to the 1^o or 0.1^o values (for which very little of the total energy remains inside the cone) one discovers that the irradiance versus off-axis angle curves are exceptionally steep for low αD and somewhat less steep for high αD. For example, with $\alpha D = 6$ the cone defined by the half irradiance (-3dB) angle (based on normalization to the 1^o value) contains only about 5% of the total energy; and for $\alpha D = 12$, it contains about 28%. It is apparent from the shape of the Duntley curves that small angle forward scattering predominates. The percentage of far off-axis energy which can be scattered back to the nadir is thus vanishingly small. It has thus been demonstrated that neither geometric refraction from waves nor small angle scattering in the water column can cause significant bottom return energy to be returned to the receiver from any effective bottom return energy surface source diameter greater than the effective diameter of the bottom source itself. The bottom return energy which can potentially reach the receiver consequently comes from a surface source with effectively the same diameter as the percentile limited illuminating energy on the bottom. For definition of this effective bottom source diameter, the Duntley angle encompassing 90% of the total energy has been arbitrarily selected. Any other percentile could be used as preferred. For example, the ratio of the 90% energy diameter to the 50% energy diameter is large (5.1 at $\alpha/a = 5.88$) for $\alpha D = 3$ and decreases to a value of 2.3 for $\alpha D = 12$.

Quantifying the effect of operating with a sub-optimal receiver field of view at large αD's requires knowledge of the radial energy distribution within the defined boundary. This distribution is not easily obtained because it is strongly dependent on scattering and sea surface structure. In the limiting case of a perfectly flat sea surface, all off-nadir energy is refracted even more off nadir; this leads to an energy distribution above the water (in the direction of the receiver) slightly broadened by small angle scattering but basically similar to the distribution incident on the bottom. This case is of no practical interest because of reduced surface return probability. With capillary and larger waves excited, the distribution is apparently somewhat modified as indicated in the following section.

Field of View Model

A straightforward, computerized model has been developed which, for given αD and α/a, calculates the 90 th percentile bottom return energy effective surface source diameter from transmitter divergence, wind driven surface refraction, depth, and a 90% energy boundary angle from the Duntley distribution modified for incidence on a flat plate. The Duntley, or any alternate energy density distribution, is then integrated numerically in two dimensions to produce a normalized expression for the modification of bottom return energy as a function of receiver field of view for selected altitudes. Alternately, for given α, α/a, altitude, and fixed receiver field of view, the normalized response can be obtained as a function of bottom depth. The latter is useful in straightening out a downward bend in the log bottom signal strength versus depth curves (caused by progressively insufficient field of view at increasing depths) whose straight line slopes are used for the calculation of the system attenuation coefficient.

Witt, et al., (12) contains airborne measurements of bottom return signal peak power versus receiver field of view from three altitudes for a KD of 1.7 ($\alpha D \cong 5.2$) and winds in excess of 10 knots. The shapes of the three curves are not in good agreement with the model prediction based on the Duntley energy density expression. The Witt, et al., results rise to their asymptotic value much more slowly for small fields of view and far more rapidly for large fields of view. An energy density function of the form $(1 + \cos \pi R/R_m)^n$ (where R is a radial distance measure and R_m is the radius of the 90 th energy percentile) with n = 2 has been found to provide a better empirical fit to the Witt, et al., data, although it tends to

have a bit too much of the opposite trends: the empirical distribution needs to be a bit more peaky in the beginning and have a slightly broader tail. The reason for the substantial deviation from the Duntley distribution is being investigated. This type of deviation could, as will be described in the next section, result from a decrease in expected peak return power due to pulse stretching, but pulse stretching is not felt to be a factor in this particular case.

Much more experimental data is needed to confirm the validity of the model and identify the proper form of the radial energy density function over a wide range of αD. Unfortunately, AOL field test results are of marginal utility in this pursuit because of the unwieldy beam geometry from the neon laser/unstable resonator combination dictated by AOL fluorosensing requirements. A high density, high aspect ratio rectangle containing about 50% of the total energy is surrounded by a much broader, low density rectangle containing the other half. This combination alters results for both the size and distribution compared to that expected for a simple circular spot. It is somewhat surprising, therefore, that experimentally measured AOL bottom return peak power versus field of view data for $\bar{\alpha}D = 4.8$ ($KD \cong 1.2$) are in excellent agreement with the model prediction based on the same $(1 + \cos \pi R/R_m)^2$ density function which fits the Witt, et al., data. An additional problem is that test results cannot be accurately compared with the normalized model predictions unless the asymptotic limit is measured (or unless one assumes an inverse square relationship with altitude for fixed receiver surface spot diameter). Finally, the AOL 20 milliradian maximum receiver field of view is quite insufficient to encompass a large fraction of the bottom return energy except for relatively shallow depths or high altitude operation (above 300 m). This shortcoming accentuates the need for careful system design based on experimentally confirmed performance models.

Temporal Limitations

The maximum receiver field of view requirement for an airborne lidar system is an important design parameter. Other things being equal, the physical length of the optical train will be linearly proportional to it (because of acceptance angle restrictions on the interference filter used for suppression of ambient sunlight). Neglecting wind, wave, and transmitter beam divergence effects for simplicity, the geometry of the lidar bathymetry model dictates that

$$FOV_N = 2 \tan^{-1} \left(\frac{D}{H} \tan \theta_N\right) \qquad (2)$$

where: FOV_N is the field of view required to encompass N percent of the potential bottom return energy,

D is the water depth,

H is the aircraft altitude, and

θ_N is the N percentile Duntley angle.

Based on this model, the field of view necessary to encompass 90% of the total potential bottom return energy can become unrealistically large for high αD cases with clean, deep water and altitudes below about 600 m. For example, $\alpha = 1\ m^{-1}$, $D = 12$ m, and $H = 150$ m leads to a field of view requirement of 160 milliradians.

This field of view model, however, is purely geometric and deals with return energy. Bottom return strength is generally measured in terms of peak power. The bottom energy returning from the extremities of the effective surface source is delayed (on its downward path) with respect to the energy from the center of the source by a time which can be approximated from the geometry as:

$$\Delta t\ (\theta_N) \cong \frac{40}{9} D\ (\sec \theta_N - 1) \qquad (3)$$

where θ_N is the cone half-angle enclosing the N th percentile of total energy,

D is the depth in meters, and

Δt is in nanoseconds.

Equations (2) and (3) can be utilized to generate families of curves of $\Delta t\ (\theta_N)$ versus FOV_N for various values of α, D, and H. The delay to the 90 th percentile, $\Delta t\ (\theta_{90})$, can be considered roughly equivalent to the duration of the impulse response. Pulse stretching results from beam spreading in the water column due to scattering. The late arrival at the receiver of light traveling longer paths in the water to the outside fringes of the distribution results in an increased length or "stretching" of the bottom return pulse, and a consequential drop in peak power. For small Δt's (less than several laser pulse lengths), increases in received energy are manifested as increases in peak power. For large Δt's, the laser pulse length becomes insignificant compared to the dominant impulse response. Under these circumstances any increase in received energy results in a longer or "stretched" pulse with no significant increase in peak power. Depending on the form of the energy density distribution, the maximum peak power is generally achieved for times from one-third to one-half the impulse response duration. Thus, in situations where D and θ_{90} are large enough to produce a Δt longer than about twice the laser pulse length, the peak bottom return power versus field of view curves will saturate at under half the field of view predicted by the geometric model. This means that, although increasing the field of view could increase the received energy, it cannot increase the peak power. It also means that for signal detection procedures based on peak power, the maximum receiver field of view requirement can be approximately half that predicted by a purely geometric, energy based model.

While pulse stretching is a problem from the point of view of pulse detection, it is even more damaging in terms of pulse location when depth is calculated from the centroid of the bottom return energy -- as it is in the NOS Processor. Pulse stretching in this case causes results to be biased on the deep side by an amount depending on the field of view, altitude, water clarity, and depth. Proper selection of a field of view for given altitude, water clarity, and depth can be used to limit pulse stretching to any desired value, although this may consequently be detrimental to peak power. In the most difficult case of deep, clear water, it is expected that modelling and prediction can be used to facilitate correction of any bias incurred. Threshold detection is not seriously affected by pulse stretching but can result in reduced accuracy at low signal-to-noise ratios (15). The AOL data generally have fairly low signal strengths, due to low laser power, and hence require centroid detection for accuracy. Numerous tradeoffs exist between threshold and centroid type pulse locators, and detailed theoretical and experimental evaluations remain to be conducted.

Optical Resolution

One customarily perceives propagating laser energy as a narrow, highly collimated beam and propagating sound energy as broad and diffuse; in water the rules are different. Because of their relatively long wavelengths (typically in the centimeter range), sound pulses are not significantly scattered in relatively clear water (free of particles with characteristic size an appreciable fraction of wavelength) and are propagated over long distances with minimal degradation in angular beam width. Laser pulses, with characteristic wavelengths on the order of 40 millionths of a centimeter, are strongly scattered through small angles in the forward direction by all types and sizes of microscopic particulate matter. For this reason, light originating from a highly collimated source is spread over a cone angle which increases significantly with each successive attenuation length of penetration. The effects of this spreading on bathymetric resolution will now be discussed.

The NOS "standard" acoustic beam has an angular spread of 7.5° as defined at the -3dB intensity points. The fraction of the total energy in the main lobe which resides within the 7.5° cone is approximately 70%. The previously described Duntley irradiance distribution (modified to a flat plate) dictates lidar resolution. The -3dB cone angle from the Duntley expression varies considerably with αD, ranging from 3° to 23° for αD's of 3 and 12 respectively. These angles cannot be directly compared with their acoustic counterparts, however, because the light distribution is such that only 5% to 28% (depending on αD) of the total energy resides within. The -3dB cone for the $(1 + \cos \pi R/R_m)^2$ function, like that for the acoustic distribution, contains approximately 70% of the total energy. The cone angles range between 20° and 40° for αD's of 3 and 12 respectively. This leads to equivalent bottom spot diameters of from 0.36D for $\alpha D=3$ to 0.72D for $\alpha D=12$ which are from 3 to 5 times larger than for the 7.5° acoustic beam widths. The effects of this resolution degradation on accuracy must be investigated. One result of this beam spreading is that significant energy can reach the bottom at nadir even for the scanning situation with off-nadir incidence. Depending on the pulse location technique in use, the measured depth will lie somewhere between the true depth and the slant range to the bottom along the beam axis. The maximum difference between these two, for off-nadir scanner angles up to 15° (an 11.25° off-nadir energy axis in the water), is small for moderate water depths (i.e., 10 cm for D = 5m at 15° scan angle), but can become significant at great depths (i.e., 1 m for D = 50 m at 15° scan angle). This error can most likely be reduced by modelling with appropriate energy density distributions.

Degradation of accuracy with increasing beam widths can be caused both by small features being lost in deep water and by adjacent large features affecting nearby results. The loss of small, localized features in deep water is not overly disturbing considering the fact that such features are generally missed completely with present low sampling densities. Features large enough to be important are not missed. For unrealistically large features such as bumps, holes, and cliffs, the largest error would occur for the case of a small diameter, deep hole for which a significantly shallow result would be obtained. A centroid-type pulse locator will perform well, even under such adverse circumstances, with most results being biased slightly shallow. A threshold-type pulse locator would produce the correct result in several cases ("top of bump" and "down cliff" nearby) but would be significantly shallow for "up cliff" nearby and "bottom of hole." Nearby features of realistic size and shape have virtually no effect on accuracy at a given location. Limiting the receiver field of view for given circumstances to a value no larger than dictated by the temporally modified geometric model assures that resolution and bottom return peak power are simultaneously optimized. If, for some reason, additional resolution is required, it can be gained by further decreasing the field of view at a cost of reduced bottom return peak power. The situation in which resolution is at its worst is that of high αD with clear, deep water. Because the extinction depth is proportional to the logarithm of the laser transmitter power, significant changes in laser power do not greatly alter the extinction depth; i.e., the differential change in extinction depth for a change in laser power is small--the higher the αD, the lower the change. Similarly, for high αD, a moderate decrease in bottom return peak power does not significantly reduce the extinction depth. This means that, if desired, bottom return peak power can be traded for resolution without greatly reducing the extinction depth. Overall, in other than very shallow water, a lidar bathymeter does not have as high a resolution for small features as the sonar equivalent, and the penetration distance is significantly less; but the effects of this reduced resolution on accuracy are generally negligible. For hydrographic (i.e., chart making) purposes, however, these drawbacks are not significant when cost and areal coverage benefits over present techniques are considered.

Accuracy Results

Investigation of the basic sounding accuracy of the system has, to date, been based (for simplicity) on data acquired in the "fixed" or non-scanning mode at various off-nadir angles. This technique permits straightforward comparisons with acoustic data and precludes additional errors due to possible uncertainties in wave correction procedures. (Scanning data contains large variations in air-to-sea slant range caused by scanner eccentricity and aircraft roll and pitch. Wave correction for non-scanning data is accomplished with the simple averaging technique previously described.)

Precision

Precision is a measure of self-consistency and is related to random noise. Dominant environmental noise sources for a lidar bathymetric system are solar background reflection in daylight and volume backscattering of the laser pulse in the water column at night. A narrowband interference filter centered on the laser wavelength reduces the solar background level by a large factor. AC-coupling in the electronics further reduces this noise source. Volume backscatter has not been particularly evident in the relatively murky waters used for AOL testing, because it occurs in close conjunction with the surface return, and because it is effectively removed by a deep water subtraction technique utilized to suppress system noise. An upper bound on the actual system precision under given conditions can be estimated as the lower bound of the RMS deviation of given depth data about a linear fit to the data over a representative interval (i.e., 40 points, or about 15 meters of track length). This is true, because this measure also unavoidably includes actual small bottom variations and residual uncorrected wave noise in addition to actual system random noise components. This worst case measure will henceforth be called "precision" for purposes of discussion.

A mean precision of 4-5 cm for data with bottom signal strengths greater than about 10 times the minimum resolvable level was observed during a low wind/wave test (without wave correction) with a 15^{o} off-nadir scan angle. This value compares favorably with simulation results (15) from a model of expected system performance based on laser pulse width and shape, charge digitizer gate width, photon arrival rates, pulse detection algorithms, and similar matters. At low bottom return signal strengths (several times the minimum detectable limit) the precision may typically increase into the 10-20 cm range (trending as predicted by the simulation). Because of limitations in the AOL altitude intervalometer (minimum discrete jumps of 15 cm, as operated), the mean precision for wave corrected data generally has a minimum of about 10 cm. Wave correction thus adds about 5 cm error to the optimum performance level but, on the other hand, performs admirably for the more usual case where wave heights above 10 cm predominate.

When speaking of AOL depth precision, it must be recalled that the AOL was not conceived with high precision bathymetry in mind. This is evidenced by the following equivalencies of distance (depth) measures related to AOL timing parameters: physical pulse length (7.5 ns) = 84 cm; gate length (4 ns) = 45 cm; gate separation (2.5 ns) = 28 cm. The 10 cm mean precisions quoted are the result of sophisticated processing software necessitated by the relative crudeness of the AOL design. This software has performed so successfully that similar techniques are also expected to be recommended for the next generation NOS system.

Controls

Vertical control consists of bathymetry and tide control. A high density bathymetric survey of the Tangier Sound flightline was conducted by a NOS vessel from the Atlantic Marine Center utilizing standard, automated, acoustic techniques. Tide control for both acoustic and laser missions was furnished by three continuously recording NOS tide gages at appropriate locations. Horizontal control for this survey was a line-of-sight, high frequency electronic positioning system with ground stations. Positions have an expected uncertainty of 5 m.

Two flightlines in the Chesapeake Bay were surveyed. The first extends completely across Tangier Sound between Janes Island and Smith Island (a distance of approximately 12 kilometers), and the second is centered on a line of buoys (off Janes Island) approximately 3 kilometers long. The former was accomplished with 25 meter line spacings, while a more concentrated effort on the latter led to roughly 10 meter line spacings on the average. Depths were digitized every six seconds or approximately 25 meters along the tracks, and a continuous, low depth resolution analog record was also maintained to record peaks or valleys between digitizations. Even with such close spacing of "truth" measurements, it is noteworthy that a small (and typical for the area) linear slope of 2^{o} produces a vertical deflection of 0.35 meter (more than one foot) in 10 meters. Practically, this means that a one foot high feature can reside undetected between lines spaced 25 m apart, given only a scant 2^{o} slope. Because of this, the acoustic data, while vital, is not the ultimate in "truth"; and differences between the two systems must be classed as "residuals", not errors.

Navigation and positioning of the aircraft were accomplished primarily with the tracking radar and plot-board capabilities available at NASA/Wallops Flight Center. The on-board LTN-51 Inertial Navigation System was prone to drift and used only for a rough indication of general location (as well as roll and pitch data). The accuracy of real time radar vectoring, at the low elevation angles required for the test site location, was limited to about $\pm$100 m. Visual aids for the pilots, such as buoys, lights, flags, etc., were only marginally successful. Consequently, attempts to fly particular, precisely located flight paths were not generally successful; each pass typically had an individual character and location within the stated bounds. After the flights, radar data are smoothed with a Kalman filter program to provide the highest possible accuracy. The post flight aircraft position data have an expected uncertainty of at least 10 m. Combining this in quadrature with the 5 m uncertainty from the acoustic bathymetry leads to a combined uncertainty of about 11 m. Because a vertical error of 35 cm can accrue in this distance for only a typical 2^{o} slope, agreement between laser and acoustic data sets to better than 30 cm cannot be guaranteed even for a "perfect" laser system. It is hoped, however, that the accuracy of the laser system can be assessed to perhaps the 5-10 cm level.

Bias

Fully automated comparisons of AOL soundings with NOS acoustic soundings are not yet available (though pending), and the comparison has consequently involved comparisons of several processed data sets by hand. Results in general are quite encouraging. Datum free comparisons of laser and acoustic bottom profiles yield mean RMS deviations in the range of 2 to 4 cm! This excellent agreement proves that both lidar and sonar depth sounders were "seeing" the same bottom. With appropriate datums applied, however, distinct biases of about 30 cm have been observed in several cases, while in others,

agreement remains in the 5-15 cm range. Careful analysis of the data indicates no apparent fault with the basic techniques, and hardware anomalies are suspected. Ground test data (from simulated bottom and surface targets), presently being analyzed to test this hypothesis, appear to contain somewhat similar inconsistencies. Biases, as a class, are generally causal and hence correctable; the high precision and correlation noted in the data are considered to be better measures of system performance at this point in time. Ultimately, biases of less than approximately ± 10 cm are expected. Detailed error budgets, calculated for the AOL and for an optimized design, indicate that this is a quite reasonable goal in the relatively shallow coastal waters of interest.

Conclusions

1) The feasibility of obtaining high precision bathymetric soundings in a typical operational environment with a scanning, airborne lidar system has been confirmed.

2) Excellent penetration ($\alpha D_{max} \cong 15$) of typical coastal waters has been achieved with a relatively low power laser (0.5 kW effective peak power).

3) Performance in the scanning mode at off-nadir angles up to 15^{o} is satisfactory for conducting bathymetry.

4) The operational window for various system variables and environmental parameters is not unduly restrictive and should not lead to unreasonable mission constraints.

5) The mean precision of AOL soundings is excellent (typically less than 20 cm) and predictable with an existing model.

6) Mean RMS deviations between NOS acoustic survey soundings and AOL datum free lidar soundings, for three arbitrarily selected data sets, range from 2 to 4 cm. This is much better than expected.

7) Biases of up to 30 cm presently noted in a limited number of passes exceed NOS accuracy standards but are expected to be explainable (in terms of hardware instabilities) if not correctable. Such biases will not appear in a well designed system.

8) Wave correction using altitude intervalometer data has been successfully demonstrated for some non-scanning data. Further work is required to assess reliability and to extend this result to scanning data.

9) Sophisticated peak detection and location software has been developed and is performing well both in low signal-to-noise ratio conditions and for depths as shallow as 45 cm (1.5 feet).

10) An elementary model has been developed to describe the effects of receiver field of view and aircraft altitude on system performance. This model requires considerably more validation with experimental results.

11) The selection of pulse detection and location algorithms for optimum accuracy remains to be addressed. NOS data processing techniques for AOL data--involving the use of a peak power detection tracking algorithm and pulse location based on the centroid of pulse energy--have proven quite successful. Pulse stretching must be properly handled to preclude incurring a bias towards the deep side.

12) Underwater angular resolution for a bathymetric lidar depends strongly on αD and is generally inferior to that obtainable with sonar. This problem can be minimized with appropriate parameter selection, and it is not felt to pose a serious threat to overall system accuracy.

13) Eye safety requirements pose a potentially serious threat to the preferred technique of wave correction based on wave profiling. Eye safety requirements will be a major consideration in the final selection of operational variables such as altitude, transmitter divergence, receiver field of view, laser power, etc.

14) Selection of system variables for the proposed NOS bathymetric lidar system must be made with full knowledge of their intricate interrelationships; they cannot be chosen arbitrarily or independently.

15) Separate studies indicate that a relatively high powered (200 kW peak), eye safe, low risk lidar bathymetry system can be configured to operate from a small (Beech "King Air" equivalent) aircraft (16) and should provide a significant gain in cost-effectiveness over present acoustic techniques.(17,18)

Acknowledgements

AOL bathymetry mode testing could not have been accomplished without the dedication of over forty individuals. We wish to specifically thank Frank Arbusto, Wayne Barbley, Chris Blue, Kurt Borman, Marion Butler, Bob Chase, Dave Enabnit, Earl Frederick, Al Guzik, Tom Harmon, Frank Hoge, Doug Mason, Rober Navarro, Bob Scott, Bob Swift, Bob Thomas, and Bill Townsend for their assistance, and the aircrew who flew long, tedious missions at low altitude. Finally, we owe a special debt of gratitude to Bill Krabill whose faith, support, and ideas made it all possible.

References

1. Kim, H., P. Cervenka, and C. Lankford, "Development of an Airborne Laser Bathymeter," NASA Technical Note TND-8079, October 1975.

2. Goodman, L.R., ed., "Laser Hydrography User Requirements Workshop Minutes," NOAA/NOS; January 1975.

3. Melfi, S.R., Chairman, "Minutes of the Laser Fluorosensor Workshop," NERC/Las Vegas, February 1975.

4. Goodman, L.R., ed., "Laser Hydrography Technical Review Workshop Minutes," NOAA/NOS; August 1976.

5. AVCO Everett Research Laboratory, Inc., "Presentation for Airborne Oceanographic Lidar System Applications Workshop Seminar," December 1976.

6. AVCO Everett Research Laboratory, Inc., "Airborne Oceanographic Lidar System," NASA Contractor Report CR-141407, prepared under contract #NAS6-2653, October 1975.

7. Jerlov, N.G., Optical Oceanography, (Elsevier, Amsterdam), 1968.

8. Swift, R.N., "Preliminary Report on Pre-Flight Seatruthing for the Airborne Oceanographic Lidar Project," prepared for NASA/Wallops Flight Center, February 1977.

9. Shannon, J.G., "Correlation of Beam and Diffuse Attenuation Coefficients Measured in Selected Ocean Waters," SPIE Ocean Optics, Vol. 64, p. 3, 1975.

10. Borman, K.L., "Airborne Oceanographic Lidar Post-flight Bathymetry Processor Program Documentation, Version 4.0," EG&G/WASC Planetary Sciences Department Report #004-78, March 1978.

11. Petri, K.J., "Laser Radar Reflectance of Chesapeake Bay Waters as a Function of Wind Speed," IEEE Trans. Geoscience Electronics, GE-15, #2, April 1977.

12. Witt, A.K., J.G. Shannon, M.B. Rankin, and L.A. Fuchs, "Air/Underwater Laser Radar Test Results, Analysis, and Performance Predictions," Naval Air Development Center Report #NADC-76005-20, January 1976, (Report is classified "CONFIDENTIAL").

13. Duntley, S.Q., "Underwater Lighting by Submerged Lasers and Incandescent Sources," SIO Ref. 71-1, Scripps Institution of Oceanography, University of California, San Diego, June 1971.

14. Cox, C.S., and W.H. Munk, "Slopes of the Sea Surface Deduced from Photographs of Sun Glitter," Bull. Scripps Inst. Oceanog., Univ. Calif., 6, No. 9 (1956).

15. Thomas, R.W.L., "A Quantitative Analysis of Errors in the Interpretation of AOL Charge Digitizer Output," EG&G/WASC Report #4820-10, January 1977.

16. AVCO Everett Research Laboratory, Inc., "Airborne Hydrography System Limited Design Report," prepared under contract #7-35373 for NOAA/NOS, January 1978.

17. GKY & Associates, Inc., "Laser Hydrography Analysis (A Cost Comparison Study)," prepared under contract for NOAA/NOS, Januaray 1977.

18. GKY & Associates, Inc., "Cost Benefit Analysis Study of Airborne Laser Hydrography," prepared under contract #7-35364 for NOAA/NOS, February 1978.

LASER BATHYMETRY FOR NEAR-SHORE CHARTING APPLICATION
(PRELIMINARY FIELD TEST RESULTS)

Gary C. Guenther
Lowell R. Goodman
David B. Enabnit
NOAA/National Ocean Survey
EDL, C61
Rockville, Maryland 20852

Robert N. Swift
Robert W.L. Thomas
EG&G/WASC
6801 Kenilworth Avenue
Riverdale, Maryland 20840

Abstract

An airborne lidar* system has been extensively flight tested to study the operational feasibility of using a scanning, rapidly pulsed laser beam, projected into water from a fixed wing aircraft, for near-shore hydrographic applications. Field test results for vertical accuracy, environmental constraints, and effects of system parameters are discussed. Detailed utilization studies indicate that such a system should yield significantly reduced cost as well as increased volume of near-shore bathymetric data for charting purposes.

1. Introduction

During the past ten years, a number of increasingly sophisticated airborne laser ranging (lidar) devices have been tested to determine technical feasibility for hydrographic and other oceanographic applications. (Ref. 1) In 1974, a development program for a versatile airborne laser and data acquisition system, to be sponsored by the NASA Advanced Applications Flight Experiment (AAFE) program, was proposed jointly by NASA/Wallops Flight Center and AVCO Everett Research Laboratory, Inc. The purpose of this collaboration was to produce and demonstrate, for a select community of potential users, a state of the art system utilizing NASA's expertise in space-age technology. Requirements, specifications, evaluation procedures, and applications for this "Airborne Oceanographic Lidar" (AOL) system were solicited and established through a series of meetings with interested parties. (Refs. 2-5) The system evolved with two major and separate modes of operation: bathymetric lidar, and fluorosensing.

Preliminary shakedown and experimentation with the instrument in the bathymetric mode has been sponsored by NOAA/National Ocean Survey (NOS) and the Defense Mapping Agency (DMA), and conducted jointly by NASA and NOS. In this paper we shall discuss the results of the NOS test program. (Ref. 6)

* light detection and ranging: the equivalent of "radar," but at optical frequencies.

Near-shore bathymetric measurements are presently accomplished by NOS primarily with narrow-beam acoustic (sonar) equipment mounted in small boats which work at relatively low speeds. An airborne laser bathymetric system has the potential to provide a higher quality product with more timely and less costly (Refs. 7 and 8) results in critical coastal and inland waters. It also permits new or improved services and shows great promise as a member of the hydrographic team. The objectives of the Laser Hydrography Development Project within NOS are to determine the capability of an optimized airborne laser system to meet or exceed NOS near-shore vertical accuracy requirements within a bounding set of system variables and environmental parameters; to perform preliminary design work on a realizable, NOS operations oriented system; to assess its cost effectiveness under "typical" operational conditions; and to investigate any potential outstanding problem areas which may develop. Flight testing of the AOL was primarily dedicated to the first of these, while also acting as a valuable input to the second.

2. AOL System Description

The Airborne Oceanographic Lidar (AOL) system, (Ref. 9) designed and built by the AVCO Everett Research Laboratory, Inc. under NASA contract, is installed in the NASA/Wallops Flight Center C-54 aircraft. An open hatch is used to pass transmitted and received energy to and from a large scanning mirror which is mounted between the floor and exterior skin of the aircraft. Water depths are determined for each laser pulse by measuring the time of flight difference between that portion of the pulse reflected back to the receiver from the water's surface and that reflected by the underwater "bottom" topography.

The AOL bathymetric configuration includes the following:

- an AVCO C-5000 gas (neon/nitrogen) laser with an unstable resonator (to improve beam divergence), an adjustable beam expander (for control), and an optional polarizer;

- a 56 cm scanner mirror with drive motor and 14-bit angle encoder;
- a 30.5 cm diameter Cassegranian f/4 telescope with adjustable field stop and baffles (0-20 milliradian field of view) and an optional polarizer;
- a narrow band (4A) interference filter to suppress ambient background;
- a photomultiplier tube (PMT) detector with appropriate electronics;
- 40 charge digitizers (A/D converters);
- CAMAC interface;
- a computer controlled data acquisition, processing, display, and recording subsystem; and
- appropriate power and control provisions.

The laser wavelength of 5401A (green) is near the minimum of the Jerlov (Ref. 10) curves of diffuse attenuation coefficient for coastal water types. The laser output power is typically 2 kilowatts (peak), while approximately 500 watts (peak) exits the aircraft in the primary beam. Divergence is variable from 0-20 milliradians, and maximum pulse repetition rate is 400 Hz.

The scanner is a nutating design whose mirror normal is offset slightly from the axis of rotation. The resulting pattern on the earth's surface is a tightly interlocked series of pseudo-ellipses (actually slightly "egg"-shaped) which provides relatively uniform areal coverage. The scanner can be operated either at a 5 Hz rotation rate or locked in a fixed position for non-scanning (fixed off-nadir angle) data acquisition. The nominal angle of the output beam with respect to the nadir is adjustable in 5° increments between 0° and 15° maximum deflection (this angle varies slightly during scanner rotation).

An altitude intervalometer, operating in conjunction with a surface return detector, triggers the electronics upon detection of the surface return and permits digitization of just the event data--automatically, independent of aircraft altitude. Delay lines are used to permit digitization of the surface return, as well as the bottom return, in the same output vector. (This feature is extremely important, as it allows use of the surface return shape and location for subsequent analysis.) The altitude data is also utilized to facilitate the removal of wave height variations from the depth calculations; this permits correction of the depths to mean sea level.

The 40 charge digitizers are gated sequentially at 2.5 ns intervals to provide 100 ns (or approximately 10 meters) of usable depth range. The digitized signals are transmitted through the CAMAC interface to a Hewlett-Packard 21 MX minicomputer with disk and tape storage and CRT display capability.

Aircraft attitude and rough positional data are supplied to the computer from a Litton LTN-51 Inertial Navigation System (INS). A Universal Time Code Translator interfaced with the system provides precise "real time of day" for each laser pulse. The entire system (electronics, laser, optics, and computer for both bathymetry and fluorosensing modes) weighs 2100 pounds and fits comfortably in a small section of the C-54 cabin.

3. AOL Bathymetric Field Test Program

Goals:

The goals of the NOS flight test program with the AOL system are to: validate the overall feasibility of a bathymetric lidar system to provide high quality data under typical operations-oriented circumstances; determine vertical error under a bounding range of system variables and environmental parameters and correlate error contributions with sources; quantify system and environmental usage constraints to establish the operational "window"; and model major contributions in a return signal strength equation to provide a sound basis for extrapolation of these results to the design specifications of an NOS prototype bathymetric lidar system.

Site Selection:

Site selection for the AOL field tests was based on the following criteria: depths must range between one and ten meters; a combination of both flat and relatively high relief topography is preferred; radar tracking of the aircraft is imperative due to poor performance of the LTN-51; the sites must be logistically easy to reach by both aircraft and ground support vessels; the area must have suitable tide "control"; typical water clarities must be appropriate to permit penetration to the bottom over sufficiently long portions of a flightline; and adequate meteorological support should be available 24 hours in advance for daily mission go/no-go decisions.

Two test sites meeting these requirements were selected (Ref. 11): one in the Atlantic Ocean over Winter Quarter Shoal (several miles offshore from Assateague Island), and one in Chesapeake Bay -- Tangier Sound between Jane's Island and Smith Island. These dissimilar sites

provided the opportunity to investigate the effects of diversity in water clarity, depth, wind, and surface wave structure. The probability of successful missions in the Wallops Island vicinity based on precipitation, fog, and wind speed data from historical records was calculated and found to be acceptable. (Refs. 11 and 12)

Supporting Data:

A wide variety of ancillary supporting data was required for the flight tests in order to permit quantitative description of the system performance and the environmental restrictions on the operational window. The performance of the AOL is limited primarily by the product of water depth and optical attenuation coefficient. The latter is, for a given location and season, modulated temporally by wind, waveheight, precipitation, and currents; also affecting performance are such things as bottom reflectivity and solar illumination. These parameters interact with system variables such as receiver field-of-view, altitude, scanner angle, and beam divergence to yield a highly complex set of interactions which must be unraveled to permit the quantization of specific effects. Adequate testing of the AOL thus depended on the quality and quantity of ground data specifically tailored to meet needs. Primary support data acquired in conjunction with the flight tests include vertical control, horizontal control, water clarity, sea surface conditions, meteorology, and bottom reflectivity.

Vertical control consists of bathymetry and tide control. A bathymetric survey of the Tangier Sound flightline was conducted by an NOS vessel from the Atlantic Marine Center utilizing standard, automated, acoustic techniques. Horizontal control for this survey was a line-of-sight, high frequency electronic positioning system with ground stations. Tide control was furnished by three continuously recording NOS tide gages at appropriate locations.

Navigation and positioning of the aircraft were accomplished with the tracking radar and plot-board capabilities available at NASA/ Wallops Flight Center. Radar data are smoothed with a Kalman filter program to provide the highest possible accuracy. Radar data are merged with AOL data offline during processing.

Water clarity measurements were made throughout the water column with a narrow beam transmissometer and were backed up with Secchi disk readings. (A well correlated linear regression of beam attenuation coefficient (α) against inverse Secchi depth was noted. This lends credence to both sets of readings.) Measurements were made in the vicinity of the flightline before, during, and after overflights. Attempts to measure diffuse attenuation coefficients (K) were foiled, with few exceptions, by baulky equipment. The observed relationship between and K, based on a very small data set, is not inconsistent with the Shannon (Ref. 13) equation ($K \cong \alpha/5$).

Winds were measured at the Wallops Island National Weather Service at several levels. Wind, waves, and visibility were measured subjectively from vessels at the flightline.

Bottom reflectivities in green and blue wavelengths were measured with a laboratory reflectometer. Grab samples were transferred in sealed plastic bags. Various handling and sample preparation techniques were investigated and yielded essentially identical results.

The support data was obtained as near to the time of overflights as possible. A total of over one hundred vessel "sorties" or "cruises" were mounted in support of the program. Cruise data was coded directly into an 80-column format and punched onto computer cards for inclusion in a "sea-truth" data base.

Test Description:

"Independent" variables and parameters chosen for investigation during the test phase are: water depth, water clarity, wind speed/ wave height, solar illumination, bottom character, aircraft altitude, scanner off-nadir angle, receiver field of view, transmitter beam divergence, and receiver polarization. "Dependent" variables studied for effects of the above are accuracy (precision and bias), repeatability, hit probabilities, extinction coefficients, system attenuation coefficients, minimum resolvable depth, surface return signal strengths, bottom return signal strengths, noise levels, and detection algorithms. Data for these relationships was obtained within a four phase program. The data base for each mission includes a mission plan, the AOL system output tape(s), a digitized flight log of equipment settings and notes, a digitized ground data log, filtered radar tracking tapes, ground calibration data, a list of tape and data file numbers, a debriefing report, measured tide correctors, and sometimes ancillary materials such as footprint camera films, scope photos, and video tape of the monitor.

In 1977, 18 missions were flown with a total of 161 separate passes for an estimated total distance of 1000 linear nautical miles and 400 minutes of recorded data comprised of five million soundings. Aircraft speed was maintained at approximately 150 knots with altitudes ranging from 150 to 600 meters. Missions were flown in river, bay, and ocean waters, in hot and cold weather, clear and cloudy, night and day, for winds from 0 to 15 knots, with and without capillary waves, in water clarities with narrow beam attenuation coefficients varying from less than $1m^{-1}$ to greater than $4m^{-1}$, and with water depths from 0 to over 10 m.

Data Processing:

The tremendous volume of data acquired on even a single pass causes computer analysis to be mandatory. A wide variety of programs on a number of computers have been developed for data verification, reduction, display, analysis, and troubleshooting. The primary analytic tool for AOL data analysis is a sophisticated multi-function program called the "Processor." (Ref. 14) This program is extremely versatile because it is based on a freeform "keyword" input procedure with liberal defaults. Desired functions or procedures are easily activated and quantified by the inclusion of a single card in the setup deck. Briefly, the Processor unpacks and interpolates the asynchronous system data tape, identifies surface and bottom returns and quantifies their location and amplitude under control of a highly parameterized tracking algorithm, performs wave height correction, prints and plots altitudes, depths, waveforms, statistics, and other requested information, and supplies regressions and correlation values for all combinations of eleven specially selected parameters. An additional program is being developed to compare airborne lidar soundings with corresponding launch acoustic soundings and regress differences against a given parameter set.

4. Results

Preliminary:

Return waveforms from the initial flight tests were badly contaminated with electronic ringing and other spurious but repeatable noise sources whose amplitudes were greater than those of the desired bottom returns. To suppress this noise, a technique was developed which subtracts the system response to a surface return in deep water (with no possible bottom return) from the waveforms with bottom returns to yield a "residual" waveform in which only the bottom return pulse (and any uncorrected noise) appears. This subtraction is parameterized on surface return amplitude which drives the system response. Excellent resolution of bottom returns was achieved for even very weak returns approaching the digitization limit of the system (approximately 50 nanowatts at the scanner). An added benefit of this technique is the resultant subtraction of the surface return (and average solar noise and volume backscatter signal as well) which permits resolution of bottom returns at very shallow depths where they might otherwise be masked. Processor output results indicate bottom resolution to as shallow as approximately 30 cm.

Engineering:

Dominant environmental noise sources for a lidar bathymetric system are solar background reflection in daylight and volume backscattering of the laser pulse in the water column at night. A narrow-band interference filter centered on the laser wavelength reduces solar background level by a large factor. AC-coupling in the electronics further reduces this noise source. Volume backscatter has not been particularly evident in the relatively murky waters used for AOL testing because it occurs very close to the surface return, and because the deep water subtraction technique effectively removes it.

Bottom returns as low as 100 nanowatts can be tracked successfully. Surface returns range from ten to several hundred times larger. Probability of a successful surface return under most circumstances approaches 100% rapidly as the mean surface return signal strength reaches several times the trigger threshold. Typically for the AOL this occurs at about 2.5 microwatts optical power into the scanner. A glassy or mirror-like water surface during totally calm wind conditions causes the surface return probability to decrease while the dynamic range of amplitudes and overall mean amplitude increase. Operation under these conditions would not be recommended.

Penetration capability is probably the most important performance parameter for a laser bathymetric system next to accuracy. The maximum penetration depth, in general, is dependent on a large number of variables and parameters including laser power, altitude, water clarity, bottom reflectivity, off-nadir angle, receiver aperture, receiver field of view, receiver sensitivity, noise sources, and many more (Ref. 9); but for a given (appropriately designed and operated) system, the ultimate concern is water clarity. The reduction in bottom return signal strength with increasing depth can be described by the expression:

$$SSB \sim e^{-2kD}$$

where

SSB = bottom signal strength,

D = depth, and

k $\equiv$ "system" attenuation coefficient as defined by this expression.

The coefficient, k, has no particular theoretical basis, but simply provides a straightforward empirical parameter for describing system performance.

It has been established (Ref. 15) that for a sufficiently large receiver field of view, the value of "k" somewhat coincidentally approaches very close to the value of depth averaged diffuse attenuation coefficient ($\bar{K}$) for the water in question. Because of this fact, the product of $\bar{K}$ and the depth beyond which successful returns cannot be detected (D_{max}) is commonly referred to as the "extinction coefficient" ($\bar{K} D_{max}$); and penetration capability is frequently reported in terms of this unitless parameter. In addition, because an apparently linear relationship ($\alpha \cong 5K$) (Ref. 13) exists between diffuse attenuation coefficient (K) and

beam attenuation coefficient (α) for water clarities of interest in coastal waters, extinction coefficients may also be reported in terms of $\bar{\alpha} D_{max}$. (AOL results will take this form because most cruise data is for α rather than K).

Calculation of "k" for the AOL (from the slope of ℓn SSB vs. D curves) resulted in values generally consistent with K. Maximum extinction coefficients observed in processed AOL data are $\bar{\alpha} D_{max} = 12$ during the day and $\bar{\alpha} D_{max} = 15$ at night! The latter was accomplished in December off Janes' Island with $\bar{\alpha} = 2.75 m^{-1}$ and $D_{max} =$ 5.5m. These results, considered to be excitingly high for such a low power laser, were defined at the maximum extent of high quality data, where hit probabilities remain in excess of 90% and precision (pulse to pulse agreement) remains no worse than 15-20 cm. Because of the sophisticated processing techniques applied to the raw signals, the loss of soundings at extinction tends to occur quite abruptly at bottom return signal strengths not greatly in excess of the minimum hardware digitization level. Projecting these results to a higher laser power system (100-200 kW peak) leads to expectations of $\bar{\alpha} D_{max}$ in the 18-20 range. Such estimates are consistent with independent high power results (Ref. 16).

Wind and wind generated waves (throughout the entire wavelength spectrum from capillaries to off-shore swell) unquestionably influence system performance through a number of interactions, but few are overly significant except at the extremes--considered for our purposes to be 2-20 knots wind speed. Surface return energy from non-nadir scanner angles reaches the receiver only if capillary waves are excited sufficiently to present a large number of tiny facets perpendicular to the beam. These capillaries tend to die out below about 2 knots, and, as noted above, this leads to a reduced hit probability. On the other end of the spectrum, high winds generate waves with sufficient energy and depth to resuspend bottom sediments and decrease water clarity to unacceptable levels. From 2-20 knots, beam spreading through the air/sea interface due to wave slope augmented refraction is not large compared to beam spreading in the water column due to scattering. Surface return amplitudes at higher off-nadir scanner angles actually benefit slightly from higher winds where less variation of amplitude with angle is also noted.

If mean surface return signal strength versus altitude data are estimated with power law curves, the exponents thus obtained range between 1.0 and 2.0 for altitudes from 150-600m. No correlation between the value of the exponent and any variable or parameter (such as off-nadir angle or wind speed) could be established; rather, the value seems to be a complex function of these plus the direction of the beam relative to the wind direction. The median exponent value observed is approximately 1.3, which indicates that the surface returns generally contain a high specular component, rather than being diffuse in nature (for typical illuminated areas from 0.5-6m in diameter at the water's surface).

The effect of altitude on bottom return signal strength is indirect. The amount of bottom return energy reaching the receiver depends on the fraction of the bottom return energy refracted through the air/sea interface (in the direction of the receiver) within the field of view of the receiver. The factors determining that fraction are water clarity, depth, altitude, wind speed, and receiver field of view. An analytic model has been developed which calculates the field of view necessary to intercept 90% of the potential bottom return energy for specific values of the other parameters. This model is in good agreement with experimental data and can be used for future system design applications.

The off-nadir "scanner" angle affects both surface and bottom return signal strengths. Surface returns at nadir are quite strong and can easily exceed the input capabilities of the system. With increasing off-nadir angle, the returns decrease rapidly in the first five degrees and then much more slowly thereafter. Bottom return signal strength is also highest at nadir but falls off more gradually with increasing angles. A scanner pattern which does not intersect the nadir is highly desirable because it avoids the dynamic range problem caused by the strong nadir surface returns. Although the AOL was configured for a maximum off-nadir angle of 15°, extrapolations of test data indicate that angles of up to 30° or more may not be unreasonable. At such large angles, calculations of a depth bias due to pulse stretching from long slant ranges would become increasingly more important.

The transmitter beam divergence, varied from two to ten milliradians, had virtually no effect on results. The only potential restriction is that the beam must be large enough to provide high surface return probability; resolution is not degraded with a larger divergence because the beam spreading in the water is several orders of magnitude greater.

Dark, muddy bottoms, typical in Chesapeake Bay, caused no bottom detection difficulties. Reflectivities for sediments consisting of various grades of mud, sand, and shell fragments ranged between 4% and 12% with a median of approximately 9%. Significant bottom vegetation was present in neither test site. Future testing of the system will be planned for bottoms populated by various forms of broad and narrow leaf plants. It is expected that various types of vegetation will attenuate the bottom signal or cause a shallow bias in soundings.

Sunglint proved to be no problem in AOL testing, because scanner off-nadir angles were not large enough to permit viewing of the glint

pattern at the 38° latitude of the test sites. For low latitudes, noon-time summer operations might be difficult, and a system with larger scan angle could experience a glint problem.

Vertical Accuracy:

Investigation of the basic sounding accuracy of the system to date has been based on data acquired in the "fixed" or non-scanning mode at various off-nadir angles. This technique permits simple comparisons with acoustic data and precludes additional errors due to possible uncertainties in wave correction procedures. (Scanning data contains large variations in air to sea slant range caused by scanner eccentricity and aircraft roll and pitch.) Wave correction procedures for scanning data based on careful modeling of the aircraft and scanner parameters are presently being investigated. Wave correction for non-scanning data is accomplished with a simple averaging technique based on altitude intervalometer data.

Accuracy is divided into two basic measures: precision and bias. Precision is a measure of self-consistency and is related to random noise, while bias errors are determined by comparison with an external "standard" and are fixed offset or "systematic" errors.

An upper bound on the actual system precision under given conditions can be estimated as the lower bound of the RMS deviation of given data about a linear fit to the data over a representative interval (typically chosen to be a single page of computer output: 40 points, or about 15 meters of track length). This is true, because this measure also unavoidably includes actual small bottom variations and residual uncorrected wave noise in addition to actual system random noise components. This worst case measure will henceforth be called "precision" for purposes of discussion.

A mean "precision" of 4-5 cm for data with reasonable signal strengths was observed during a low wind/wave test (without wave correction) with a 15° off-nadir scan angle. This value compares favorably with simulation results (Ref. 17) undertaken to derive a model of expected system performance based on laser pulse width and shape, charge digitizer gate width, photon arrival rates, pulse detection algorithms, and similar matters. At low bottom return signal strengths (several times the mimimum detectable limit) the "precision" may typically increase into the 10-20 cm range (trending as predicted by the simulation). Because of limitations in the AOL altitude intervalometer (minimum discrete jumps of 15 cm, as operated), the mean precision for wave corrected data generally has a minimum of about 10 cm. Wave correction thus adds about 5 cm error to the optimum performance level, but on the other hand performs admirably for the more usual case where wave heights above 10 cm predominate.

Fully automated comparisons of AOL soundings with NOS acoustic soundings are not yet available (though pending), and the comparison has consequently involved comparisons of several data sets by hand--a tedious task. Results in general are encouraging. Datum free comparisons of laser and acoustic bottom profiles yield mean RMS deviations in the range of 5-15 cm. With appropriate datums applied, however, distinct biases of about 30 cm have been observed in several cases. Careful analysis of the data indicates no apparent fault with the basic techniques, and hardware anomalies are suspected. Ground test data (from simulated bottom and surface targets), presently being analyzed to test this hypothesis, appear to contain somewhat similar inconsistencies. Biases as a class are generally causal and hence correctable; the high "precision" noted in the data is considered to be a better measure of system performance at this point in time. Ultimately, biases of less than approximately $\pm$ 15 cm are desired. Detailed error budgets, calculated for the AOL and for an optimized design, indicate that this is a quite reasonable goal in the reasonably shallow coastal waters of interest.

5. Conclusions

1) The feasibility of obtaining high precision bathymetric soundings in a typical operational environment with a scanning airborne lidar system has been confirmed.

2) Excellent penetration ($\bar{\alpha}$ D $\cong$ 15) of typical coastal waters has been achieved with a relatively low power laser.

3) Performance in the scanning mode at off-nadir angles up to 15° is satisfactory for performing bathymetry.

4) The operational window for various system variables and environmental parameters is not unduly restrictive and should not lead to unreasonable mission constraints.

5) The mean precision of AOL soundings is excellent (typically less than 20 cm) and predictable with an existing model.

6) Biases of up to 30 cm presently noted in a limited number of soundings are slightly greater than NOS accuracy standards but are expected to be explainable (in terms of hardware instabilities) if not correctable. Such biases are not expected to appear in a well designed system.

7) Wave correction using altitude intervalometer data has been successfully demonstrated for non-scanning data. Further work is required to extend this result to scanning data.

8) Sophisticated peak detection and location software has been developed and is performing well in low signal-to-noise ratio conditions.

9) Separate studies indicate that a relatively high powered (200 kW peak), eye safe, lidar bathymetry system can be configured to operate from a small (Beech "King Air") aircraft (Ref. 18) and should provide a significant gain in cost-effectiveness over present acoustic techniques (Refs. 7 and 8).

6. Acknowledgements

AOL bathymetry mode testing could not have been accomplished without the dedication of over forty individuals. We wish to specifically thank Frank Arbusto, Wayne Barbley, Chris Blue, Kurt Borman, Marion Butler, Bob Chase, Earl Frederick, Tom Harmon, Frank Hoge, Doug Mason, Roger Navarro, and Bill Townsend for their assistance, and the aircrew who flew long, tedious missions at low altitude. Finally, we owe a special debt of gratitude to Bill Krabill whose unending faith, support, and ideas made it all possible.

References

1. Kim, H., P. Cervenka, and C. Lankford, "Development of an Airborne Laser Bathymeter," NASA Technical Note TND-8079, October 1975.

2. "Laser Hydrography User Requirements Workshop Minutes," edited by L.R. Goodman, NOAA; January 1975.

3. "Minutes of the Laser Fluorosensor Workshop," NERC/Las Vegas, S.R. Melfi, Chairman, February 1975.

4. "Laser Hydrography Technical Review Workshop Minutes," edited by L.R. Goodman, NOAA; August 1976.

5. "Presentation for Airborne Oceanographic Lidar System Applications Workshop Seminar," AVCO-Everett Research Laboratories, Inc., December 1976.

6. "Laser Hydrography Development Project Plan, A Working Document," L.R. Goodman, February 1977.

7. "Laser Hydrography Analysis (A Cost Comparison Study)," prepared under contract for NOAA/NOS by GKY & Associates, Inc., January 1977.

8. "Cost Benefit Analysis Study of Airborne Laser Hydrography," prepared under contract #7-35364 for NOAA/NOS by GKY & Associates, Inc., February 1978.

9. "Airborne Oceanographic Lidar System," NASA Contractor Report CR-141407, prepared under contract # NAS6-2653 by AVCO-Everett Research Laboratory, Inc., October 1975.

10. Jerlov, N.G., Optical Oceanography, (Elsevier, Amsterdam), 1968.

11. Swift, R.N., "Preliminary Report on Pre-Flight Seatruthing for the Airborne Oceanographic Lidar Project," prepared for NASA/Wallops Flight Center, February 1977.

12. Scott, R., "Probability of Success of AOL Bathymetry," NOS Internal Report, December 1976.

13. Shannon, J.G., "Correlation of Beam and Diffuse Attenuation Coefficients Measured in Selected Ocean Waters," SPIE Ocean Optics, Vol. 64, p. 3, 1975.

14. "Airborne Oceanographic Lidar Post-flight Bathymetry Processor Program Documentation, Version 4.0," K. Borman, EG&G/WASC Planetary Sciences Department Report #004-78, March 1978.

15. Witt, A.K., et. al., "Air/Underwater Laser Radar Test Results, Analysis, and Performance Predictions," Naval Air Development Center Report #NADC-76005-20, January 1976, (Report is classified "CONFIDENTIAL").

16. Petri, K., Naval Air Development Center, personal communication.

17. "A Quantitative Analysis of Errors in the Interpretation of AOL Charge Digitizer Output," R.W.L. Thomas, EG&G/WASC Report # 4820-10, January 1977.

18. "Airborne Hydrography System Limited Design Report," prepared under contract #7-35373 for NOAA/NOS by AVCO-Everett Research Laboratory, Inc., January 1978.

THEORETICAL CHARACTERIZATION OF BOTTOM RETURNS FOR BATHYMETRIC LIDAR*

Robert W.L. Thomas
EG&G/WASC
6801 Kenilworth Avenue
Riverdale, Maryland 20840

and

Gary C. Guenther
NOAA/National Ocean Survey
EDL, C61
Rockville, Maryland 20852

Abstract

The two parameters most important to describing and evaluating the performance of an airborne, pulsed lidar bathymetry system are accuracy and penetration. In this paper, Monte Carlo simulation results for multiple scattering and diffusion in a homogeneous medium are extended analytically to provide estimates of expected temporal response shape, depth bias errors, and round trip signal loss profiles as a function of optical depth and scattering parameters. These formulations will provide several of the key relationships necessary for extrapolation of performance parameters in an optimized system from existing experimental data sets.

Background

Airborne laser radar (lidar) is being investigated in the National Ocean Survey's Office of Marine Technology (NOS/OMT) as a potential method for acquiring bathymetric data (water depths) in costal regions for charting purposes. Similar programs are presently being pursued in both Canada and Australia. The basic technique involves the use of a scanning, pulsed laser transmitter and a suitable receiver--consisting of a reflecting telescope and photomultiplier tube (PMT) detector--operating under computer control. Depth measurements are determined by the time differential between the return pulses from the air/water interface and the water/bottom interface.

The ability to acquire lidar bottom soundings with great confidence over a wide range of system and environmental parameters has been amply demonstrated[1] during bathymetric flight testing of the Airborne Oceanographic Lidar (AOL) system built for NASA/Wallops Flight Center by the AVCO Everett Research Laboratory, Inc. A data base of some 5 million laser soundings in Chesapeake Bay and the Atlantic Ocean was created, and detailed analysis is being actively pursued. The AOL is a low power (1 kilowatt peak), general purpose research tool for both bathymetry and fluorosensing; it was not designed optimally as an engineering model for a high performance bathymetric system. Consequently, test results from this program must be extended via simulation and modelling to provide predictions for important performance parameters over a range of input variables.

The two most important performance requirements for an airborne lidar bathymetric system are accuracy and maximum penetration depth. Predicted precision, bias, and repeatibility of depth measurements over the entire range of expected working conditions must be demonstrated, with reasonable confidence, to fall within NOS charting requirements. The predicted maximum penetration depth for typical water clarities is a key to the cost and operational effectiveness of the system through determination of the location and maximum geographic extent of the chartable areas. These results cannot be obtained solely from tests utilizing a low power, shallow water research system such as the AOL, but the data so gathered can be manipulated to provide a basis for and confidence in the necessary, farther reaching theoretical formulations.

Introduction

Microwave radar signals are generally passed through the intervening medium with little scattering or attenuation (other than geometric). For a known target, the return waveform is deterministic and delayed by a simply predictable function of the separation distance.

*This work was supported in part by the Defense Mapping Agency under Interagency Cost Reimbursement Order No. HM0050-8-326 monitored by CDR V. Nield.

This is not, however, the case for lidar and laser communications systems, wherein scattering and absorption in the signal path play dominant roles in altering the shape and time delay of received pulses. The temporal spreading, in the case of a bathymetric lidar bottom return signal, leads to a bias error in the depth measurement. Knowledge of the expected (or measured) bottom return shape and duration from a given medium could be used to permit prediction of this bias error and thus recovery of an accurate estimate of the true depth. It would also facilitate formulation of optimal signal detection and location algorithms. For the bathymetric application, the maximum permissable laser power is constrained by eye-safety considerations, hardware limitations, and reliability factors: it cannot be increased at will to meet penetration requirements. Accurate prediction of the dominant signal loss term (absorption and scattering in the water column) would permit confident extrapolation to expected penetration depth limitations for laser powers significantly in excess of that available on the AOL.

A Monte Carlo solution of the radiative transfer problem for an optically thick medium has been developed for atmospheric transport. The application of this formalism to bathymetric lidar signals, for the case of unlimited receiver field of view, will be presented in the following section. Results will be reported for the predicted bottom return pulse shape, fractional depth error, and bottom return energy and peak power versus optical depth. The sensitivity of the model results to variations in input parameters is discussed.

Theory

Analytical formalisms have been developed in two transport regimes to characterize the transport of a laser beam through turbid media. The first,[2] applicable to high scattering orders, describes the consequences of the approach to and development of an isotropic radiation field through the application of Monte Carlo simulation results and diffusion theory. The second[3] applies to low scattering orders for which the strong forward peak in the scattering function dominates or continues to influence the directional redistribution. The goal is to characterize the temporal distribution of radiation which has traversed a medium and been reflected back through the same medium to a receiver. It is assumed that the transport of reflected radiation has a statistical description equivalent to that for the incoming radiation in the medium. It is therefore sufficient to begin by deriving the temporal distribution for one-way transport. For simplicity the problem will be solved for an input beam vertically incident onto a flat surface in a homogeneous medium. The following symbols will be used throughout the ensuing discussion:

D = physical thickness of the medium,
R = reflection coefficient of the bottom,
α = beam attenuation coefficient (=scattering, s + absorption, a),
τ = optical depth of the medium ($=\alpha D$),
θ = single event scattering angle,
$\langle\cos\theta\rangle$ = mean cosine of the scattering angle,
ω_o = albedo for single scattering ($=S/\alpha$),
τ_d = momentum transfer optical depth or effective scattering thickness ($=\tau(1-\langle\cos\theta\rangle)$), and
c = velocity of light in water.

Depth Bias

"Multipath time delay" is a term used to denote traverse times through a medium measured from the time required for a straight through path; i.e., the multipath time delay of an unscattered photon, along the shortest path through the medium, is zero. In a homogeneous medium, the mean total travel time through the medium for elastic scattering ($\omega_o = 1$) has been given historically as[4,5]

$$\bar{t} = D\tau_d/2c. \qquad (1)$$

Through Monte Carlo simulations it has been determined[2] that this relationship better describes the mean multipath time delay and is approximately valid for τ_d as small as 0.2. Bucher's[6] Eq. (12) (converted from distance to time), based also on Monte Carlo simulation, predicts more precisely a mean multipath time delay

$$\bar{t} = 0.62\ D\ \tau_d^{0.94}/c \qquad (2)$$

for τ_d at least as small as 0.6. These results are virtually independent of the exact form of the scattering function for $\tau_d \geq 1$.

More generally, the simulations[2] indicate that, except for very small multipath time delays, the multipath temporal delay impulse response of the model is exponential in character. Therefore, by inference, the scattering number is also exponentially distributed. The collision frequency, f, is $c\tau/D$; and using Eq. (1), the mean scattering number is thus given by

$$\bar{n} = f\bar{t} = \frac{1}{2}\tau\ \tau_d = \frac{1}{2}(\alpha D)^2\ (1-\langle\cos\theta\rangle). \tag{3}$$

The probability distribution of the number of elastic scatterings, n, incurred in crossing the medium can then be written approximately as

$$p_e(n|T) = \frac{1}{\bar{n}}\, e^{-n/\bar{n}}. \tag{4}$$

When inelastic scattering is considered, the weight of n^{th} order scattering must be reduced by ω_o^n since the fraction ω_o of all photons is not absorbed at each scattering. The probability density of scattering numbers crossing the medium under the constraint of absorption then takes the form

$$p(n|T) = \omega_o^n\, p_e(n|T) = \frac{\omega_o^n}{\bar{n}}\ e^{-n/\bar{n}} = \frac{1}{\bar{n}} \exp\left[-n\left(\frac{1}{\bar{n}} - \ln\omega_o\right)\right]. \tag{5}$$

If $\bar{n}_o$ is the mean number of scatterings under the influence of absorption, then a comparison of equations (4) and (5) reveals that

$$\bar{n}_o = (\bar{n}^{-1} - \ln\omega_o)^{-1}. \tag{6}$$

Using $\bar{n}_o$ in Eq. (3) leads to

$$\bar{t} = \left[\frac{\tau c}{D}\left(\frac{2}{\tau\tau_d} - \ln\omega_o\right)\right]^{-1} \tag{7}$$

for the multipath time delay characterizing one-way transport. For ω_o=1, this expression reduces simply to Eq. (1).

The form of the signal arriving at the ocean bottom for multiple scattering or diffusion conditions has been found, as previously noted, to be of the form

$$p_B(t) = \frac{1}{\bar{t}}\, e^{-t/\bar{t}}. \tag{8}$$

A similar form applies to the reflected radiation with the multipath time delay, t, referenced to the instant of scattering from the bottom. If $\bar{t}_1$ is the mean multipath time delay for upward transport, then the temporal description of the round trip signal is given by the convolution of the two exponential functions:

$$p_s(t) = \frac{1}{\bar{t}\,\bar{t}_1} \int_o^t e^{u/\bar{t}}\, e^{-(t-u)/\bar{t}_1}\, du. \tag{9}$$

Invoking reciprocity in the scattering medium, it seems reasonable to assume that the downwelling and upwelling transport exhibit the same mean multipath delay time, $\bar{t}$, for those paths which exit the medium perpendicular to the interface--just as the incident energy entered. It is just those paths which are of specific interest to the airborne lidar problem, because they are the only ones which have any appreciable chance of reaching a coaxial receiver. Integrating Eq. (9) and setting $\bar{t}_1 = \bar{t}$ leads to

$$p_s(t) = \frac{t}{\bar{t}^2}\, e^{-t/\bar{t}}. \tag{10}$$

The general form of this relationship is illustrated in Fig. 1. It can be seen that the signal exhibits a peak at $t=\bar{t}$; for signal detectors that search for the peak of the bottom return, there will be a timing bias of this amount. The corresponding fractional error in the depth estimate is given by

$$\frac{\Delta}{D} = \frac{c\bar{t}}{2D} \quad . \tag{11}$$

Using Eq. (7), this becomes

$$\frac{\Delta_1}{D} = \frac{1}{2}\left\{ 2\left[\alpha D(1-\langle\cos\theta\rangle)\right]^{-1} - \alpha D \ell n \omega_o \right\}^{-1}, \tag{12}$$

where the subscript "1" denotes the multiple scattering situation. Note that the fractional depth error is a function of the parameters αD, ω_o, and $\langle\cos\theta\rangle$ alone.

Simulations performed for small scattering numbers indicate that while the tail of the multipath time delay distribution for one-way transport is exponential, the early return (including directly transmitted light) can be much greater than suggested by the exponential form. It follows that, in this case, the peak of the bottom reflected round-trip return signal will probably occur before $\bar{t}$, so that Eq. (12) is an upper bound on the bias in this regime. Stotts[3] has derived a closed form solution for the multipath time delay, which he feels is valid in the single and low order multiple scattering regime, as follows:

$$\bar{t}_2 = \frac{D}{c}\left\{ \frac{0.30}{\omega_o \tau \overline{\theta^2}} \left[\left(1 + \frac{9}{4}\omega_o \tau \overline{\theta^2}\right)^{3/2} - 1 \right]^{-1} \right\}. \tag{13}$$

Using Eqs. (11) and (13) with $\tau = \alpha D$ leads to

$$\frac{\Delta_2}{D} = \frac{1}{2}\left\{ \frac{0.30}{\alpha D \omega_o \overline{\theta^2}} \left[\left(1 + \frac{9}{4}\alpha D \omega_o \overline{\theta^2}\right)^{3/2} - 1 \right]^{-1} \right\}. \tag{14}$$

Thus, for low scattering orders, the fractional depth error is a function of only one parameter, $\overline{\phi^2} = \alpha D \omega_o \overline{\theta^2}$, which is the mean squared angle between the beam axis and the radius of incidence on the bottom at a range of αD optical depths. Equation (14) is plotted in Fig. 2. As expected, the fractional depth error increases with the mean off-axis angle of incidence at the bottom. The result will eventually break down at high values of $\overline{\phi^2}$ where small angle approximations are no longer valid.

Signal Strength

The strength of the lidar return from the bottom, for an unlimited receiver field of view, can be computed for the two transport regimes. For the low scattering order case, energy losses occur principally through absorption, and the energy in the return signal for a large receiver field of view is expected to behave exponentially in the form

$$\frac{E_2}{R} = C e^{-2kD}, \tag{15}$$

where R is the albedo of the ocean bottom and k is a constant close in value to the diffuse attenuation coefficient, K[7]. It has been found experimentally[8] that K may be written approximately as

$$K = a + s/b = \alpha\left\{1 - \omega_o(1-b^{-1})\right\} \tag{16}$$

where $b \cong 20$ (H.R. Gordon -- personal communication). This shows that, in addition to loss from absorption, a small fraction of the scattered energy is also lost from the signal. Substituting Eq. (16) into Eq. (15) with k=K, one obtains

$$\frac{E_2}{R} \approx C \exp\left\{ -2\alpha D\left[1 - \omega_o(1-b^{-1})\right]\right\}, \tag{17}$$

indicating dependency on αD and ω_o only.

For the multiple scattering and diffusion dominated regime, a different treatment is necessary. The empirical formula for the transmission probability, T, through a non-absorbing turbid medium with effective scattering thickness τ_d is

$$T = \frac{A}{B + \tau_d}, \tag{18}$$

where A and B are constants equal to 1.69 and 1.42, respectively, for normal entry. The probability distribution $p(n|T)$ of scattering orders for transmitted photons is listed in Eq. (4); the probability that an incident photon will be transmitted with exactly n scatterings is then

$$p(T|n) = T\, p(n|T). \tag{19}$$

If absorption is introduced, the energy fraction associated with these photons becomes

$$e(n) = T\, p_e(n|T)\, \omega_o^{\,n}. \tag{20}$$

For low scattering numbers and large optical depths, the actual probability distributions for photons traversing a medium differ somewhat from the pure exponential forms used in Eqs. (4) and (5). Monte Carlo simulation results[6] indicate that for increasing scattering numbers (or multipath time delays), the transit probability rises sharply from a low value, achieves a peak at a relatively low scattering number, and then decays exponentially for the remainder. Equations (4) and (5) thus significantly overestimate the contribution from the low scattering numbers. Ideally one should calculate the fraction of incident energy transmitted through the medium, E_T, by obtaining and integrating the required distribution. Lacking these functions, one can nevertheless proceed by substituting Eqs. (5) and (18) into Eq. (20) and summing over appropriate scattering numbers as follows:

$$\begin{aligned} E_T = \sum_{n=m}^{\infty} e(n) &= \frac{A}{\bar{n}(B+\tau_d)} \sum_{n=m}^{\infty} \exp\left\{(\ell n\, \omega_o - 1/\bar{n})\right\}^n \\ &= \frac{A}{\bar{n}(B+\tau_d)} \frac{\exp\left\{m(\ell n \omega_o - 1/\bar{n})\right\}}{1-\exp(\ell n \omega_o - 1/\bar{n})} \end{aligned} \tag{21}$$

If the summation is started at m=0, the undesirable form of the exponential probability distribution at low scattering numbers will lead to an excess of transmitted energy from these little attenuated paths, particularly for low ω_o where other paths are much more highly attenuated. The number of low order paths to be truncated depends ultimately on ω_o, τ, and τ_d (i.e., on ω_o, αD, and $\langle\cos\theta\rangle$). In order to provide some quantitative results from Eq. (21), an ad hoc value of $m=\bar{n}/3$ will be selected. This value is not inconsistent with the distributions presented graphically by Bucher[6].

Once again invoking statistical reciprocity for the return path, one can calculate the round trip bottom return energy fraction for an unlimited receiver field of view as

$$\frac{E_1}{R} = \frac{E_T^{\,2}}{R} = FA^2(GH)^{-2}\, J^2 \tag{22}$$

where

$G = 1-\exp\left\{\ell n \omega_o - 2\, N^{-1}\right\}$,

$H = (B+N/\alpha D)\, N$,

$J = \exp\left\{N(\ell n\, \omega_o - 2N^{-1})/6\right\}$,

$N = (\alpha D)^2\, (1-\langle\cos\theta\rangle)$, and

F = a constant.

Eq. (3) has been substituted for $\bar{n}$, and R is the albedo of the bottom. Note that E_1/R is a function of αD, ω_o, and $\langle\cos\theta\rangle$.

In computing the peak received power, it is important to determine whether the impulse response function given by Eq. (10) is significantly wider than the excitation width of the laser source pulse. If the source pulse is broad compared to the impulse response, then the peak power will be proportional to the return energy given by Eq. (17) or (22). For narrow source pulses, however, the peak power will be dictated by the spread function modal time, $\bar{t}$, since this will dominate the temporal distribution of the received pulse. For a spread function of the type given in Eq. (10), the peak power, P, is related to the integrated energy by the equation

$$P = E/e\bar{t}, \tag{23}$$

where e = 2.718 is the natural logarithm base, and $\bar{t}$ is given by Eq. (7) or (13). Both of these equations can be written in the form

$$\bar{t} = Dg(\alpha D, \omega_o, \bar{S}), \tag{24}$$

where g is a function of αD, ω_o, and some parameter, $\bar{S}$, relating to the scattering function. Eq. (24) can be rewritten as

$$\bar{t} = \alpha^{-1} h(\alpha D, \omega_o, \bar{S}), \tag{25}$$

where $h = \alpha Dg$. Substituting Eq. (25) into Eq. (23) yields

$$P = \alpha E/e\, h(\alpha D, \omega_o, \bar{S}), \tag{26}$$

which indicates that for mean multipath time delays significantly longer than the exciting laser pulse, the peak power for given values of αD, ω_o, and $\bar{S}$ will be proportional to α. The impact of this result is that, for an unlimited receiver field of view and a given value of optical depth, αD, stronger returns will be received from shallower depths and weaker returns from deeper depths, if the laser pulse is short compared to the impulse response.

Discussion

One of the principal problems in using a scattering distribution is the need to establish the portion which is relevant to the transport process for the round trip lidar bottom return. If the receiver field of view is considered to be unlimited (large), then the small amount of highly scattered energy returning at large distances from the incoming beam axis (and with correspondingly large multipath time delays) will cause the calculated time delay (and hence fractional depth error) to be significantly larger than for a case with even moderate field of view limitation. If one makes the first order approximation that the returning energy truncated by a limited field of view comes from the high angle portion (10 or 20 percent) of the scattering function, then trends for limited field of view cases can be approximated by truncating the scattering function and thereby increasing the effective value of $\langle\cos\theta\rangle$. The scattering function which will now be used to quantify the scattering parameters $\langle\cos\theta\rangle$ and $\overline{\theta^2}$ in the foregoing formulations was measured by W.H. Wilson at Scripps Institution of Oceanography and reported by Funk[10]. This function exhibits a strong forward bias with 50% of the scattering occurring through angles of less than 10 degrees. To simulate the expected qualitative effects of moderate field of view limitation and to examine the sensitivity of the predictions to $\langle\cos\theta\rangle$, several ad hoc percentiles of the scattering function (100, 90, and 80) were arbitrarily selected for study. For the complete distribution, a value of $\langle\cos\theta\rangle$=0.908 was estimated, while the forward 90th and 80th percentiles yielded values of 0.971 and 0.986 respectively.

In Fig. 3, the fractional depth bias for the multiple scattering and diffusion regime from Eq. (12) is plotted against αD for various values of ω_o and $\langle\cos\theta\rangle$. The result can be seen to be fairly sensitive to the portion of the scattering function used to compute $\langle\cos\theta\rangle$, with the fractional error increasing as one permits the distribution to be more isotropic. It follows that a restriction in the receiver field of view, which is equivalent to restricting the range of scattering angles for which energy will be accepted, will cause the associated fractional depth error to be somewhat smaller. The curves for

$\langle\cos\theta\rangle = 0.908$ must, therefore, be considered absolute upper bounds on the potential errors for a physical system. In general, the fractional depth error is seen to be reduced for lower values of scattering albedo (higher absorption). For $\omega_o = 0.5$ the error is only weakly dependent on the scattering function for $\alpha D \gtrsim 15$ and is nearly constant with increasing αD. It is interesting to note that when the complete scattering function is considered ($\langle\cos\theta\rangle = 0.908$), the peak in the fractional error occurs for αD values from 6 to 14. The decrease in fractional error for higher αD is due to increasing dominance of the absorption term.

In light of the large potential bias errors noted in Fig. 3, it will be important to attempt to correct depth measurements for the impact of the spread function. If the form of the source pulse is known, the deconvolution of this pulse from the lidar bottom return pulse should yield a form which can be described by Eq. (10). The peak time, $\bar{t}$, can then be measured and applied as a corrector to largely remove the bias present in the original measurement.

An estimate of the validity for low αD of all the formal expressions presented herein should be considered. A weak condition is to require $\bar{n} \gtrsim 1$; using Eq. (3) and $\langle\cos\theta\rangle = 0.908$, this leads to $(\alpha D)_{min} = 4.7$. A stronger restriction such as $\bar{n} \gtrsim 3$ ($m \gtrsim 1$) is probably more realistic and leads to $(\alpha D)_{min} = 8.1$. This approximate value has been noted on Figures 3-6 as a lower boundary for the region of validity of results with respect to αD.

An attempt was made to reconcile the fractional depth error predictions of Eqs. (12) and (14) for intermediate values of αD. If equivalent percentiles of the scattering function are used to calculate $\langle\cos\theta\rangle$ and $\overline{\theta^2}$ for the two expressions, the predicted errors, as seen in Fig. 4 for $\langle\cos\theta\rangle = 0.971$ ($\overline{\theta^2} = 0.060$), are not in good agreement for any range of αD because Eq. (14) predicts consistently larger values. The Stotts formula depends on the validity of small angle expressions and is not accurate for larger values of αD. Further it tends to underestimate the impact of absorption as αD increases. Eq. (14) can thus be valid only as an absolute upper bound, and Eq. (12) would, indeed, be expected to provide lower (and more accurate) error estimates.

The relative, round trip, bottom return signal energy, E_1/R, predicted for the multiple scattering and diffusion regimes (Eq. 22) is plotted in Fig. 5 as a function of αD for several values of ω_o. As previously noted, E_1/R depends on αD, not α and D separately. For source pulse widths significantly wider than the spread function, this is also the form of the peak power. For a given optical depth, the received energy increases with increasing single scatter albedo, ω_o, because the corresponding absorption is less. The $\omega_o = 1$ curve is the asymptotic limit corresponding to no absorption. A model including both the exit from the medium of backscattered energy which has not reached the bottom and multiple reflections from the bottom would yield a horizontal line. In Eq. (22) and Fig. 5, only the energy first reaching the bottom and then returning through the entrance interface is considered to be "signal energy." This accounts for the attenuation present in the limiting case of the $\omega_o = 1$ curve. The "lost" non-signal energy would be more or less uniformly distributed over a long time span and not directly associated with the bottom return pulse.

In general, the effective attenuation coefficients describing the exponential decay (e.g., the slopes of the curves) are seen to be virtually independent of αD for $\alpha D \gtrsim 6$. Associated with each curve in Fig. 5 are several additional line segments representing the low αD prediction of Eq. (17) as well as the limiting cases of exp (-2aD) and exp (-2αD) -- no loss due to scattering and complete loss due to scattering, respectively. It can be seen that the slopes predicted by Eq. (22), under the very arbitrary assumption of $m = \bar{n}/3$, fall between the slopes from Eq. (17) and exp (-2aD) for $\omega_o = 0.8$ and 0.9; for $\omega_o = 0.5$ the slope falls completely outside the acceptable boundaries of exp (-2aD) and exp (-2αD). The reason for this disparity can be traced directly to the previously discussed divergence between the assumed exponential distribution and the actual peaked distribution for low scattering orders which is accentuated in the realm of high absorption (low ω_o). One should note that the slopes predicted by Eq. (22) might be expected to be greater than those from Eq. (17) for which very little of the scattered energy is considered actually lost from the return signal. In fact, this is not the case. The curves can arbitrarily be made steeper by using a larger value for the summation index m; such numerical juggling is, however, artificial and not the point. The necessary distributions must be obtained from Monte Carlo simulations and integrated if a more accurate prediction of the exact slopes is desired. The $\bar{n}/3$ estimate is certainly good enough to permit general features and trends in the results to be meaningfully extracted.

The peak received signal power, calculated in Eq. (23) from Eqs. (7) and (22), is plotted in Fig. 6 as a function of αD and ω_o with a default value of $\alpha = 1$. This function is presented with the previously mentioned caveat that the range of validity is limited to

that for which $\bar{t} \gtrsim t_p$, where t_p is the incident laser pulse width. As $\bar{t}$ approaches t_p, the actual measured peak power curves will gradually behave more and more like the signal energy prediction curves. Unlike the signal energy curves which they somewhat resemble, the peak power curves depend both on αD and on α and D separately. This relationship, as denoted by the dotted curves of α=0.5 and 4.0 for ω_o=0.8 in Fig. 6, is a multiplicative one which simply translates the curves up or down by the factor α. The prediction is that for a fixed value of αD, the peak received power (for $\bar{t} \gtrsim t_p$) will be proportional to α. The reason for this is that with αD fixed, a larger α implies a correspondingly smaller D; and this shallower depth leads to a stronger peak return by permitting the scattering (loss) to be effective over a lesser throw distance. A more precise way of looking at this is to note that the fractional depth error is invariant for fixed αD, so for shallower depths the absolute depth error decreases, and the spread function gets narrower. Since the signal energy is also invariant, the peak power increases in direct proportion to α.

Overall, the peak power curves exhibit the same general behavior as the signal energy curves for variations in ω_o. Like the signal energy curves, the peak power curves exhibit fairly constant exponential decay slopes for $\alpha D \gtrsim 10$. The slopes for $\omega_o \lesssim 0.9$ tend to decrease slightly with increasing D--particularly for high values of ω_o. In actuality, if one compares the asymptotic behavior in Figs. 5 and 6 for $\omega_o \lesssim 0.9$ and large αD, the slopes are seen to be virtually identical--the lower the ω_o, the lower the αD at which this takes place. The peak power curves also reach an asymptotic limit at ω_o=1, but the slope is much steeper than for signal energy. This behavior can be easily understood by reviewing the behavior of Eqs. (7), (22), and (23): for large αD, $\bar{t}$ is dependent on α, not αD, except when $\omega_o \rightarrow 1$. Thus P behaves like E. For $\omega_o \rightarrow 1$, $\ell n \omega_o \rightarrow 0$, and the behavior of $\bar{t}$ again becomes dependent on αD; this explains how the asymptotic slopes in Figs. 5 and 6 for environmentally typical values of ω_o can be equal, while for ω_o=1, they are not.

The steeper slopes of the peak power curves (compared to the signal energy curves) for moderate values of αD and/or high values of ω_o indicate that scattering affects peak power more adversely than it does signal energy; for high scattering orders, the energy may eventually return (for this unlimited field of view case) but at too late a time to be useful to a pulse amplitude detector. Since a large proportion of this late arriving, highly scattered radiation intersects the entry interface at fairly large radial distances from the beam axis, a receiver field of view small enough to exclude it does not necessarily reduce the peak received power. Further calculations and/or simulations are necessary to permit the quantitative prediction of peak power versus receiver field of view, which is of interest to the system designer.

Conclusions

The effects of the radiation transfer process, for light in natural waters, on penetration and depth measurement accuracy for an airborne lidar bathymetry system have been investigated. Straightforward analytic extensions of Monte Carlo scattering simulation results have been employed to derive a simple form for the temporal dispersion of pulsed radiation traversing a turbid medium. The application of this theory to two-way transport through the water column has resulted in the computation of the character of the (optical) depth dependencies of the expected depth measurement bias and bottom return signal energy and peak power. The theory indicates that both the depth error (expressed as a fraction of the total depth) and the bottom return signal energy depend (solely) on three parameters: the optical depth, the single scattering albedo, and the scattering anisotropy (represented as the mean value of the cosine of the scattering angle). The prediction of significant depth errors caused by pulse stretching is moderated by the fact that in quantifying the error we have also identified and quantified the appropriate correction procedure. The prediction of peak received bottom return power, from a given optical depth, proportional to the beam attenuation coefficient (for multipath time spreading in excess of the incident laser pulse duration) is a significant departure from the contemporary theory[7] of exponential dependence on optical depth alone.

Because these predictions are based on a number of assumptions and approximations, it is vital that they be severely tested for physical validity by experimentation and/or specific, detailed simulation over a wide range of parameters. A desirable topic of major interest not in this presentation is the quantitative effect of receiver field of view. In the future, the theory described herein should also be merged with a good low order scattering theory valid to zero optical depth. This would permit the prediction of absolute bottom return signal energy and power.

References

1. Guenther, G.C., and L.R. Goodman, "Laser Applications for Near-Shore Nautical Charting," SPIE Ocean Optics V, 160 (1978).

2. Thomas, R.W.L., and A.C. Holland, "Geometry Dependence of Optical Pulse Broadening in Multiple Scattering Media," SPIE 168 (1978).

3. Stotts, L.B., Appl. Opt. Let., 17, 4, 504 (1978).

4. Harries, W., and G. Hertz, Z. Phys. 46, 177 (1927).

5. Didlaukis, M., Z. Phys. 77, 352 (1932).

6. Bucher, E.A., Appl. Opt. 12, 10, 2391 (1973).

7. Witt, A.K., J.G. Shannon, M.B. Rankin, and L.A. Fuchs, "Air/Underwater Laser Radar Test Results, Analysis, and Performance Predictions," Naval Air Development Center Report No. NADC-76005-20, (1976). (Report is classified "CONFIDENTIAL")

8. Sorenson, G.P., R.C. Honey, J.R. Payne, "Analysis of the Use of Airborne Laser Radar for Submarine Detection and Ranging," SRI Report 5583, 1966. (Report is classified "CONFIDENTIAL")

9. Danielson, R.E., D.R. Moore, and H.C. van de Hulst, J. Atmos. Sci. 26, 1078 (1968).

10. Funk, C.J., Appl. Opt. 12, 2, 301 (1973).

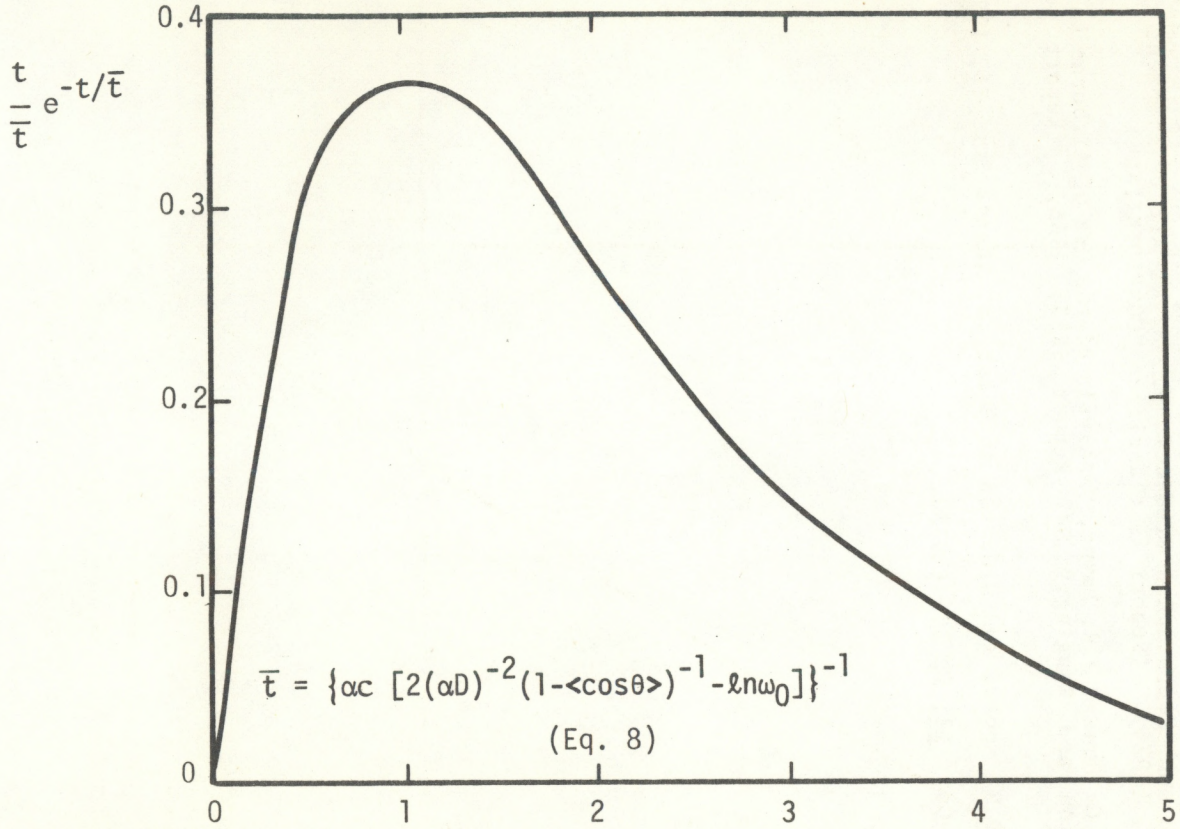

Figure 1. General Form of Round-Trip Impulse Response for Diffusion Limited Case

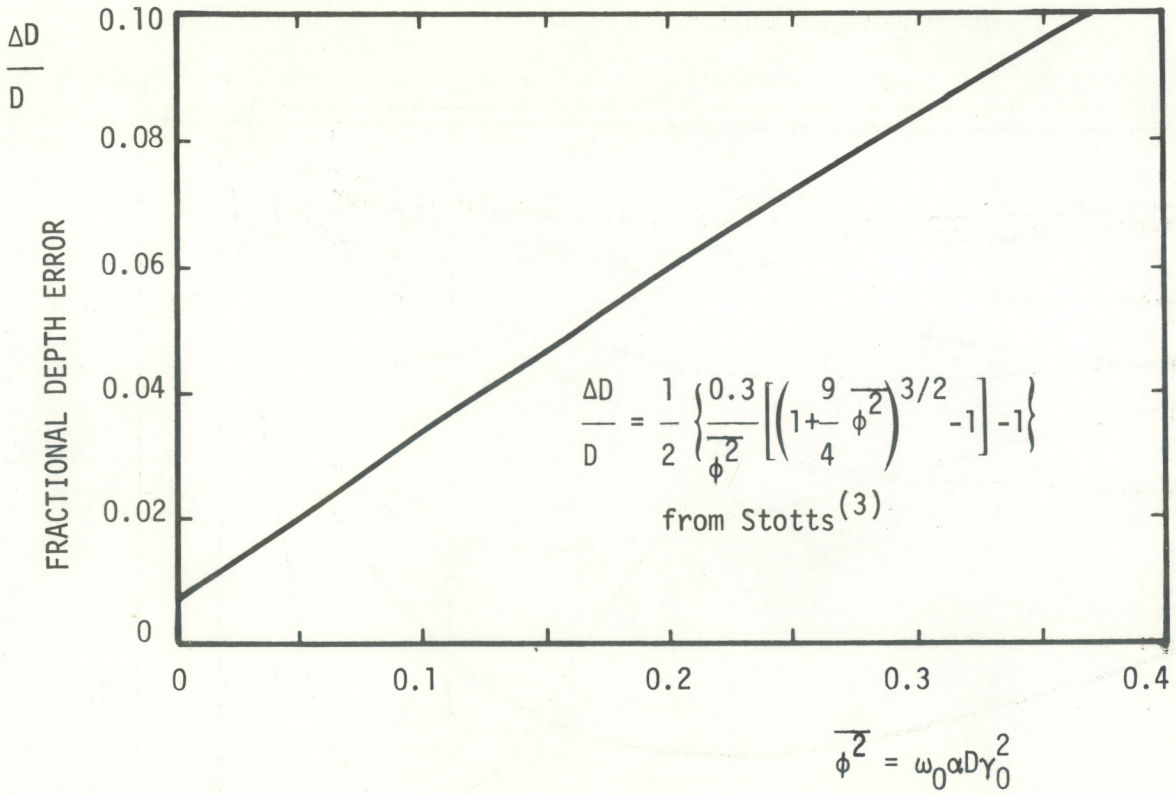

Figure 2. Fractional Depth Error vs. Mean Square of Projected Angle

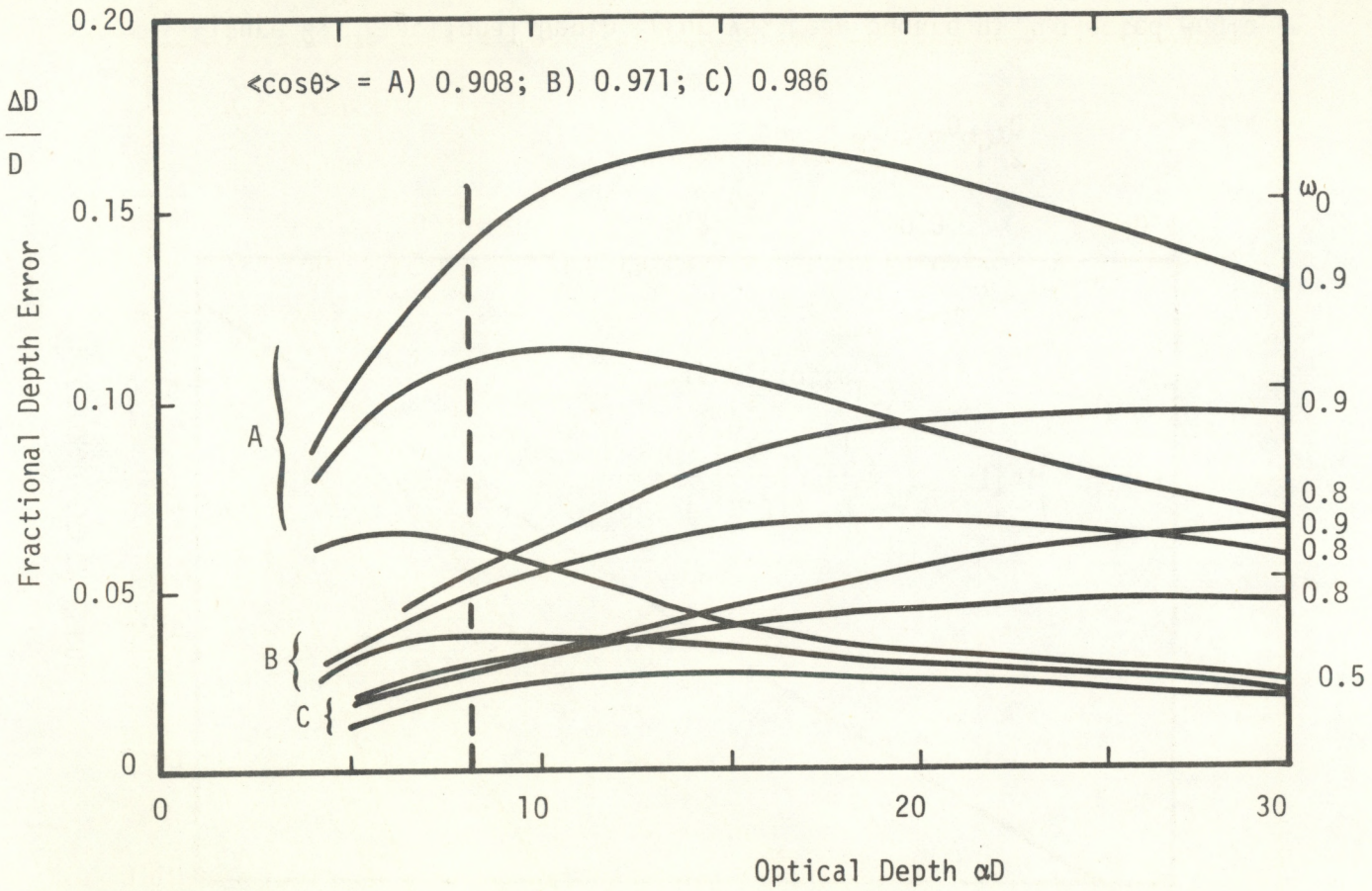

Figure 3. Predicted Fractional Depth Error for the Diffusion Limited Case. $\omega_0 = S/\alpha$

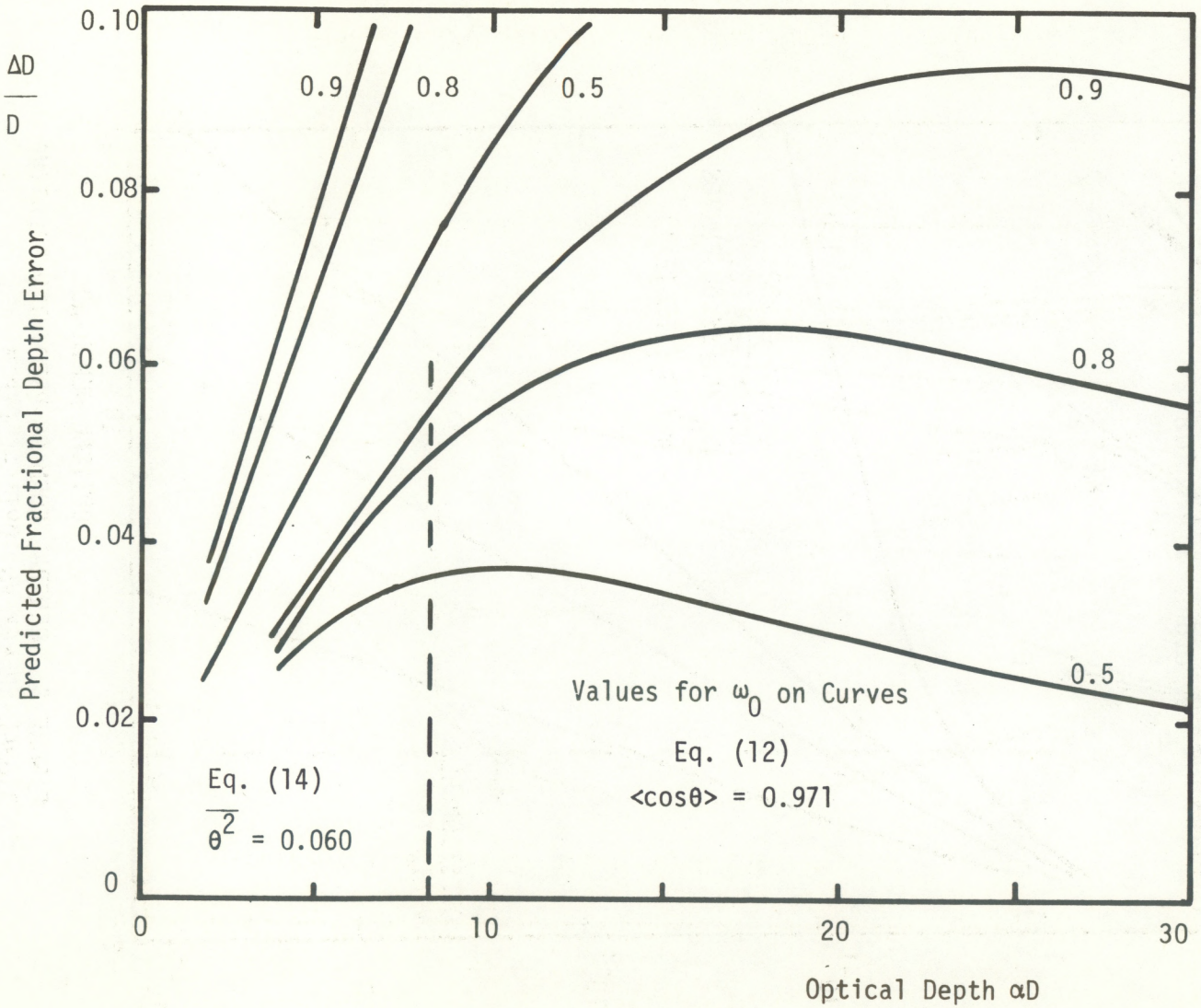

Figure 4. Comparison of Predicted Time Delays with Stotts[3] Theory

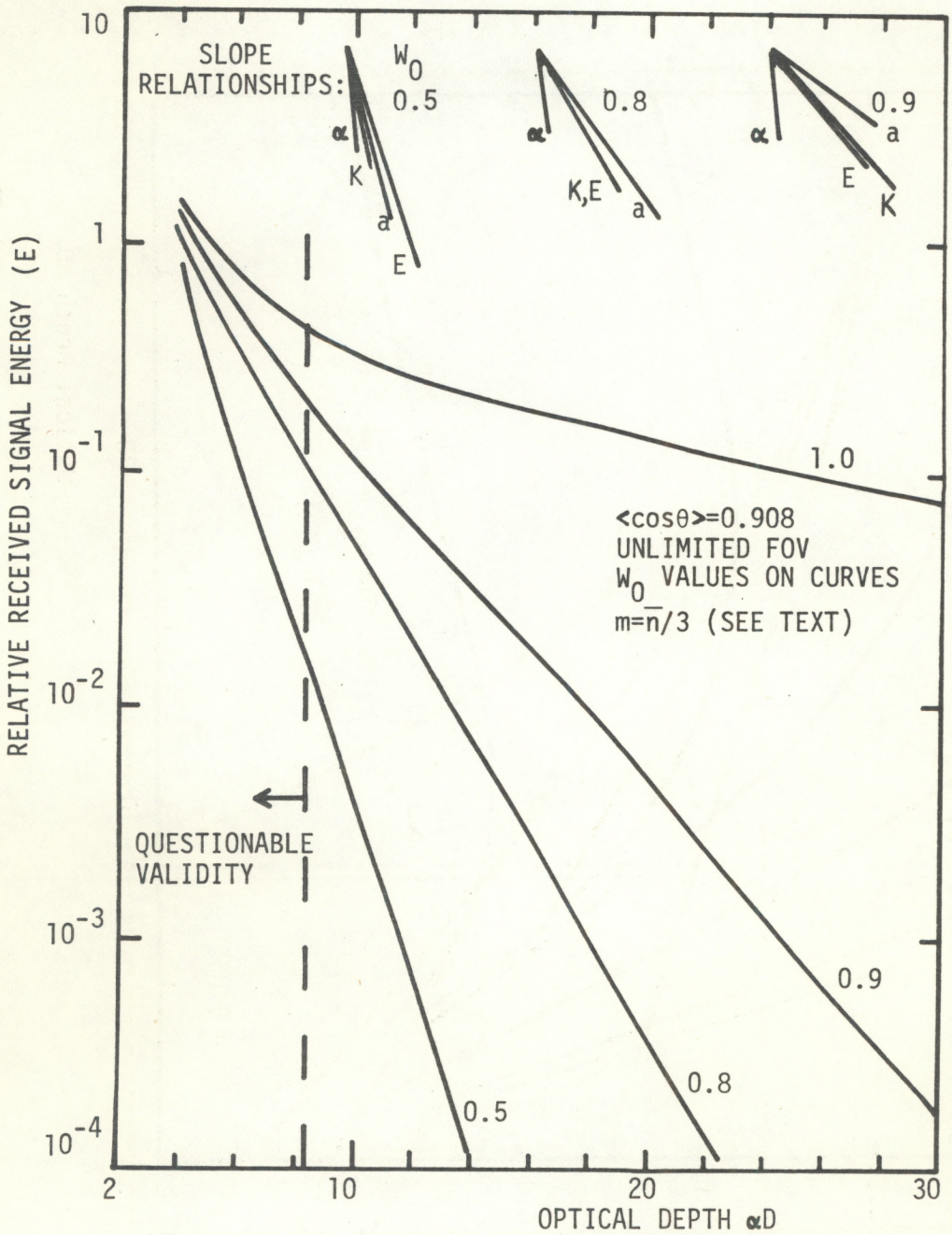

FIGURE 5. GENERAL FORM OF PREDICTED RELATIVE SIGNAL ENERGY VS. OPTICAL DEPTH

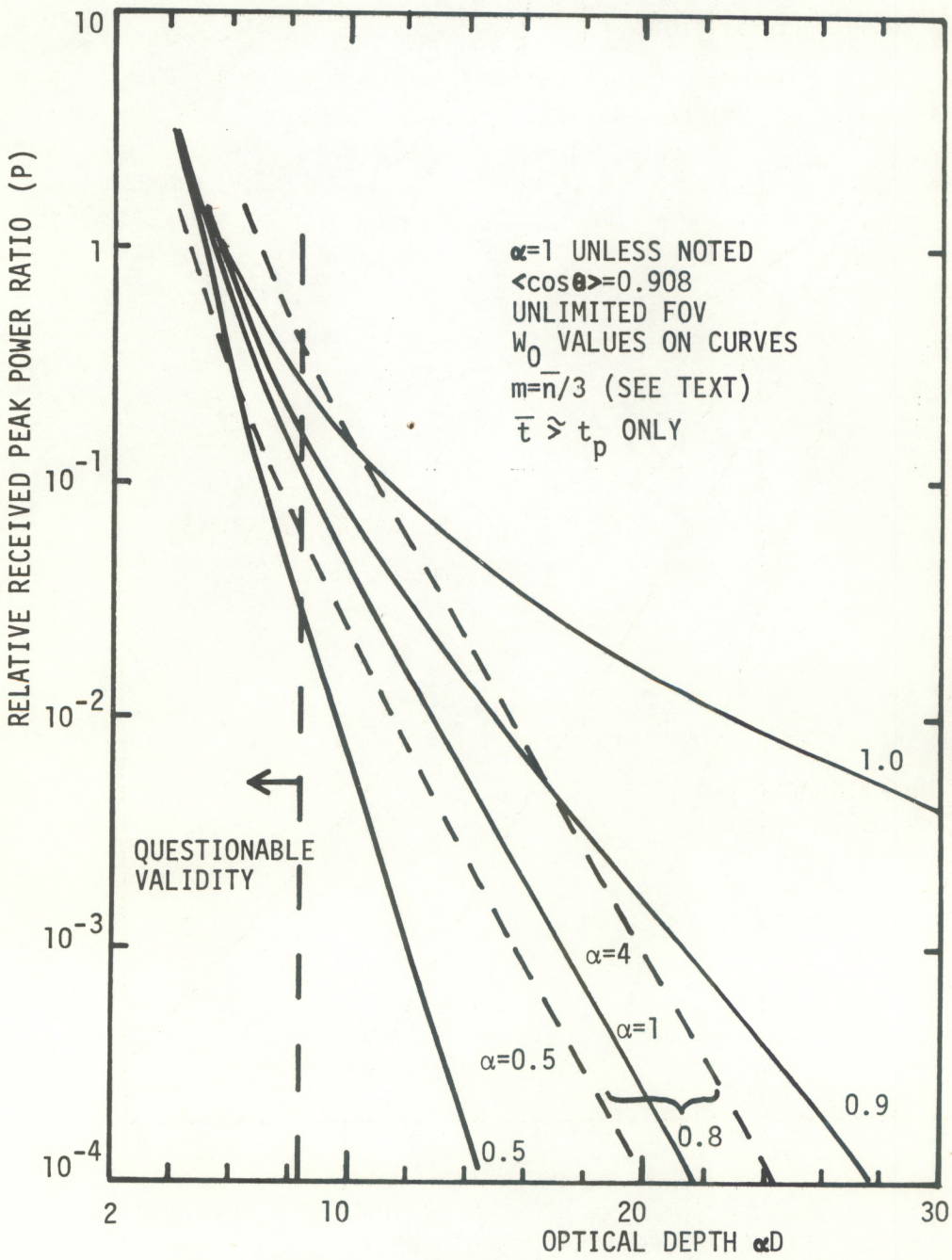

FIGURE 6. GENERAL FORM OF PREDICTED RELATIVE PEAK POWER VS. OPTICAL DEPTH

(Continued from inside front cover)

NOS 16 Deep Sea Tide and Current Observations in the Gulf of Alaska and Northeast Pacific. Carl A. Pearson, December 1975.

NOS 17 Deep Sea Tide Observations Off the Southeastern United States. Carl A. Pearson, December 1975. (PB-250072)

NOS 18 Performance Evaluation of Guildline Model 8400 Laboratory Salinometer. James E. Boyd, July 1976.

NOS 19 Test Results on an Electromagnetic Current Sensor With an Open Design. David R. Crump, August 1976. (PB-260444)

NOS 20 Test and Evaluation of the Interocean Systems, Inc. Model 500 CTD/Oxygen pH In-Situ Monitor System. Barbara S. Pijanowski, August 1976. (PB-260442)

NOS 21 National Ocean Survey Abstracts - 1976. October 1977, 20 pp. (PB-275293)

NOS 22 Performance Evaluations of the Orbisphere Laboratories Models 2702 and 2709 Oxygen Measuring Systems. Jerald M. Peterson, Charles C. White, Barbara S. Pijanowski and Gary K. Ward, June 1979.

NOS 23 Performance Evaluation of the Martek Instruments, Inc. Mark V Digital Water Quality Analyzer System. Jerald M. Peterson, Charles C. White, Barbara S. Pijanowski and Gary K. Ward, June 1979.

NOS 24 Performance Evaluation of the Horiba Instruments, Inc. Model U-7 Water Quality Checker. Jerald M. Peterson, Charles C. White, Barbara S. Pijanowski and Gary K. Ward, June 1979.

NOAA SCIENTIFIC AND TECHNICAL PUBLICATIONS

The National Oceanic and Atmospheric Administration was established as part of the Department of Commerce on October 3, 1970. The mission responsibilities of NOAA are to assess the socioeconomic impact of natural and technological changes in the environment and to monitor and predict the state of the solid Earth, the oceans and their living resources, the atmosphere, and the space environment of the Earth.

The major components of NOAA regularly produce various types of scientific and technical information in the following kinds of publications:

PROFESSIONAL PAPERS — Important definitive research results, major techniques, and special investigations.

CONTRACT AND GRANT REPORTS — Reports prepared by contractors or grantees under NOAA sponsorship.

ATLAS — Presentation of analyzed data generally in the form of maps showing distribution of rainfall, chemical and physical conditions of oceans and atmosphere, distribution of fishes and marine mammals, ionospheric conditions, etc.

TECHNICAL SERVICE PUBLICATIONS — Reports containing data, observations, instructions, etc. A partial listing includes data serials; prediction and outlook periodicals; technical manuals, training papers, planning reports, and information serials; and miscellaneous technical publications.

TECHNICAL REPORTS — Journal quality with extensive details, mathematical developments, or data listings.

TECHNICAL MEMORANDUMS — Reports of preliminary, partial, or negative research or technology results, interim instructions, and the like.

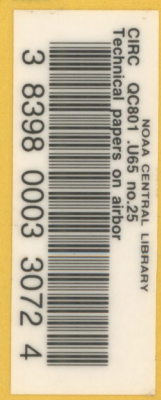

Information on availability of NOAA publications can be obtained from:

ENVIRONMENTAL SCIENCE INFORMATION CENTER (D822)
ENVIRONMENTAL DATA AND INFORMATION SERVICE
NATIONAL OCEANIC AND ATMOSPHERIC ADMINISTRATION
U.S. DEPARTMENT OF COMMERCE

6009 Executive Boulevard
Rockville, MD 20852

NOAA--S/T 79-262